AD-A061 145 CALIFORNIA UNIV BERKELEY OFFICE OF RESEARCH SERVICES F/G 8/7
FABRIC ANALYSIS OF UNDISTURBED SANDS FROM NIIGATA, JAPAN.(U)
SEP 78 J K MITCHELL, F J GUZIKOWSKI DACA39-76-M-0344
UNCLASSIFIED WES-TR-S-78-11 NL

LEVEL II

TECHNICAL REPORT S-78-11

FABRIC ANALYSIS OF UNDISTURBED SANDS FROM NIIGATA, JAPAN

by

James K. Mitchell, Frank J. [illegible], William C. B. Villet
Office of Research Services
University of California, Berkeley, California 94720

DACA39-76-M-0344

11 Sep 1978

Final Report

Approved for Public Release; Distribution Unlimited

WES TR-S-78-11

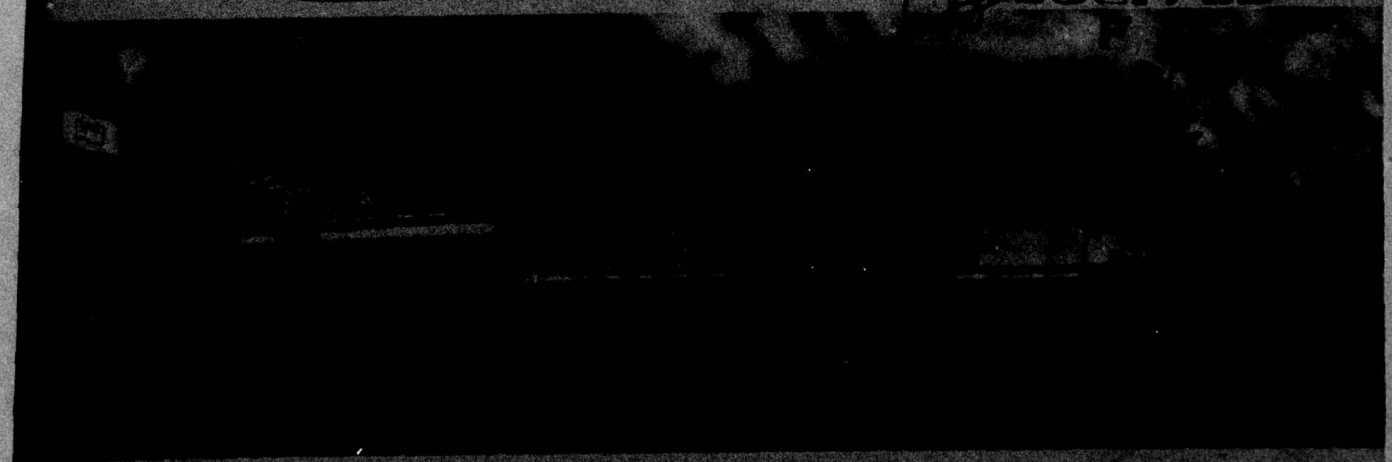

Prepared for Office, Chief of Engineers, U. S. Army
Washington, D. C. 20314

Work Unit No. [illegible] Task A2, Work Unit 005)

Soils and Pavements Laboratory
U. S. Army Engineer Waterways Experiment Station
P. O. Box 631, Vicksburg, Miss. 39180

Destroy this report when no longer needed. Do not return it to the originator.

Unclassified

SECURITY CLASSIFICATION OF THIS PAGE (When Data Entered)

REPORT DOCUMENTATION PAGE

READ INSTRUCTIONS BEFORE COMPLETING FORM

1. REPORT NUMBER: Technical Report S-78-11
2. GOVT ACCESSION NO.:
3. RECIPIENT'S CATALOG NUMBER:

4. TITLE (and Subtitle): FABRIC ANALYSIS OF UNDISTURBED SANDS FROM NIIGATA, JAPAN
5. TYPE OF REPORT & PERIOD COVERED: Final report
6. PERFORMING ORG. REPORT NUMBER:

7. AUTHOR(s): James K. Mitchell; Frank J. Guzikowski; Willem C. B. Villet
8. CONTRACT OR GRANT NUMBER(s): Contract No. DACA39-76-M0344 new

9. PERFORMING ORGANIZATION NAME AND ADDRESS: College of Engineering, Office of Research Services, University of California, Berkeley, Calif. 94720
10. PROGRAM ELEMENT, PROJECT, TASK AREA & WORK UNIT NUMBERS: Project 4A161102AT22, Task A2, Work Unit 005

11. CONTROLLING OFFICE NAME AND ADDRESS: Office, Chief of Engineers, U. S. Army, Washington, D. C. 20314
12. REPORT DATE: September 1978
13. NUMBER OF PAGES: 112

14. MONITORING AGENCY NAME & ADDRESS (if different from Controlling Office): U. S. Army Engineer Waterways Experiment Station, Geotechnical Laboratory, P. O. Box 631, Vicksburg, Miss. 39180
15. SECURITY CLASS. (of this report): Unclassified
15a. DECLASSIFICATION/DOWNGRADING SCHEDULE:

16. DISTRIBUTION STATEMENT (of this Report)

Approved for public release; distribution unlimited.

17. DISTRIBUTION STATEMENT (of the abstract entered in Block 20, if different from Report)

18. SUPPLEMENTARY NOTES

19. KEY WORDS (Continue on reverse side if necessary and identify by block number)

Liquefaction (Soils)
Niigata, Japan
Sands
Soil structure
Soils -- Japan
Undisturbed soil samples

20. ABSTRACT (Continue on reverse side if necessary and identify by block number)

The fabric of undisturbed sand samples, six from a location known to have liquefied and five from a location that did not, from a site in Niigata, Japan, has been studied using petrographic thin sections and water content-soil water suction measurements. All samples were frozen after sampling but prior to transportation from the site to the laboratory.

The gradational and particle shape characteristics of the medium to fine sands from the two locations are similar, but the void ratios of (Continued)

Cont

DD FORM 1 JAN 73 1473 EDITION OF 1 NOV 65 IS OBSOLETE

Unclassified

SECURITY CLASSIFICATION OF THIS PAGE (When Data Entered)

20. ABSTRACT (Continued).

CONT

samples from the location known not to have liquefied were generally somewhat higher than for samples from the site that liquefied. Particle arrangements in the horizontal plane were slightly more random for the samples from the location that did not liquefy. These samples also exhibited a stronger degree of particle long axis orientation in vertical planes, a finding consistent to their higher resistance to liquefaction in cyclic triaxial tests. Significant differences in orientations of normals to interparticle contacts were not detected for samples from the two locations.

The results of the suction-water content determinations indicated that samples from the location where the sand liquefied had a greater volume of small size pores than did the samples of sand that did not liquefy.

As the samples were not frozen until after sampling, any disturbance that may have occurred during sampling is unknown. The results do suggest, however, that fabric in-situ is related to susceptibility to liquefaction.

THE CONTENTS OF THIS REPORT ARE NOT TO BE USED FOR ADVERTISING, PUBLICATION, OR PROMOTIONAL PURPOSES. CITATION OF TRADE NAMES DOES NOT CONSITIUTE AN OFFICIAL ENDORSEMENT OR APPROVAL OF THE USE OF SUCH COMMERCIAL PRODUCTS.

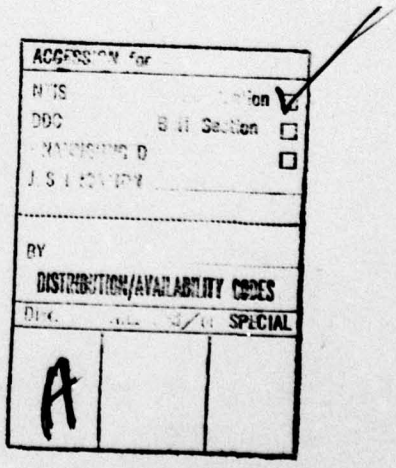

PREFACE

This report was prepared by Professor J. K. Mitchell and Messrs. F. J. Guzikowski and W. C. B. Villet under Contract No. DACA39-76-MO344 as part of on-going work conducted at the U. S. Army Engineer Waterways Experiment Station (WES) under the sponsorship of the Directorate of Military Construction, Office, Chief of Engineers, U. S. Army, under Research in Military Construction, Project 4A161102AT22, Task A2, Work Unit 005, Study of Engineering Classification of Cohesionless Soils.

The work was directed by Dr. F. C. Townsend, Research Civil Engineer, Soil Mechanics Division (SMD), Geotechnical Laboratory (GL). General guidance was provided by Mr. J. P. Sale, Chief, GL, and Mr. C. L. McAnear, Chief, SMD.

Director of the WES during this study and preparation and publication of this report was COL J. L. Cannon, CE. Technical Director was Mr. F. R. Brown.

TABLE OF CONTENTS

LIST OF TABLES*

LIST OF FIGURES

* Tables and figures follow the main text in numerical order as listed.

I. INTRODUCTION

The purpose of this study was to determine fabric characteristics of undisturbed sand samples from Niigata, Japan. The results of these studies in combination with results of completed and continuing studies on the sampling and testing of sands from Niigata (Silver and Ishihara, 1977), as shown in Table 1, have as their objective development of improved understanding of the liquefaction behavior of sands in-situ. It has already been established that liquefaction properties of sand samples compacted in the laboratory bear some relationship to method of sample preparation (Ladd, 1974; Mulilis et al, 1977) and to the sand fabric as characterized by interparticle contact orientations and particle long axis orientations (Mitchell, 1976). Previous work by Oda (1972, 1976), Mahmood (1973) and Mitchell (1976) has shown that the static strength and compressibility of sands and silts also depend upon soil fabric. It is therefore suspected that in-situ liquefaction behavior of sand deposits in response to seismic loading may be related to some degree with the sand fabric.

A fabric analysis was performed on undisturbed sand samples from two sites in Niigata, Japan, as shown in Fig. 1. One site, the "River Site", experienced significant distress from liquefaction during the 1964 earthquake, while the other, the "Road Site," showed no surface evidence of liquefaction during the earthquake. Site profiles are presented in Fig. 2. A complete description of the site profiles and topography has been presented by Silver and Ishihara (1977), who state that it is generally believed that liquefaction at the River site only occurred in the upper 9 meters (30 ft) of the soil profile.

A large number of samples were obtained at the Niigata site using both an Osterberg Sampler and a newly developed Japanese Large Diameter Sampler. Only Osterberg samples were chosen for use in this study as the Japanese sampling method was not used at the Road site. Depths and identification numbers are indicated in Fig. 2 for the eleven samples chosen.

It is important to emphasize at the outset that as the sand at the River site liquefied during the 1964 earthquake, present fabric differences between samples from the Road and River sites cannot be related to liquefaction potential prior to that earthquake. They may, however, relate to present liquefaction potential.

II. SAMPLING PROCEDURE

Introduction

An important aspect of this overall project was the development of new soil sampling, sample handling and sample storage techniques in an effort to minimize sample disturbance between the field and the laboratory. A complete description of these procedures is provided by Silver and Ishihara (1977). In the following section, details of sampling technique will be discussed only as they pertain to the subsequent fabric study.

Sampler Description and Operation

The samples used in this study were obtained by means of a U.S. Osterberg Sampler, a hydraulically operated piston sampler (Osterberg, 1952). A schematic illustration showing the operation of the Osterberg Sampler is presented in Fig. 3.

Sampling at Niigata was performed in a mud filled borehole 100 mm (4 in.) in diameter. The hole was advanced with a fish-tailed bit, which was modified with baffles that directed the drilling fluid away from the bottom of the borehole to reduce disturbance. Fresh drilling mud was introduced into the borehole as the sampler was withdrawn to prevent caving. When the sampling tube cleared the riser casing, a small amount of soil was removed from the core tube, an expandable O-ring packer installed in the tube and locked to prevent the loss of sand. A small hole was then drilled below the piston to release the vacuum developed by the sampler and to make it easier to remove the sample tube. After removing the sample tube, the dimensions of the sample were recorded.

The bottom packer was equipped with small vertical drainage holes. When the vacuum under the piston was released, water from the soil voids

could flow out of the sample. Samples were drained for 24 hours in a vertical position to prepare them for subsequent freezing.

The horizontal orientation of the samples was not recorded on the sampling tubes. This means that a truly three dimensional comparison of sample fabrics from different locations cannot be made.

Specimen Handling

After 24 hours of free drainage, the samples were quickly frozen in liquid nitrogen in the field and stored in dry ice while they were transported from Japan to the laboratory at the University of California. In the laboratory, the samples were stored in a commercial freezer at -10°C.

The quality of the frozen specimens was checked by determining the specimen volume before and after freezing (Silver and Ishihara, 1977). No measurable difference was noted, although an average one percent volume decrease accompanied subsequent thawing. The fact that freezing did not change the dimensions of the sample led Silver and Ishihara (1977) to conclude that the drainage procedure effectively cleared the soil voids of excess water and only provided enough water at the intergranular contacts to provide particle binding when the specimen was frozen.

The lack of measurable sample deformation during freezing indicates that in-situ void ratio was preserved, but since sands at equivalent void ratios may possess radically different fabrics, the possibility of an induced change in fabric as a result of freezing does exist. To investigate this possibility further, a limited study was made by Guzikowski* using Monterey No. 0 sand. It was found that for samples prepared by moist tamping

*Guzikowski, F. J., Unpublished Research Report, Department of Civil Engineering, University of California, Berkeley, 1977.

freezing had no statistically significant effect on the particle long axis orientations for relative densities of 50 and 80 percent. The distributions of interparticle contact normal orientations were not statistically different for frozen and unfrozen samples at a relative density of 80 percent. For samples at a relative density of 50 percent, however, it was found that on the order of 15 percent of the interparticle contacts were disturbed, as evidenced by changes in the interparticle contact distribution function.

Soil water suction - water content determinations were also made by Guzikowski on samples that had been previously frozen for comparison with results for unfrozen samples. From these data estimates of pore size distribution could be made. No significant difference was observed for samples compacted to 80 percent relative density. Small differences, attributable to either real pore size differences or to sample seating in the test cell, were observed for samples at 50 percent relative density.

It seems, therefore, that freezing may cause fabric changes for samples at low relative densities, although preliminary results by Walberg (1977) indicate that freezing may not influence cyclic triaxial results.

It should be noted further that as the sand at Niigata was sampled prior to freezing rather than frozen in-situ prior to sampling (coring would be required), the observed fabric may differ from the actual fabric in the ground.

III. SAMPLE PREPARATION

Introduction

The frozen Osterberg samples as received at the laboratory were 2.8 inches (71 mm) in diameter and approximately 7 inches (178 mm) in length. The top portion of each sample was used for the preparation of thin-sections, as well as sections for X radiographs, while the bottom portion was used in measuring the relationship between water content and soil-water suction. Thin-section and X radiograph section preparation necessitated resin impregnation of dried samples, while the dimensions of the "Tempe-Cell" soil suction device dictated that the samples be cut and trimmed prior to testing. In an effort to preserve the fabric, samples were trimmed while frozen.

Sample Cutting

To obtain portions of the samples for both resin impregnation and frozen trimming, the sample tubes were cut with a pipe cutter into two sections of approximately 5 and 2 inches (127 and 50 mm) in length. Once the tubes were cut, a fine toothed hacksaw was used to cut the sample itself. The entire cutting operation could be performed in a few minutes. In each case, visual inspection indicated that no significant thawing of the sample had occurred outside the immediate cutting zone.

Sample Thawing

The portion of the sample to be impregnated was fitted with a specially fabricated base cap equipped with a threaded drainage port and wire mesh filter. The sample tube was placed vertically, and the sample height was measured at different points to the nearest .01 in. (0.25 mm).

The sample was allowed to thaw and drain freely overnight. No measurable change in sample height was observed as a result of thawing. It was noted, however, that on the order of 0.5-1.0 ml. of water had flowed out of the drainage port during thawing. This outflow may be traced to two possible sources: 1) atmospheric condensation on the cold sample and sample tube, 2) additional drainage from the sample which could be attributable to incomplete drainage before freezing, to a change in the pore size distribution during freezing, handling or thawing, and/or to a reduction in the water adsorption tendencies of the sand grains.

Resin Impregnation

After thawing, the moist samples were dried in a forced air oven at 60°C. Warm air was drawn slowly through the sample by connecting the base cap to a vacuum of about 1 psi and allowing warm air to enter through the top. The samples were allowed to dry in this manner for 8 hours or more.

The sample to be resin impregnated was then cooled, fitted with a plexiglas cap and subjected to a vacuum of 5 psi. Koppers polyester resin No. 1086-4, mixed with 24 percent (by volume) styrene (Koppers No. VM-901) to reduce viscosity and 1 percent (by volume) organic peroxide (Witco Chemical HI-Point-180) as catalyst, was introduced at the bottom of the sample. After saturation the sample was left undisturbed until initial set of the resin had occurred. The sample was then placed in a forced air oven at 60°C for 24 hours to permit the resin to cure.

After curing, the samples were removed from the oven and allowed to cool. The sample tubes were cut longitudinally with a bandsaw and the impregnated samples extruded.

Thin Sections

Three thin sections were cut from the central portions of the impregnated samples at orthogonal orientations as shown in Fig. 4. By determining grain and contact orientations in each of these thin sections, their distributions in all directions within the sample could be determined.

Petrographic thin sections, about 60 μm thick, 20 mm wide, and 30 mm long, were prepared using standard methods.

X-Radiograph Sections

The portions of the resin impregnated samples remaining after thin section preparation, were used for X-radiograph inspection. The largest remaining pieces of each sample were selected, and horizontal as well as vertical sections about 0.2 inch (5 mm) thick were cut by means of a circular, water cooled, rock saw. Sawing was completed in stages to prevent melting of the resin. As horizontal orientations of the samples were not determined, the orientations of the vertical sections were selected to provide maximum dimensions for each section.

Trimming of Frozen Samples

The portion of the sample to be used in the pore size distribution study was trimmed, while frozen, to the required dimensions. The sample tube was cut lengthwise with a band saw. The heat generated in this procedure produced a thawed zone in the vicinity of the cut. The sample was returned to the freezer and care was taken to note the extent of thawing to avoid the subsequent use of disturbed portions of the sample.

The frozen sample was trimmed to the dimensions indicated in Fig. 5 with the aid of teflon coated aluminum templates. A hacksaw blade was used to cut the sample into a disk and, with the templates as a guide, metal

files were used to trim the sample to size. The trimming procedure was performed in short stages and the sample was returned to the freezer for at least one hour between each stage.

After trimming, the dimensions and weights of the frozen samples were recorded.

IV. SAND PROPERTIES

Introduction

The Niigata sand is a fine to medium sand composed primarily of angular to subangular quartz particles. The Shinano River, Fig. 1, has meandered over the site, with alternate cycles of scour and deposition of silt and sand. At both the River and Road sites, the sand at depths greater than 4 m consists of fluvial river deposits. The sand from 1.0 to 4.0 m depth at the River site and 1.5 to 4.0 m depth at the Road site was dumped through water and not subsequently densified. Uncompacted fill was placed above to the present ground surface.

The sample properties which were quantitatively examined in this fabric study included void ratio, grain size distribution and particle axial ratio distribution. Portions of each sample which were disturbed or thawed during cutting and trimming were retained for grain size and axial ratio measurements. The weights and dimensions of thawed, dried samples were used in conjunction with specific gravity values obtained by Silver and Ishihara (1977) to calculate void ratios.

Grain Size Distributions

Grain size distributions were obtained by dry sieving the oven-dried portions of the sample retained after cutting and trimming. Grain size distributions of the River site samples are presented in Fig. 6. Grain size distributions of the Road site samples appear in Fig. 7. The samples from both sites are seen to fall into the medium to fine sand size range.

The mean particle size, D_{50}, and the uniformity coefficient, D_{60}/D_{10}, are plotted for each site as functions of depth in Fig. 8. Results obtained by Silver and Ishihara (1977) are also plotted for comparison.

The mean particle size of the River site samples exhibits a uniform increase with depth. Values of D_{50} obtained from Road site samples are slightly lower and more variable than those of the River site samples. The mean particle sizes measured by Silver and Ishihara (1977) are seen to agree closely with the values obtained in the present study. The uniformity coefficients of the Road site samples are slightly lower than those of the River site samples. All other factors being equal, the lower values of mean particle size and coefficient of uniformity for the sand at the Road site would suggest a greater susceptibility to liquefaction. Even for a given input ground motion, all things would not be equal, however, as the water table is almost 2 m deeper at the Road site than at the River site.

The uniformity coefficients calculated by Silver and Ishihara (1977), Fig. 8, are consistently lower than the values measured in this study. It should be noted that the grain size distributions presented by them were determined using Japanese standards. This discrepancy in measured uniformity coefficient may therefore result from differences in sieving technique, from the use of different definitions of uniformity coefficient or from genuine differences between the samples studied.

Axial ratio, AR, as discussed by Oda (1976) is an index of particle shape which is calculated by dividing the shortest dimension (L_s) of a projected particle image by the length (L_l) of a rectangle tangent to the particle image outline, as illustrated in Fig. 9. Thus, axial ratio is seen to be the inverse of the particle length/width ratio, L/W, employed in earlier studies by Mahmood (1973) and Mitchell et al. (1976). Axial ratio was selected as a particle shape index for use in this study, as the value which AR can assume is limited to the range $0 < AR \leq 1$. When the axial ratio approaches unity, the projected particle image is close to circular. The

value of axial ratio may therefore be regarded as indicating a characteristic of particle shape with similar meaning to particle sphericity as discussed by Oda (1976).

The average axial ratio, $\overline{AR}$, is determined by calculating the arithmetic mean of a number (approximately 200) of axial ratio observations. An investigation by Oda and Koishikawa (1977) indicates that statistically significant preferences of particle orientation may be measured in sands which exhibit a value of $\overline{AR}$ less than approximately 0.65.

Histograms of the particle axial ratios of the samples studied are presented in Figs. 10a and b. In all cases, the average axial ratio is less than 0.65, indicating that a statistically significant study of particle orientations is feasible. The average axial ratio distributions for the River and Road site samples are compared in Fig. 11. The River site samples exhibit a slightly wider range of particle axial ratio values and possess a higher average value (.62 vs .59) than the Road site samples.

Sample Void Ratio

Dry unit weight values were determined by measuring the dimensions of the thawed samples which were prepared for resin impregnation. The dried sample was weighed while still in the sample tube, and the weight of the base cap and a calculated weight for the tube (derived from measured tube length) were subtracted. The accuracy of calculating tube weight from measured tube length was determined by applying the procedure to a number of scrap sample tube lengths. It was found that the weight of a five inch (127 mm) length of tubing could be predicted to within .01 lb. (4.54 gm). For a typical sample, this degree of accuracy results in an uncertainty of less than two percent in the computed void ratio.

Void ratios calculated in this manner are presented in Fig. 12, together with additional void ratios measured during the preparation of samples for soil suction testing. Results obtained by Silver and Ishihara (1977) are also shown. The void ratios of samples used in this study are seen to be consistent with the range of values obtained by Silver and Ishihara from Osterberg and Large Diameter samples at similar depths. The data indicate that the in-situ void ratios for the River and Road sites are distributed erratically with depth. Void ratios at the Road site are seen to be generally higher than void ratios at the River site.

Insufficient sample quantities were available to determine maximum and minimum void ratios according to ASTM standard D2049. Limiting void ratios (e_{max}, e_{min}) as presented by Silver and Ishihara (1977) were therefore used to calculate the relative density of the samples studied. The calculated values are subject to a degree of uncertainty since the Japanese procedure used to measure e_{min} produces samples with a higher maximum density than is attainable using the more usual ASTM procedure. An additional uncertainty in the calculated relative density values arises from the fact that natural sample variation may cause the limiting void ratios as determined by Silver and Ishihara to differ from the limiting void ratios appropriate for the fabric study samples.

Relative densities for the two profiles are presented as functions of depth in Fig. 13. Results obtained by Silver and Ishihara (1977) from Osterberg and Large Diameter samples are also shown. The values obtained from the fabric study samples are seen to be consistent with the range of values obtained by Silver and Ishihara. The data indicate that the in-situ relative density values are low at both sites, typically ranging from 20 to

60 percent.* Relative densities of River site samples measured in this study are seen to be slightly larger than those of the Road site samples. However, the wide range of D_r measured by Silver and Ishihara indicates that sample density is too variable to warrant the drawing of definite conclusions from the values obtained from the samples used in this study.

---

*Were the ASTM standard procedure used to determine the maximum density, a larger value of e_{min} would have been obtained, resulting in somewhat greater values of relative density.

V. FABRIC ANALYSIS

Introduction

Fabric elements studied were the three-dimensional distributions of normals to interparticle contact planes, the orientations of apparent particle long axes in the plane of the thin section, and the distribution of pore sizes as inferred from the measurement of soil suction-water content relationships. Other fabric elements such as void variability within samples, particle clustering and particle size segregation were not examined quantitatively.

Universal Stage Microscope

A microscope equipped with a universal stage was used to determine particle and contact orientations. The universal stage, shown schematically in Fig. 14, allows independent rotation of the thin section about three orthogonal reference axes. The thin section is coated with an oil possessing the appropriate index of refraction, and covered by the upper glass hemisphere (H in Fig. 14) set in the metal mount, M. The thin section is aligned and moved with the aid of the sledge R which moves horizontally in a slot cut in the hemisphere mount. Rotation can be made about the NS, EW, and vertical axes, and the amount of rotation is measured on the appropriate vernier.

The use of the universal stage microscope is described in detail by Turner and Weiss (1963).

Sampling Methods

Selection of particles for the study of long axis orientations and contact plane orientations in a given thin section can be considered as a

two-dimensional sampling problem, because the thickness of the thin section is very small compared to its length and width. Several methods of sampling two-dimensional populations are available (Kellerhals and Bray, 1971; Koch and Link, 1970; Miller and Kahn, 1962; Pincus, 1953):

1. Sample the entire population.

This is the only method that can describe the true orientation of the entire population. This method is impractical for the typically large populations of the thin sections used in this study.

2. Grid sampling.

A grid is established over the sample and only those grains or contacts immediately below the grid points are counted. A variation of this method is to assign a number to each grid block and to count the entire populations within randomly selected grid blocks.

3. Transect sampling.

Every member of the population that falls under a straight line or narrow strip across the sample is counted.

4. Pseudo-random sampling.

Arbitrarily chosen members of the parent population are measured. This is most susceptible to sampling bias.

The transect sampling method was used in this investigation, because (1) the population was too large to sample in its entirety, (2) no grid attachment was available for the microscope and (3) it was necessary to avoid sampling bias. Traverses about eight or nine grains wide and about one inch long were chosen parallel to the long axis of the thin sections. Every grain or contact within these zones was counted until a statistically

significant number of observations had been recorded as discussed in more detail later in this report.

Apparent Longest Axis Orientations

The orientation of a particle is represented by the inclination of its true long or short axis with respect to fixed reference axes. In practice the true orientation of small particles is estimated by analyzing the orientation of apparent longest axes as seen in thin sections. The three-dimensional orientations of grains can estimated from the orientations observed in sections cut in different directions.

In this study the orientations of apparent longest axes were determined in two vertical and one horizontal section for each sample. Orientations were determined for about 200 grains in each thin section. For the vertical sections, the orientation angle θ_i is defined as the angle between the apparent longest particle axis and the reference axis parallel to the vertical direction. For the horizontal thin sections, θ_i is defined as the angle between the apparent longest axis of a particle and the arbitrarily designated X axis. All measurements are therefore made in the range $0° \leq \theta_i \leq 180°$, with $\theta = 0°$, 180° corresponding to particle axes parallel to the relevant reference axis.

Statistical analyses of the long axis orientation data were performed using a vector method and test of significance presented by Curry (1956). According to this method each long axis observation is considered to be a vector of unit magnitude in the measured direction. No distinction is made between one end of the particle and the other. All measurements are therefore made in the range $0° \leq \theta \leq 180°$.

A resultant vector which is calculated from these unit observation vectors may not reflect the true central tendency of the distribution. If

the 180° range lies in an eastern semi-circle, the distribution has no west components at all. North components would tend to cancel south components so the resultant vector would always possess a strong easterly tendency even if the true central tendency lay close to the north-south direction. To remedy this bias the angles of the observation vectors are doubled before computing a resultant vector. The calculations used to determine the components of the resultant vector are as follows:

$$\text{N-S component} = \Sigma n_i \cos(2\theta_i) \tag{1}$$

$$\text{E-W component} = \Sigma n_i \sin(2\theta_i) \tag{2}$$

where: n_i = number of observations oriented at θ_i

θ_i = angle between particle long axis and the N-S direction.

The orientation, $\overline{\theta}$, and the length, r, of the resultant vector may be calculated:

$$\tan(2\overline{\theta}) = \frac{\Sigma n_i \sin 2\theta_i}{\Sigma n_i \cos 2\theta_i} \tag{3}$$

$$r = \sqrt{(\Sigma n_i \sin 2\theta_i)^2 + (\Sigma n_i \cos 2\theta_i)^2} \tag{4}$$

The vector magnitude, L, is defined as follows:

$$L = \frac{r}{\Sigma n_i} \times 100\% \tag{5}$$

The vector magnitude may vary from 0 to 100 percent. A perfectly uniform distribution of orientations will yield a resultant vector magnitude of 0 percent. A vector magnitude of 100 percent indicates that all orientations are exactly the same or, in the case of grouped data, all orientations lie within the same class interval. According to Curry (1956),

L is a sensitive measure of data dispersion and is comparable to standard deviation with the advantage of being independent of the choice of reference axes.

The vector magnitude, L, may also be adapted for use in the Rayleigh test of significance as discussed by Curry (1956). Rayleigh's equation is:

$$p = e^{-r^2/n} \tag{6}$$

where: p = probability of obtaining a greater vector magnitude as the result of pure chance combinations of random orientations.

r = length of resultant vector

n = total number of observations

e = base of natural logarithms.

The length of the resultant vector may be expressed in terms of the vector magnitude:

$$r = \frac{Ln}{100} \tag{7}$$

Rayleigh's equation may thus be rewritten by substituting for r:

$$p = e^{(-L^2 n \times 10^{-4})} \tag{8}$$

Any level of significance, p, may be employed. In practice the 0.05 level is commonly used for the study of sand grain orientations. A value of 0.05 for p signifies that there are only 5 chances in 100 that the calculated vector magnitude is due to chance.

A previous study performed by Mitchell et al, (1976) showed that a sample size of approximately 200 orientation observations per thin section can be expected to result in a value of p less than 0.05. The procedure used in this study was first to measure and tabulate the orientations of 200

particles per thin section. The values of L, $\overline{\theta}$ and p were then calculated. If the significance level was less than 0.95 (i.e. $p > 0.05$) additional observations were made until the calculated value of p was found to be less than or equal to 0.05.

It should be noted that a truly uniform distribution of long axis orientations does not lend itself to this method of analysis. The relationship expressed in Equation 8 implies that the low values of L which would result from sampling such a uniform distribution would yield large values for p, even if an infinitely large number of observations were tabulated. As nearly uniform distributions are seldom encountered in practice, the Rayleigh test of significance remains a viable tool for use in sand fabric studies.

Interparticle Contact Orientations

The orientation of any interparticle contact can be represented by the normals, N_i^1, N_i^2, to the tangent plane, as shown in Fig. 15. A method for analyzing the orientation of contact plane normals, developed by Oda (1972), was used in this investigation.

It is convenient to express vector orientations in terms of spherical coordinates. Spherical and Cartesian coordinates are related as follows:

$$x = r \sin\beta \cos\alpha \tag{9a}$$

$$y = r \sin\beta \sin\alpha \tag{9b}$$

$$z = r \cos\beta \tag{9c}$$

where r is the vector length and the angles α and β describe vector direction as shown in Fig. 15.

An element dA of the surface area of a sphere is given by:

$$dA_{\alpha,\beta} = rd\beta \cdot r\sin\beta d\alpha = r^2 \sin\beta \, d\alpha d\beta \tag{10}$$

for a sphere of unit radius:

$$dA_{\alpha,\beta} = \sin\beta \, d\alpha d\beta \tag{11}$$

Integration yields a value for the entire surface area, A:

$$A = \int_{\alpha} \int_{\beta} \sin\beta \, d\alpha d\beta \tag{12}$$

Consider M contacts within an assemblage of granular particles. At each interparticle contact there are two contact surfaces, one belonging to each grain. Normal directions N_i^1 and N_i^2 in Fig. 15 are perpendicular to the tangent plane at the contact point. The direction of N_i^2 is described by angles α and β; whereas, the direction of N_i^1 is described by the angles $\alpha + \pi$ and $\pi - \beta$.

The distribution of interparticle contact normals can be shown by plotting their piercing points on a sphere or its graphical equivalent, the equal area stereonet discussed by Turner and Weiss (1963). The total number of plotted points is 2M, twice the number of contacts.

The total number of contact normals within the angular ranges $\alpha + d\alpha$ and $\beta + d\beta$ is:

$$2M \, E(\alpha,\beta) \, \sin\beta \, d\alpha d\beta \tag{13}$$

where $E(\alpha,\beta)$ is the probability density of points of contact within the angular intervals, a function of both α and β. All plotted points will be included if Equation (13) is integrated over the intervals of $\alpha = 0°$ to $360°$ and $\beta = 0°$ to $180°$. Thus $E(\alpha,\beta)$ must satisfy the following equality:

$$\int_{\alpha} \int_{\beta} E(\alpha,\beta) \, \sin \, d\alpha d\beta = 1 \tag{14}$$

In the present investigation absolute values of α are not known, since horizontal orientations were not marked on the Osterberg samples. Quantitative comparisons between samples have thus been limited to consideration of the distributions of β_i, the angles between contact normals and the vertical direction. To eliminate the dependance of $E(\alpha,\beta)$ on α, $E(\alpha,\beta)$ may be summed across all values of α. Thus Equation 14 becomes:

$$2\pi \int_{\beta} E(\beta)\ \sin\beta d\beta = 1 \tag{15}$$

Since the vectors N_i^1 and N_i^2 are colinear $E(\beta)$ equals $E(\pi-\beta)$. For example, the probability density in the region $\beta = 0°$ to $\beta = 10°$ is the same as in the region $\beta = 180°$ to $\beta = 170°$. As a result only the vector orientations in one hemisphere need be measured and plotted and the results doubled to obtain the density distribution over the entire sphere. Thus Equation 15 becomes

$$2\left[2\pi \int_{0°}^{90°} E(\beta)\ \sin\beta d\beta\right] = 1 \tag{16}$$

or

$$M = 4\pi M\left[\int_{0°}^{10°} E(\beta)\ \sin\beta d\beta + \ldots\ldots + \int_{80°}^{90°} E(\beta)\ \sin\beta d\beta\right] \tag{17}$$

If M_1 is the total number of normals in the range = 0° to = 10°, then:

$$M_1 = 4\pi M \int_{0°}^{10°} E(\beta)\ \sin\beta d\beta \tag{18}$$

Integration gives the mean value of $E_1(\beta)$ within the range $0° \leq \beta \leq 10°$:

$$E_1(\beta) = \frac{M_1}{4\pi M(\cos 0° - \cos 10°)} \tag{19}$$

Mean values of $E(\beta)$ for other intervals are calculated in a similar manner.

For an isotropic fabric $E_i(\beta)$ = constant = $1/4\pi$. Values of $E_i(\beta) > 1/4\pi$ mean a greater than average proportion of contact normals at an inclination of β_i. A value of $E_i(\beta) < 1/4\pi$ indicates a less than average proportion of contact normals at inclination β_i.

Pore Size Measurements

The nature of pore spaces, as discussed by Mitchell (1976), is an important element of soil fabric. A relatively simple approach to the approximation of pore sizes in intact samples is to measure the equilibrium water content at various values of negative pore water pressure (soil suction). The principle of capillary rise provides the basis for inferring pore size distribution from measured values of water content and soil suction.

Consider a glass capillary tube of radius, R, as illustrated in Fig. 16: The attraction between the glass and the water molecules combined with the surface tension of the water pulls the water up into the tube to a height, h_c, above the outside water level. The height, h_c, is known as the "height of capillary rise". The upper surface or meniscus of the water assumes a concave shape which joins the walls of the tube at an angle, α, known as the "contact angle". The value of α depends upon the material that constitutes the capillary wall and on the type of impurities that cover it. For quartz tubes with chemically clean or wetted walls, α is equal to 0°.

If σ denotes the surface tension of water and γ_w denotes the unit weight of water, equilibrium requires that

$$h_c \pi R^2 \gamma_w = 2\pi R \sigma \cos\alpha \qquad (20)$$

whence

$$h_c = \frac{2\sigma}{R\gamma_w} \cos\alpha \qquad (21)$$

Substituting the values γ_w = 1 gm/cc, α = 0° (reasonable for water in contact with quartz) and σ = 0.075 gm/cm, Equation (21) may be rewritten as follows:

$$h_c(\text{cm}) = \frac{0.15}{R\,(\text{cm})} \qquad (22)$$

If soil voids are assumed to behave as a large number of interconnecting simple capillary tubes, Equation (22) may be used to calculate an effective or average pore radius, R, which will support a capillary rise of magnitude h_c. A capillary rise of magnitude h_c corresponds to a maximum negative pore pressure or soil suction of magnitude $h_c \cdot \gamma_w$. Thus if a negative pore pressure of magnitude $h_c \cdot \gamma_w$ is applied to a sample and a certain volume of water remains in the sample at equilibrium, it can be inferred by using Equation (22) that a certain volume of pores exists within the sample with an effective radius less than or equal to R. If a series of water content measurements are obtained at different values of soil suction, the relative volumes of pore spaces with different maximum effective radii may be estimated.

In practice, the accuracy of this method is limited by the nature of the interconnecting pore drainage paths. As illustrated in Figure 17, a large void which is isolated by small pores will remain saturated until sufficient soil suction is applied to draw the meniscus through the smaller pores. The resulting outflow of water will be attributed to a volume of small pores.

A Soiltest A-98 Tempe Pressure cell was used in this study to apply accurately controlled increments of soil suction and to measure the resulting flow of water into and out of each sample. The equilibrium water content for each level of soil suction was back calculated from the initial water content and measured flow quantities.

VI. APPARENT LONG AXIS ORIENTATIONS

The distributions of apparent long axis orientations, as well as the direction, $\overline{\theta}$, and magnitude, L, of the resultant vectors were determined using the procedures previously described. The longitudinal axis (vertical axis) of the original cylindrical sample was used as the reference axis for the vertical sections. An arbitrarily chosen "X" axis was used as the reference axis for horizontal samples. Long axis orientations are expressed in terms of θ, the angle between the reference axis and the observed particle long axis. Thus, for a vertical section, a value of $\theta = 0°, 180°$ means that the particles are oriented in a vertical direction; while a value of $\theta = 90°, 270°$ indicates a horizontal orientation.

The calculated values of mean vector orientation and vector magnitude are summarized in Table 2. Frequency histograms based on 10° azimuth class intervals were prepared from the data on each thin section. The frequency histograms for each sample are reproduced in Figs. 18 through 28.

Long Axis Orientations of Particles in Horizontal Thin Sections

Resultant vector orientations, $\overline{\theta}$, obtained from the horizontal thin sections are seen to exhibit a wide degree of variation. A complete interpretation of these values is not possible since horizontal orientations of the Osterberg samples at the site were not recorded at the time of sampling.

The resultant vector magnitude, L, however, is independent of the choice of reference axes, so a comparison of different vector magnitudes can provide information concerning the relative intensity of horizontal particle orientation. Resultant vector magnitudes obtained from horizontal sections are presented in Fig. 29 as functions of depth. The magnitudes of resultant vectors obtained from the River site are seen to exhibit a general increase

with depth, ranging from values of approximately 10% at a depth of 4.5 m. to approximately 18% at a depth of 13 m. Resultant vector magnitudes obtained from the Road site exhibit a similar increase with depth, but the intensities of horizontal particle orientation are seen to be slightly less than those observed in the River site samples.

Although the intensity of particle orientation in a horizontal plane has not yet been found to be of major significance to liquefaction behavior, the lower L values exhibited by the Road site are in agreement with results obtained by Mitchell et al. (1976) which show that a more random distribution of long axis orientation will produce higher values of cyclic strength in compacted laboratory samples.

Long Axis Orientations of Particles in Vertical Thin Sections

Although direct comparisons of $\overline{\theta}$ values observed in the vertical thin sections are ambiguous in the absence of fixed horizontal axes, a qualitative approach may be taken to evaluate the average inclinations of particle long axes to the vertical axis. It is evident that preferred orientation of particles in the vertical direction will be reflected in low values of $\overline{\theta}$ as observed in both ZX and ZY thin sections. The average value of $\overline{\theta}$ observed in the two vertical thin sections may thus provide a qualitative indication of this preferred orientation. The values of $\overline{\theta}$ observed in the ZX and ZY thin sections of each sample are presented as functions of depth in Fig. 30. In the estimated zone of liquefaction, the average values of $\overline{\theta}$ from the Road site samples are lower than those of the River site samples. Cyclic triaxial strength values obtained by Silver and Ishihara (1977) are presented in Fig. 31 as functions of depth. A comparison of the particle orientations in Fig. 30 with the strength values presented in Fig. 31 shows that the higher cyclic strength of the Road site samples for depths less than 9 m

may be associated with a smaller average inclination of particle long axes to the vertical.

In the absence of known horizontal reference axes, a quantitative comparison of vector magnitude (L) values in different vertical thin sections is not possible. To illustrate this fact, a schematic illustration of a two grain sand sample is presented in Fig. 32. As shown in the figure, a thin section of the sample prepared in the ZX plane will exhibit a vector magnitude which differs from the vector magnitude observed in the thin section prepared in the ZY plane. Nonetheless, the average value observed in the ZX and ZY thin sections may be used as a qualitative index of the intensity of particle orientation. L values from vertical thin sections are presented as functions of depth in Fig. 33. The Road site samples are seen to exhibit higher L values than the River site samples implying that particles in the Road site samples are more strongly oriented. Furthermore, the variation of average L values with depth is seen to be similar at the two sites.

These results would appear to be contrary to the results reported by Mitchell et al. (1976) which showed that, for a given relative density, a more random particle orientation (lower L) produced higher strength under cyclic triaxial loading. However, in the previous study the conclusion was drawn from tests in which the preferred direction of long axis orientations was in a direction normal to the direction of the applied cyclic deviator stress. The results of the present study suggest that the greater the intensity of preferred long axis orientation in a direction parallel to the applied cyclic deviator stress, the greater the resistance to liquefaction. Thus, the results of the two studies may not be inconsistent with each other, but reflect the importance of stress direction relative

to orientation direction in determining resistance to cyclic loading.

The values of vector magnitude (L), for long axis orientations in the vertical thin sections (Fig. 33) are predominantly in the range of 10 to 20 percent. Recalling that the average axial ratio ($\overline{AR}$) for the Niigata sand is about 0.6, reference to Oda (1976) shows that values in this range are characteristic of samples prepared by up and down vibrations. Samples prepared by pouring, however, give vector magnitudes considerably larger, of the order of 35 to 40 percent.

VII. INTERPARTICLE CONTACT ORIENTATIONS

Interparticle contact orientations, expressed in terms of the normal to the interparticle contact plane, were measured in each thin section and plotted on equal area stereonets according to the procedure presented by Turner and Weiss (1963). The density function, $E(\beta)$, was calculated according to the procedure outlined in Section V of this report.

The equal area stereonets are presented in Figs. 34 through 44. On these diagrams blank areas indicate contact normal directions within which less than one percent of the normals intersect one percent of the surface area of a sphere containing all possible directions. Light stippled areas enclose regions containing 1 to 2 percent of the contact normals per one percent of the area of the circumscribing sphere. The heavily stippled areas indicate more than 2 percent of the normals per one percent of the sphere surface. Thus the darker the area on the stereonet, the greater the concentration of interparticle contact normals in the directions represented by that area.

It should be noted in viewing these stereonets that because the horizontal orientation of the samples was not known and the selection of X and Y axis directions was arbitrary, the stereonet representing the true in-situ distribution of interparticle contact normals is indeterminate. In any case the pattern would be the same as shown in the figures but "rotated" to the proper position around the Z axis.

When the influence of rotation around the Z axis is considered, it should be remembered that an axis through the center of a sphere intersects the surface of the sphere at two diammetrically opposite points. If the sphere is rotated from east to west, an axis intersection point which

disappears in the west, will immediately have its diametrically opposite point of intersection appearing in the east. The simultaneously disappearing and appearing points of intersection are equidistant from, but on opposite sides, of the equator.

The stereonets in Figs. 34 to 44 were studied by Professor Richard E. Goodman of our Geotechnical Engineering faculty. Professor Goodman is an expert on stereonets and their interpretation. His study was done without prior knowledge of where the samples were from or their groupings from two different sites. His conclusions were that the patterns appear to fall into at least two groups. One of them is represented by samples B1-S1 (Fig. 34), B1-S7 (Fig. 38) and B3-S5 (Fig. 43), where there is approximately orthogonal symmetry with three preferred orientations. All the others, except possibly those for sample B1-S6 (Fig. 37) and sample B3-S2 (Fig. 40) indicate non-orthogonal symmetry with more than three preferred orientations.

An important conclusion that results from the interpretations by Professor Goodman is that the stereonets do not indicate significant difference between the interparticle contact normal orientations for River site (B1 samples) and the Road site (B3 samples).

This lack of significant differences between the distributions of contact normals for samples from the two sites is borne out also by the distribution functions $E(\beta)$ shown in Figs. 45 and 46. The distributions do suggest that the concentration of interparticle contact normals in a near vertical direction (contact planes in a horizontal direction) increases with depth for both sites. Oda (1976) has shown that an increase in the concentration of normals in the maximum principal stress direction is related to an increase in strength of a granular material. This is because contact planes perpendicular to the major stress direction are the most effective to carry that stress.

VIII. SOIL SUCTION-WATER CONTENT RELATIONSHIPS

As described in Section III, portions of the frozen samples were cut, trimmed and allowed to thaw in the Tempe Pressure cell. After a thawing period of 4 hours successive increments of negative pore water pressure (soil suction) ranging from 1 cm. to 900 cm. of water head were induced and the amount of water which flowed from the sample was measured. The first phase of the test, in which increasing values of soil suction were applied, is termed the "drying cycle". The second phase of the test, in which the soil suction was decreased in successive increments, is termed the "wetting cycle." The equilibrium sample water content corresponding to each value of applied soil suction could be calculated from the initial and final sample weights and the amount of water which flowed in or out of the sample.

Sample water contents are plotted against the corresponding soil suction values in Figs. 47 through 57. Initial sample water contents, are seen to fall within the range of 8 to 10 percent for all samples. The results show that most of the water outflow measured during the drying cycles occurred in the soil suction range of 10 to 60 cm. H_2O.

The results for all the River site samples have been averaged and are shown in Fig. 58. An average water content vs. suction curve for the Road site samples is shown in Fig. 59. The behavior of the samples from the two sites is compared in Fig. 60 in terms of degree of saturation vs. soil suction and vs. equivalent pore radius as calculated from equation (22).

It is clear from Fig. 60 that the River site samples had a higher degree of saturation at a given value of soil water suction than did the Road site samples. As the tests followed a drying cycle (increasing suction) followed by a wetting cycle, this implies that a greater proportion of the

void space was made up of small pores in the River site samples than in the Road site samples. A part of this difference may have resulted from the fact that the Road site samples were less dense (average void ratio of 0.91) than the River site samples (average void ratio of 0.84) used for the suction tests.

Nonetheless, the degree of saturation represents the proportion of the void space that is filled with water, and the ordinate values in Fig. 60 can be interpreted as percentage of pores finer than any given size. It is clear that the River site samples contain more small pores than do the Road site samples. This may be a factor in the apparent lower resistance to liquefaction at the River site than at the Road site in spite of the higher void ratio of the Road site samples. A high proportion of small pores means a low hydraulic conductivity. A low hydraulic conductivity means limited ability for pore pressures generated during cyclic loading to dissipate rapidly, and, hence, a potentially more rapid onset of liquefaction.

IX. X-RADIOGRAPHS

As described in Section III, remaining portions of the resin impregnated samples, after thin section preparation, were prepared for X-radiographic inspection. Actual-size, positive X-radiographs of horizontal and vertical sections are shown for samples B1-S3, B1-S4, B1-S5, B1-S6 and B1-S7 (all from the river site) in Fig. 61, while horizontal and vertical sections for samples B3-S1, B3-S2, B3-S4, B3-S5 and B3-S7 (all from the road site) are shown in Fig. 62.

Comparison of Figs. 61 and 62 shows that the samples taken at 9.5 m depth (B1-S5 and B3-S5) appear reasonably similar as far as grain size is concerned. The same holds true for the samples taken at 12.5 m (B1-S7 and B3-S7) depth, while the river site sample taken at 4.5 m (B1-S3) contains larger particles than the road site sample from a similar depth (B3-S1). The larger grains in sample B1-S3, when compared to B3-S1, are not reflected in the grain size distribution curves for these samples (Figs. 6 and 7).

A slightly darker zone can be observed on the circular edges of all horizontal sections. The darker zone is probably caused by densification during sampling of a narrow annulus of soil immediately adjacent to the sampler. The disturbed zone can be seen to be approximately 1/8 to 1/4 inch (3 to 6 mm) thick.

The variation in X-radiograph intensity shown by samples B1-S3, B1-S5, B3-S1 and B3-S5 may be indicative of variations in density of these samples on the scale of the sections. It would not be possible to quantitatively assess these variations by means of relative density measurements, as the latter require relatively large samples.

Similarly a zone of lower density, about 1/8 inch (3 mm) thick, is also shown by the vertical section of sample B1-S4.

Sample B1-S6, from a depth of 11.5 m, was located near the assumed maximum depth of liquefaction (9.0 m). The striations in the vertical section may have been caused by shear displacements.

The cracks shown by light zones in the horizontal sections of samples B3-S1 and B3-S4 are probably not representative of in-situ conditions, and may have been caused by either the sampling or resin impregnation processes, while the darker lines in the horizontal section of sample B3-S4 was caused by sawing as evidenced by inspection of the section surface.

While the X-radiographs provide a reasonably good visual representation of the respective samples, the number and size of samples is insufficient to allow any conclusion regarding the observed different liquefaction behavior at the two sites.

X. SUMMARY AND CONCLUSIONS

The fabric of 11 undisturbed sand samples from Niigata, Japan, obtained using an Osterberg sampler, has been studied using petrographic thin sections and water content-soil water suction measurements. Six samples, from a depth range of 4.5 to 13.5 m, were obtained from a single boring (B1) at a location termed the River site, where the sand is known to have liquefied during the 1964 Niigata earthquake. Five samples from a depth range of 4.5 to 13.5 m were obtained from a single boring (B3) at a location termed the Road site, where no liquefaction was observed during the 1964 earthquake. All samples were frozen after they were taken from the ground prior to shipment to the University of California, Berkeley, Geotechnical Engineering Laboratory for study.

The major findings from this investigation are as follows.

1. The techniques developed for preparation of thin sections for fabric study and for samples for soil water content vs. suction measurements worked well.

2. The gradational and particle shape characteristics of the medium to fine sands at the Road and River sites are similar, although the average particle size, D_{50}, and uniformity coefficient, D_{60}/D_{10}, at the River site are slightly larger than at the Road site. Particle shape, described in terms of the average particle axial ratio ($\overline{AR}$) is quite similar for the two sites; 0.62 for the River site and 0.59 for the Road site, with the River site samples exhibiting a slightly wider range of values.

3. The void ratios of the samples are distributed erratically with depth at both sites; however, the void ratios of the Road site samples are generally higher than those from the River site.

4. Preferred orientation of particle long axes in any known horizontal direction could not be determined owing to the absence of sample orientation information. The intensity of horizontal orientation relative to arbitrary axes was determined, however, in terms of the resultant vector magnitude, L. For samples from the upper 9 m, the presumed zone of liquefaction at the River site, the Road site samples exhibited slightly lower L values (Fig. 29), indicative of more random particle arrangement. This is consistent with the results of a previous study (Mitchell et al., 1976) which indicated that samples with a more random orientation of particles in the horizontal plane were more resistant to liquefaction in cyclic triaxial tests.

5. The mean orientation direction $\overline{\theta}$ of particle long axes in vertical thin sections was closer to the vertical for samples from the upper 9 m from the Road site than for samples from the River site (Fig. 30).

6. The magnitudes of L observed in different vertical thin sections provide qualitative indices of the degree of particle orientations in vertical planes. The Road site samples exhibit a stronger degree of particle long axis orientation in vertical planes than do the River site samples. This finding is shown to be consistent with a higher resistance to liquefaction in cyclic triaxial tests for the Road site samples.

7. The values of vector magnitude L for long axis orientations in the vertical thin sections are characteristic of reconstituted samples of similar sands prepared by up and down vibrations (Oda, 1976) but not of samples prepared by pouring.

8. Analysis of equal area stereonets does not indicate significant differences between the orientations of normals to interparticle contact planes for Road and River site samples. This lack of significant differences in the distributions of interparticle contact normals for samples from the two sites is borne out also by the $E(\beta)$ distribution functions. At both sites, however, the concentration of normals to interparticle contacts in a near vertical direction increases with depth.

9. The River site samples had a higher degree of saturation at a given value of soil water suction than did the Road site samples. These results suggest that the River site samples had a greater volume of small size pores than did the Road site samples. This could be a factor in the lower resistance to liquefaction exhibited by the River site samples.

10. X-radiography of slices of resin-impregnated samples would appear to offer good potential for studying fabric characteristics on a scale of a few mm.

In interpreting these findings it should be noted firstly that the samples were taken from the ground before freezing. Any disturbance that may have occurred during this sampling will be reflected in the measured fabric characteristics. As the magnitude of this disturbance is unknown, there is uncertainty as to whether the observed fabric accurately reflects the true in-situ fabric.

Secondly, the horizontal orientation of the samples was not recorded. Consequently the possible existence of any macroscopic horizontal preferred orientations of particles or particle contacts at the two sites cannot be established.

Thirdly, the River site samples came from a zone which had liquefied during the 1964 earthquake. Thus present difference between the sand fabric characteristics at the two sites cannot be used to explain the original differences in cyclic shear strength and resistance to liquefaction.

Finally, the fact that liquefaction occurred at the River site but not at the Road site during the 1964 Niigata earthquake could be due to causes other than differences in sand fabric or density. Specifically, it is noted that the water table at the Road site is at a depth of 2.5 m, whereas it is at 0.6 m at the River site, a fact that would give a greater resistance to liquefaction, for a given intensity of shaking, at the Road site. Furthermore, whether the intensities of shaking at the two sites were the same is unknown.

Consequently, the results of this study, taken by themselves, cannot be used to establish conclusively the specific role of sand fabric in-situ in determining resistance to liquefaction or the changes in fabric that accompany liquefaction. They do suggest, however, that fabric in-situ is related to susceptibility to liquefaction as borne out by the differences in fabric observed for the two sites and the corresponding differences in cyclic triaxial strength reported by Silver and Ishihara (1977). Furthermore, the fabric relationships observed herein and corresponding cyclic strength behavior reported by Silver and Ishihara appear consistent with previous fabric property correlations reported by Oda (1976) and Mitchell et al. (1976).

Further studies are indicated to evaluate the effect of sampling on fabric, to compare the in-situ fabric of the Niigata sands with that of reconstituted samples of the same sand, and to integrate the results of the present investigation more completely with the results of fabric and liquefaction studies on other sands.

REFERENCES

Curry, J. R. (1956) "The Analysis of Two-Dimensional Orientation Data," Journal of Geology, Vol. 64, pp. 117-131.

Earth Manual (1974) U. S. Department of the Interior, Bureau of Reclamation, Washington, D. C.

Kellerhals, R. and Bray, D. (1971) "Sampling Procedure for Coarse Fluvial Sediments," Journal of the Hydraulics Division, ASCE, August, pp. 1165-1180.

Koch, G. S. and Link, R. F. (1970) Statistical Analysis of Geological Data, John Wiley & Sons, Inc., New York, Vol. 1, 375 p., Vol. 2, 438 p.

Ladd, R. S. (1974) "Specimen Preparation and Liquefaction of Sand," Journal of the Geotechnical Engineering Division, ASCE, Vol. 100, No. GT10.

Mahmood, A. (1973) "Fabric-Mechanical Property Relationships in Fine Granular Soils," Ph.D. Dissertation, Department of Civil Engineering, University of California, Berkeley.

Miller, R. L. and Kahn, J. S. (1962) Statistical Analysis in the Geological Sciences, John Wiley & Sons, Inc., New York, 483 p.

Mitchell, J. K. (1976) Fundamentals of Soil Behavior, John Wiley & Sons, Inc., New York.

Mitchell, J. K., Chatoian, J. M. and Carpenter, G. C. (1976) "The Influence of Sand Fabric on Liquefaction Behavior," Report No. TE 76-1, Geotechnical Engineering, University of California, Berkeley.

Mulilis, J. P., Seed, H. B., Chan, C. K., Mitchell, J. K. and Arulanandan, K. (1977) "Effects of Sample Preparation on Sand Liquefaction," Journal of the Geotechnical Engineering Division, ASCE, Vol. 103, No. GT2, Feb. 1977, pp. 91-108.

Oda, M. (1972a) "Initial Fabrics and their Relationships to Mechanical Properties of Granular Materials," Soils and Foundations, Vol. 12, No. 1, pp. 17-37.

Oda, M. (1972b) "The Mechanism of Fabric Changes During Compressional Deformation of Sand," Soils and Foundations, Vol. 12, No. 2, pp. 1-18.

Oda, M. (1976) "Fabrics and their Effects on the Deformation Behaviors of Sand," Report of Department of Foundation Engineering, Faculty of Engineering, Saitama University, Urawa, Saitama, Japan.

Oda, M. and Koishikawa, I. (1977) "Anisotropic Fabric of Sands," Proceedings of the Ninth International Conference on Soil Mechanics and Foundation Engineering, Vol. I, pp. 235-238, Tokyo, Japan.

Osterberg, J. O. (1952) "New Piston Type Soil Sampler," Engineering News Record, 148, April 24, pp. 77-78.

Pincus, H. J. (1953) "The Analysis of Aggregates of Orientation Data in the Earth Sciences," Journal of Geology, Vol. 61, No. 6, November, pp. 482-509.

Silver, M. L. and Ishihara, K. (1977) "Sampling and Testing of Undisturbed Sands from Niigata, Japan, to Evaluate In-Situ Liquefaction Behavior," Unpublished Report.

Turner, F. J. and Weiss, L. E. (1963) Structural Analysis of Metamorphic Tectonites, McGraw-Hill Book Co., New York, pp. 194-255.

Walberg, F. (1977) "Preliminary Draft - Effect of Freezing on Sands," Missouri River Division, Corps of Engineers.

TABLE 1

FLOWCHART OF RESEARCH ON UNDISTURBED SAMPLING AND TESTING OF SANDS FROM NIIGATA, JAPAN
(Adapted from Silver and Ishihara, 1977)

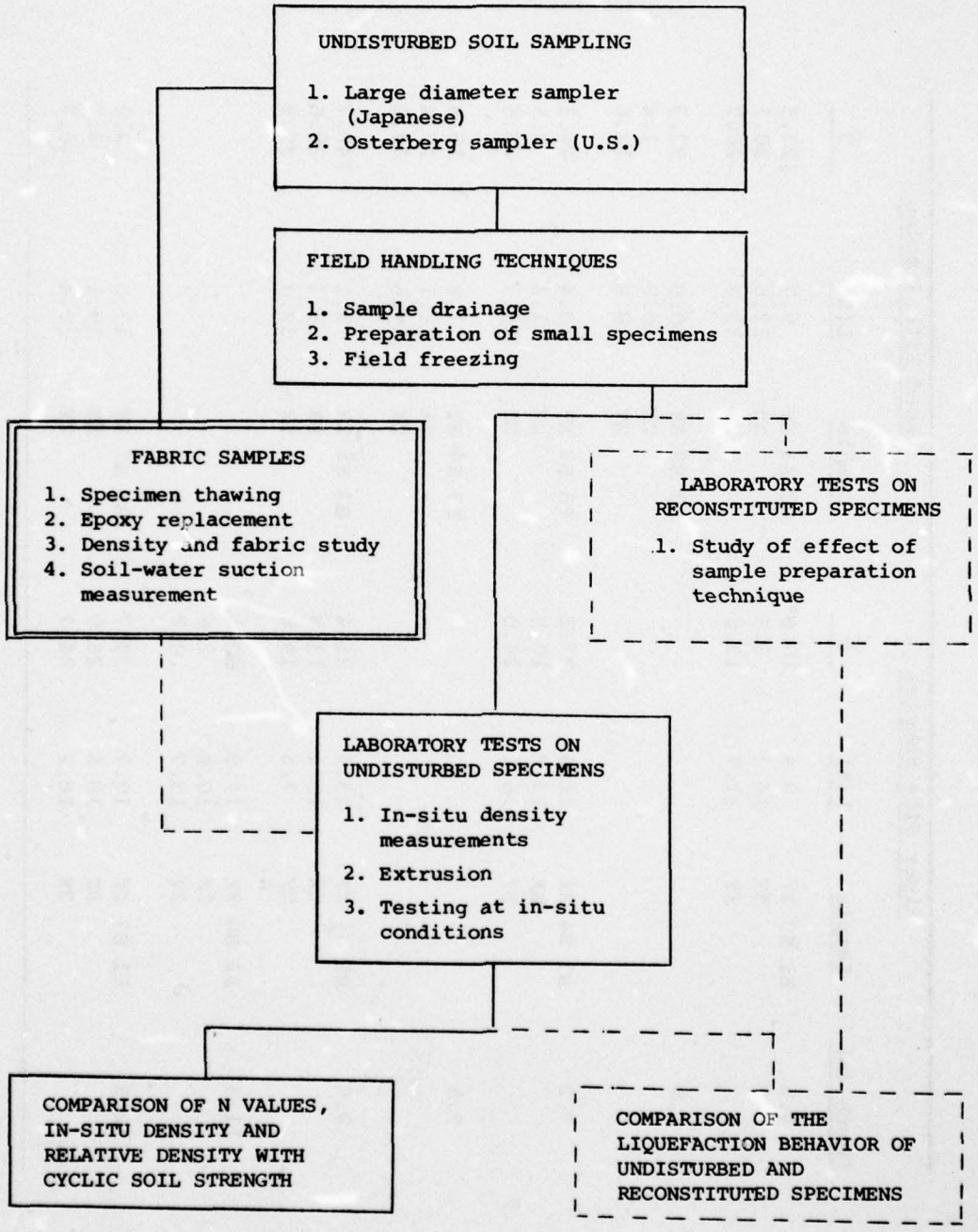

Note: ═══ studies described in this report

– – – – indicates work not yet completed

——— indicates work described by Silver and Ishihara (1977)

Table 2: Summary of Apparent Long Axis Orientation Data

	River Site Samples			Road Site Samples		
Depth (m)	Sample	L(%)	$\bar{\theta}$	Sample	L(%)	$\bar{\theta}$
4.5	B1 S3 XY	9.5	19.6°	B3 S1 XY	9.7	127.5
	ZX	14.3	3.9	ZX	13.5	20.1
	ZY	11.7	13.8	ZY	13.0	26.7
5.5				B3 S2 XY	10.9	92.3
				ZX	16.9	1.4
				ZY	18.8	12.6
7.2	B1 S4 XY	11.6	27.1	B3 S3 XY	10.4	26.1
	ZX	14.3	10.9	ZX	21.6	1.5
	ZY	16.1	24.0	ZY	15.7	23.5
8.5				B3 S4 XY	11.8	16.8
				ZX	11.1	17.4
				ZY	14.6	12.2
9.5	B1 S5 XY	13.9	21.4	B3 S5 XY	9.1	148.7
	ZX	10.1	13.8	ZX	8.7	29.6
	ZY	7.5	19.8	ZY	19.0	39.9
11.5	B1 S6 XY	11.9	80.6			
	ZX	10.9	2.6			
	ZY	13.7	0.7			
12.5	B1 S7 XY	19.7	39.7	B3 S7 XY	17.0	4.0
	ZX	18.5	26.0	ZX	19.1	8.7
	ZY	18.2	24.4	ZY	12.4	16.7

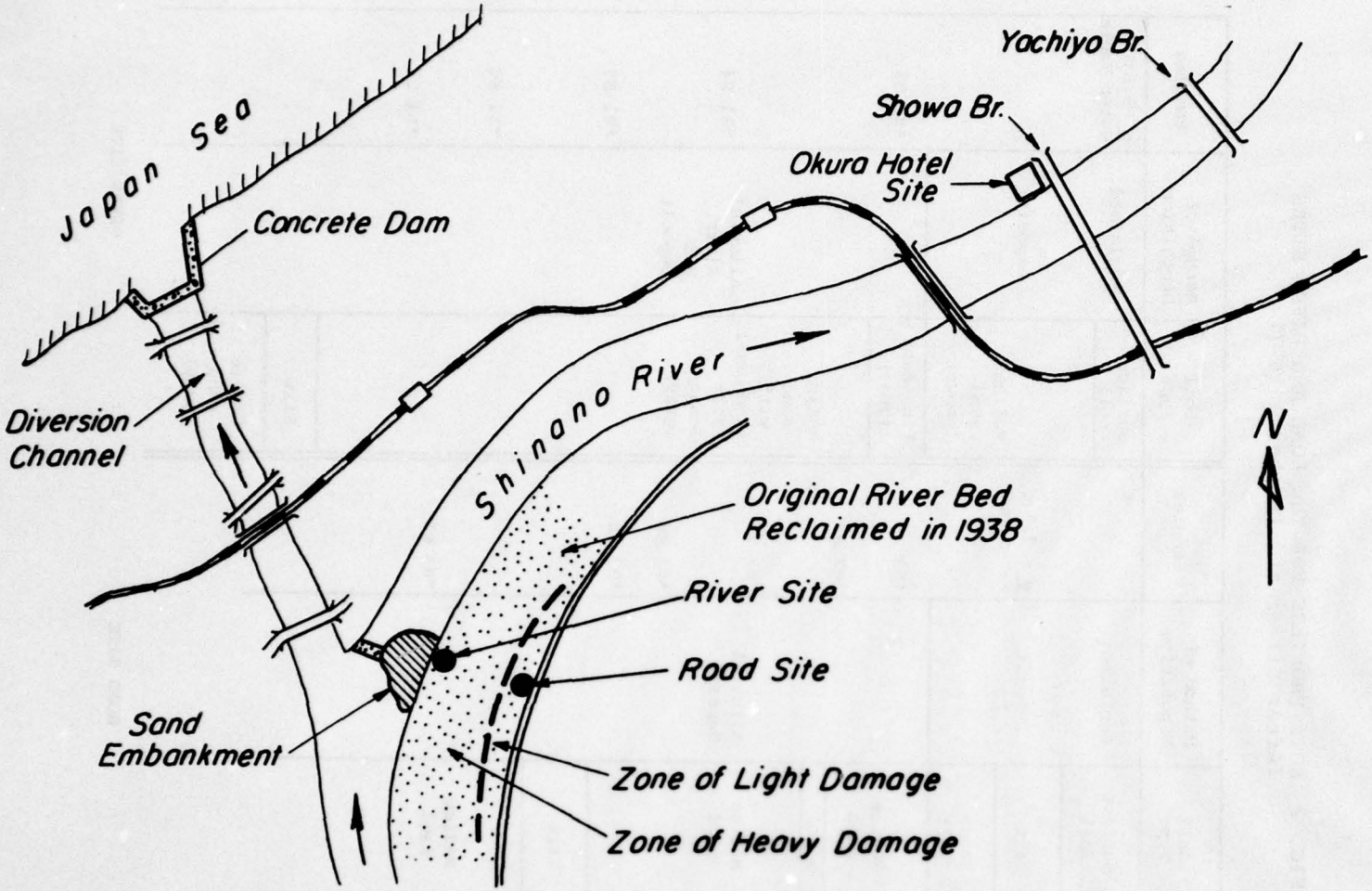

FIG. 1 LOCATIONS OF RIVER AND ROAD SAMPLING SITES IN NIIGATA, JAPAN
(After Silver and Ishihara, 1977)

FIG. 2 SOIL PROFILES FOR THE ROAD AND RIVER SITES
(After Silver and Ishihara, 1977)

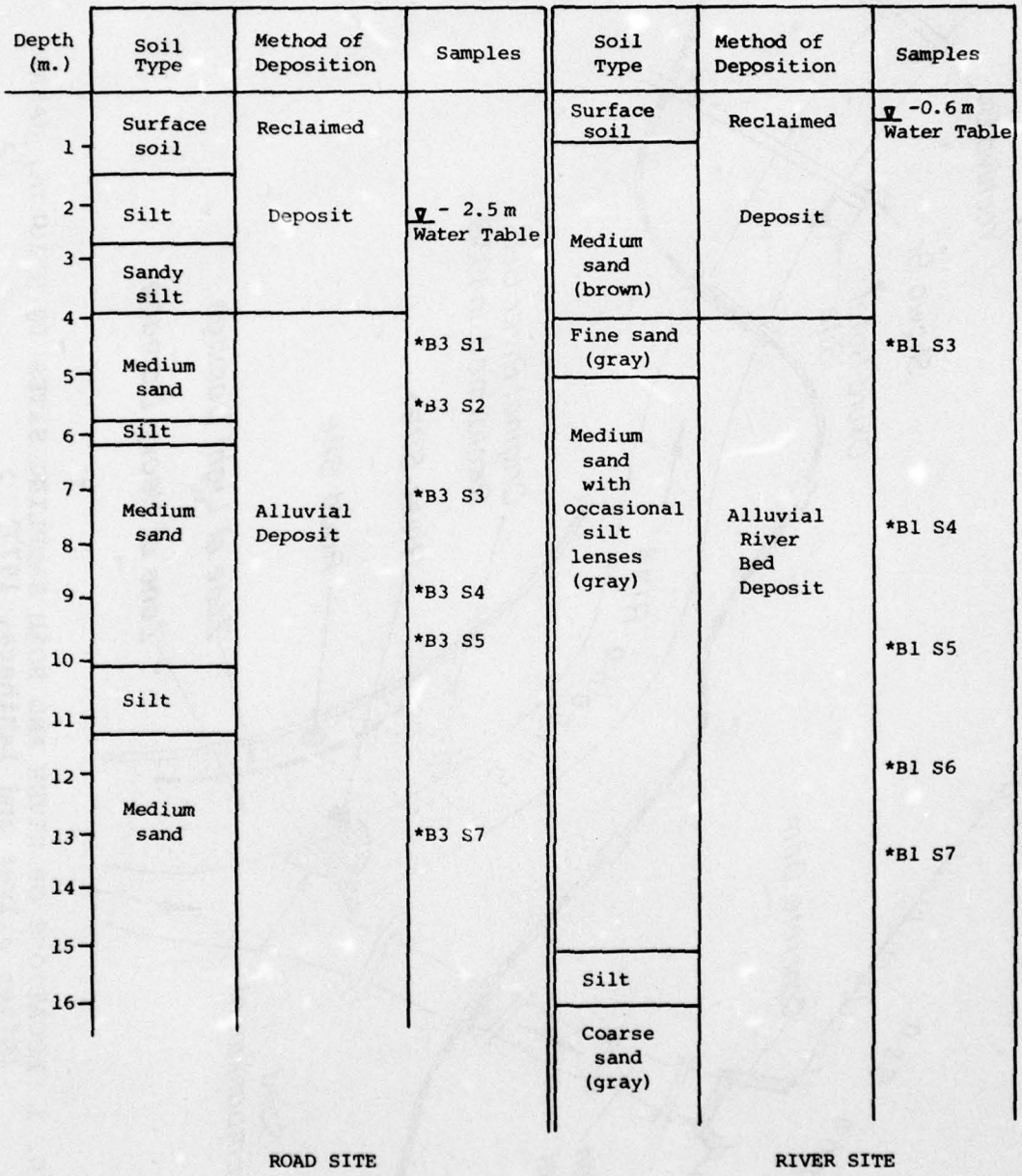

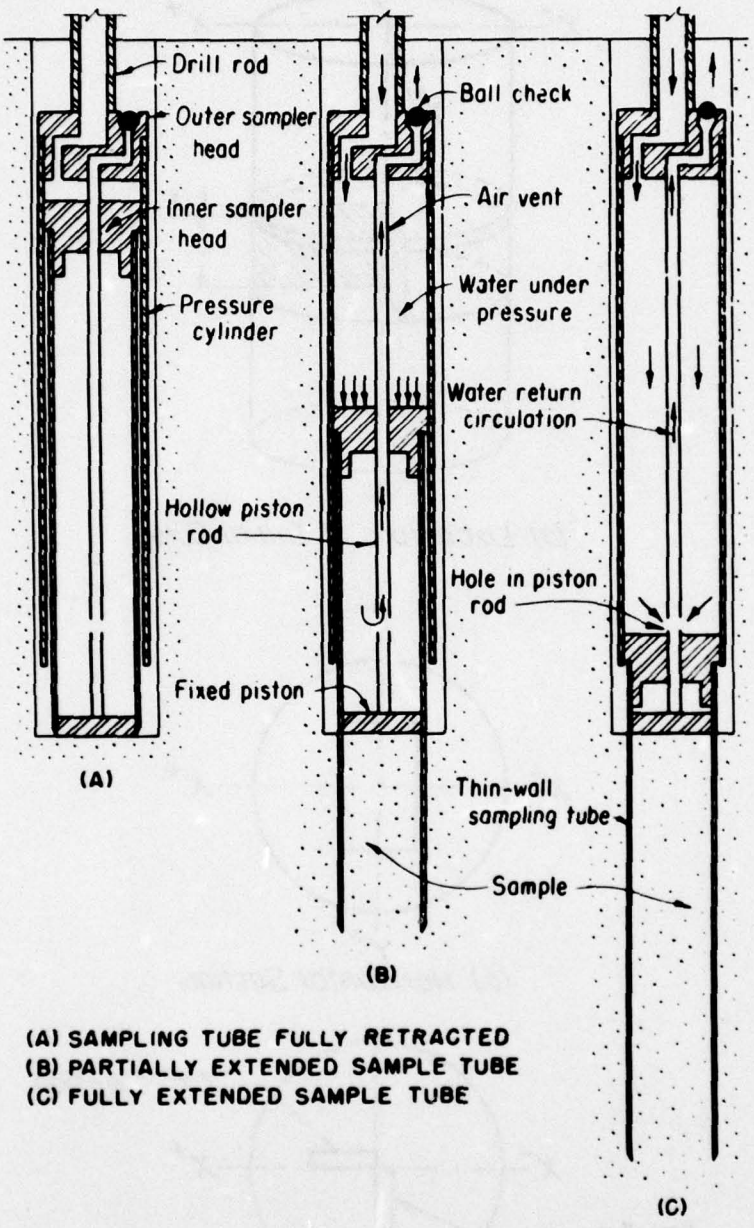

FIG. 3 SCHEMATIC ILLUSTRATION OF OSTERBERG SAMPLER OPERATION
(From U.S.B.R. Earth Manual, 1974)

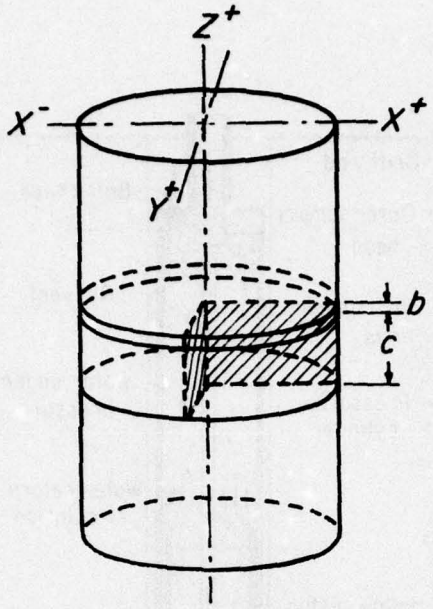

(a) Locations of Initial Cuts

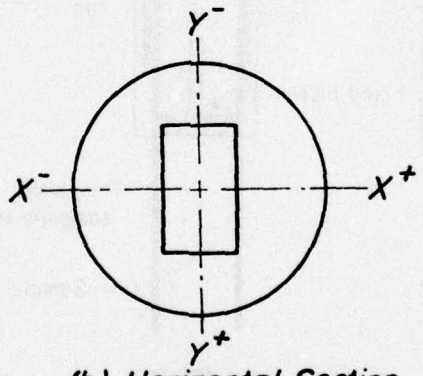

(b) Horizontal Section

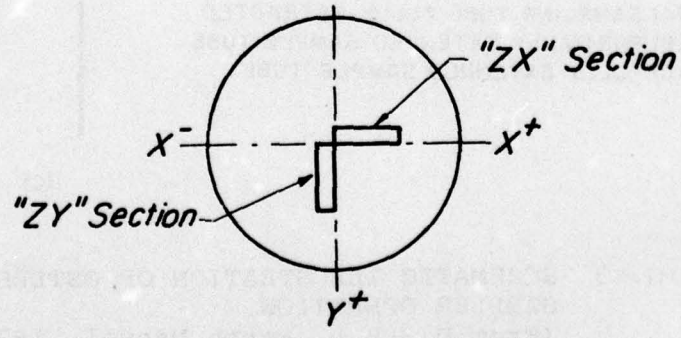

(c) Vertical Sections

FIG. 4 THIN SECTION LOCATIONS FROM WITHIN RESIN-IMPREGNATED SAMPLES

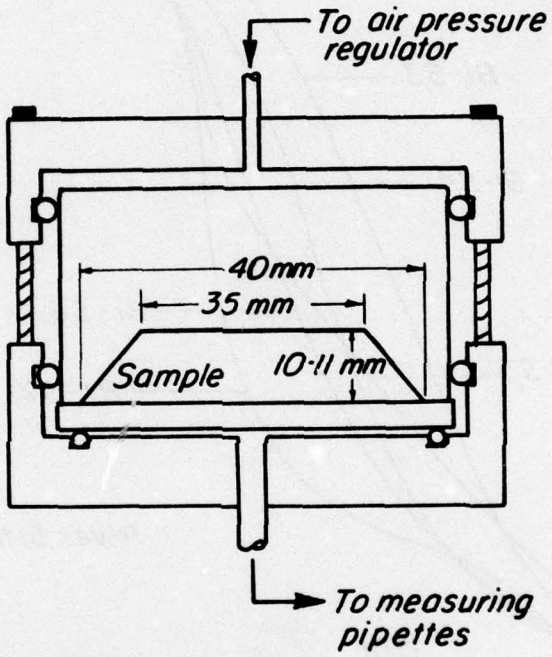

FIG. 5 SOILTEST TEMPE PRESSURE CELL WITH TRIMMED SAMPLE

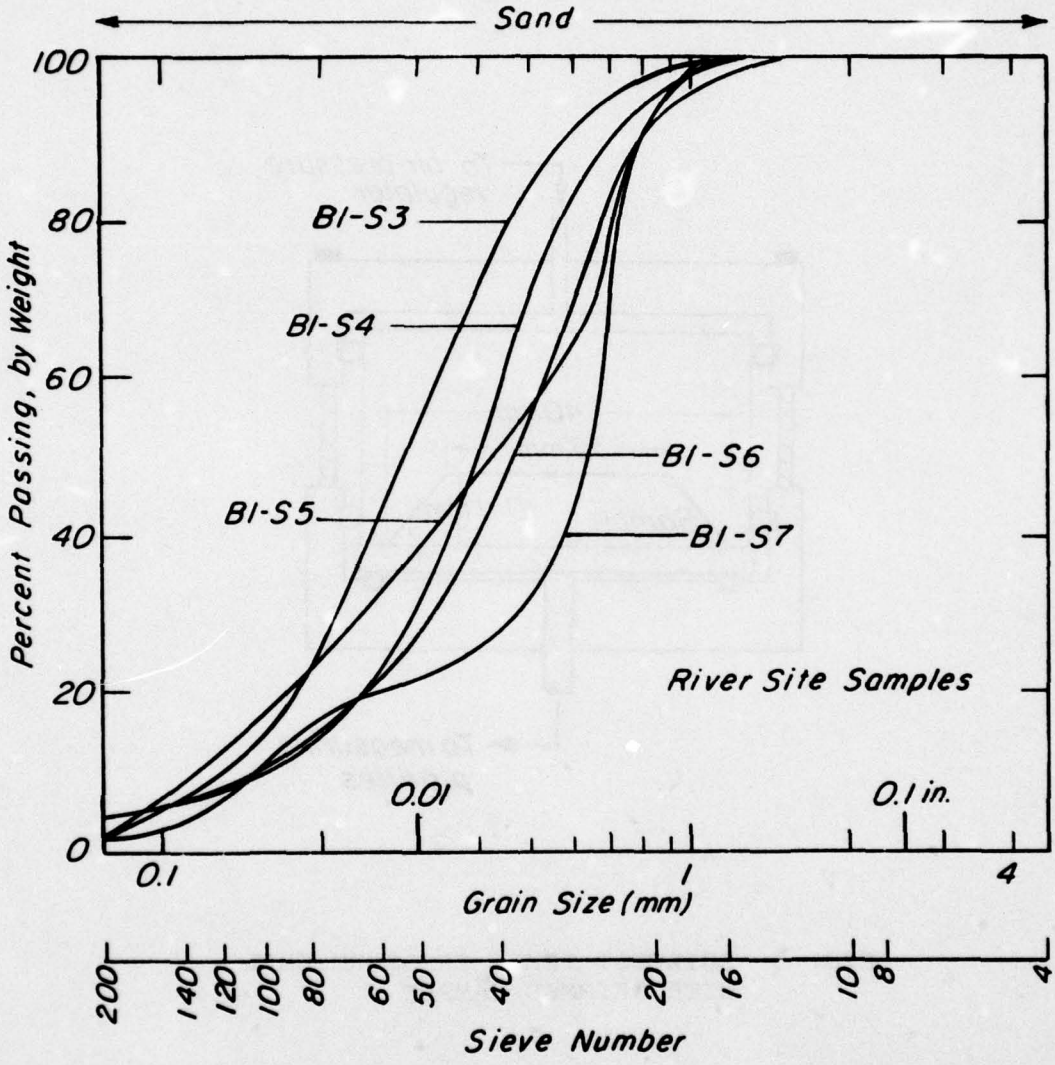

FIG. 6 GRAIN SIZE DISTRIBUTIONS OF RIVER SITE SAMPLES

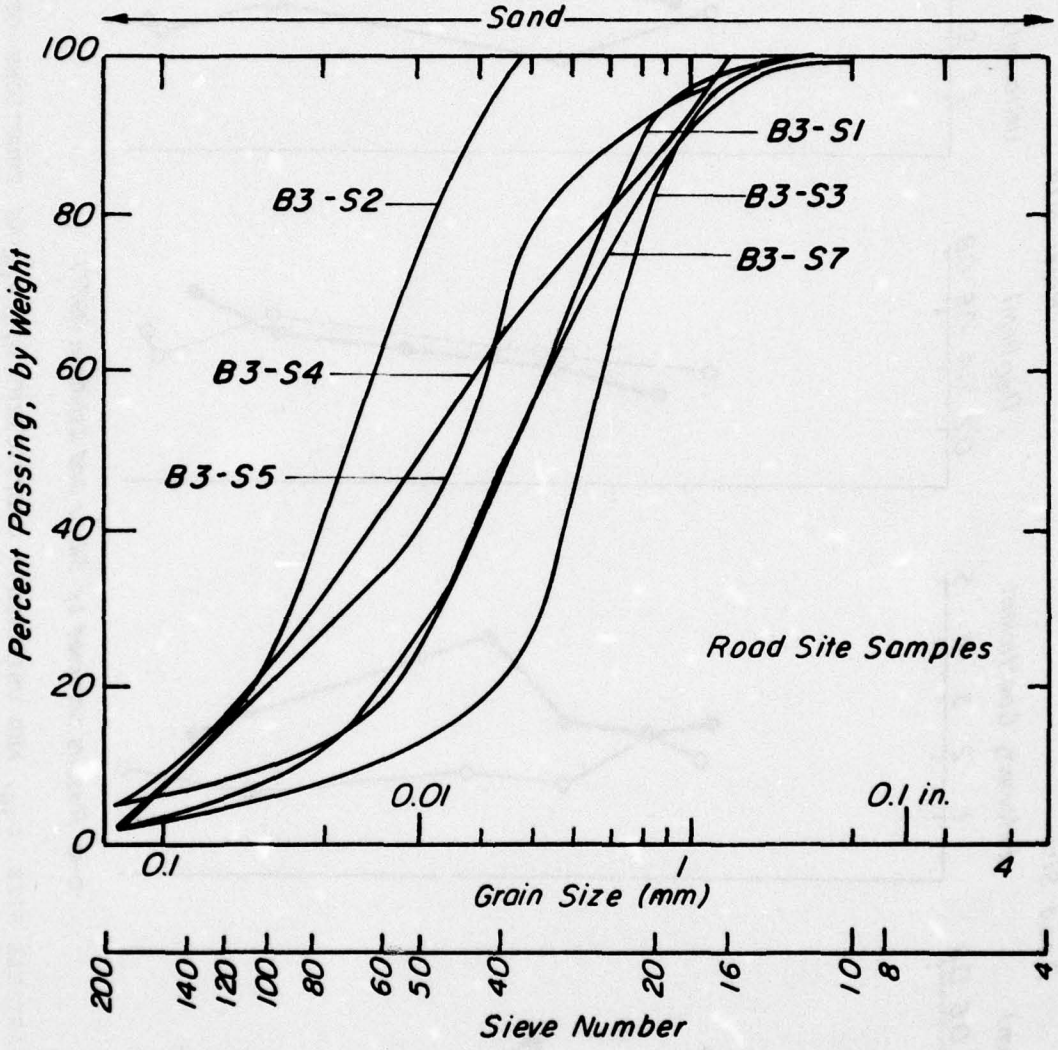

FIG. 7 GRAIN SIZE DISTRIBUTIONS OF ROAD SITE SAMPLES

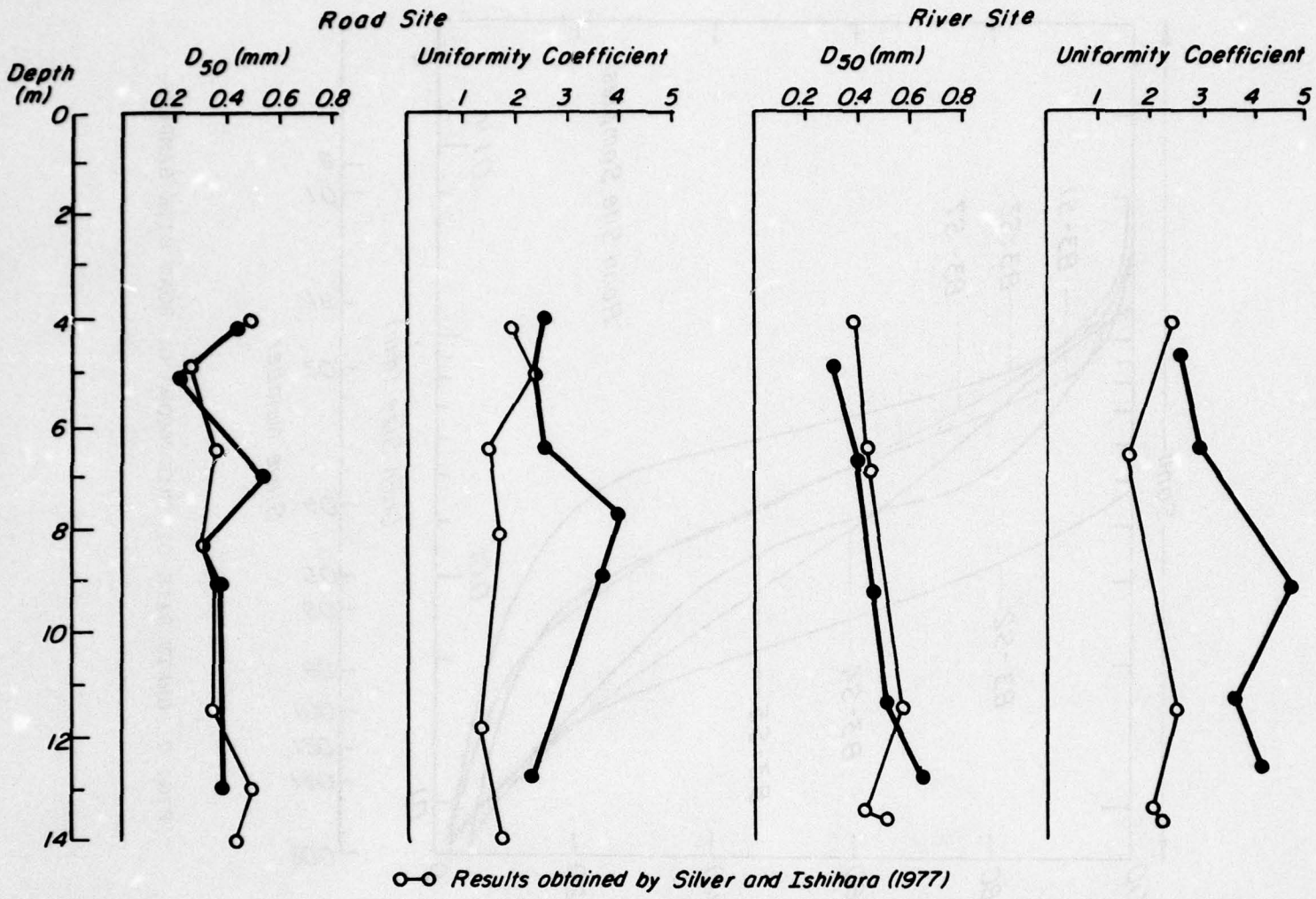

FIG. 8 MEAN PARTICLE SIZE, D_{50}, AND UNIFORMITY COEFFICIENT, D_{60}/D_{10}, AS FUNCTIONS OF DEPTH

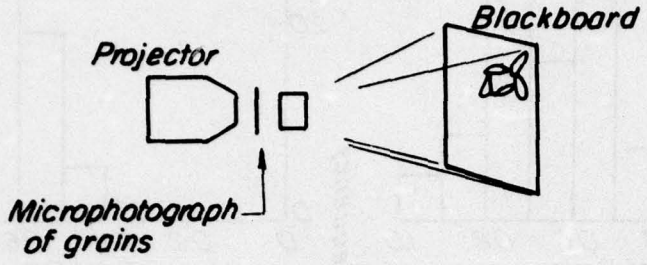

Projection Method

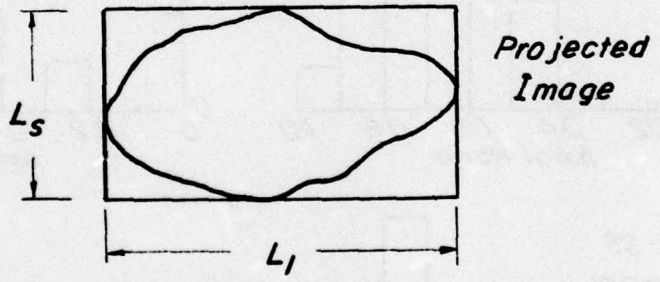

Determination of particle shape: $AR = L_s/L_l$

FIG. 9 THE MEASUREMENT OF PARTICLE AXIAL RATIO
(After Oda, 1976)

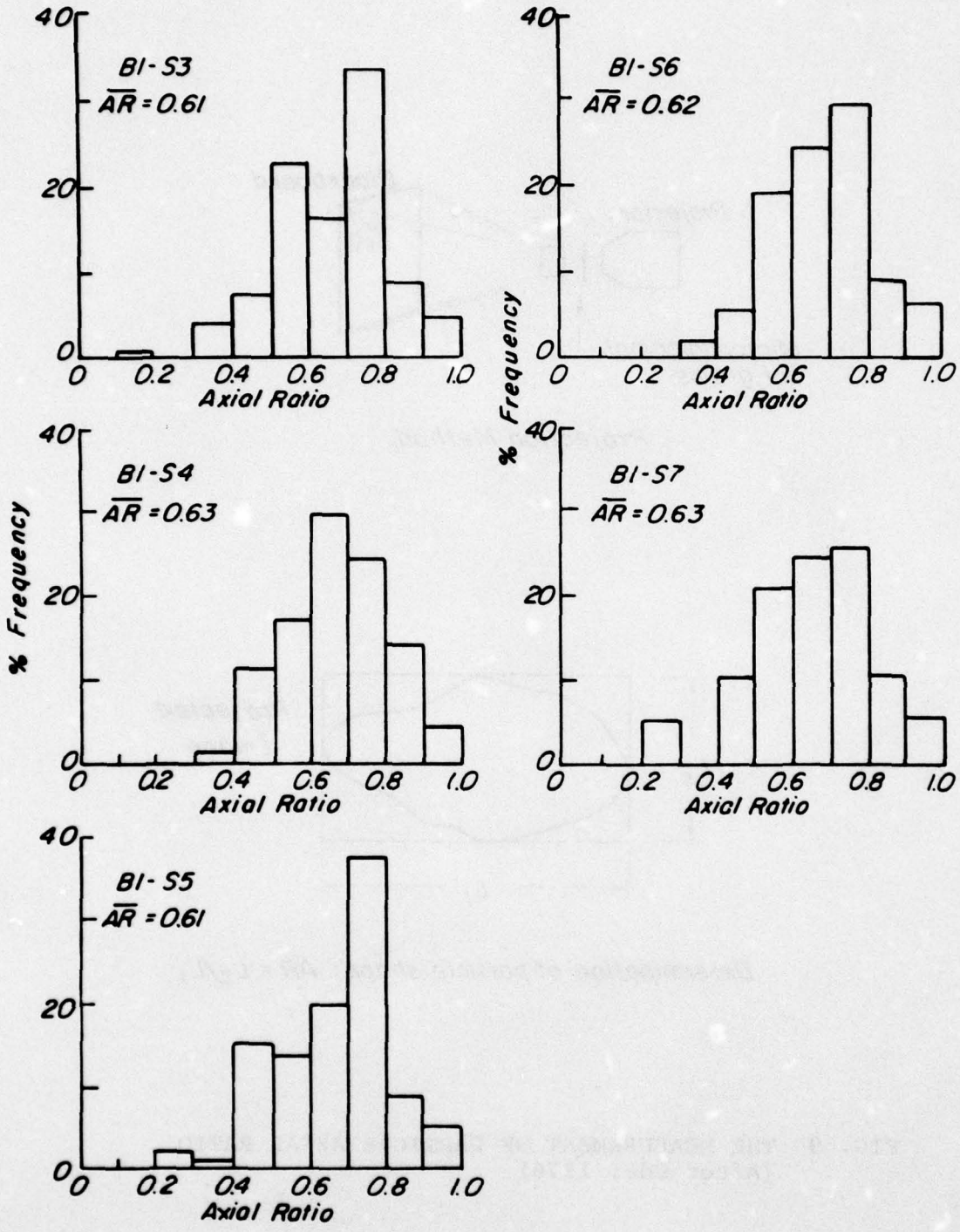

FIG. 10a PARTICLE AXIAL RATIO DISTRIBUTIONS FOR RIVER SITE SAMPLES

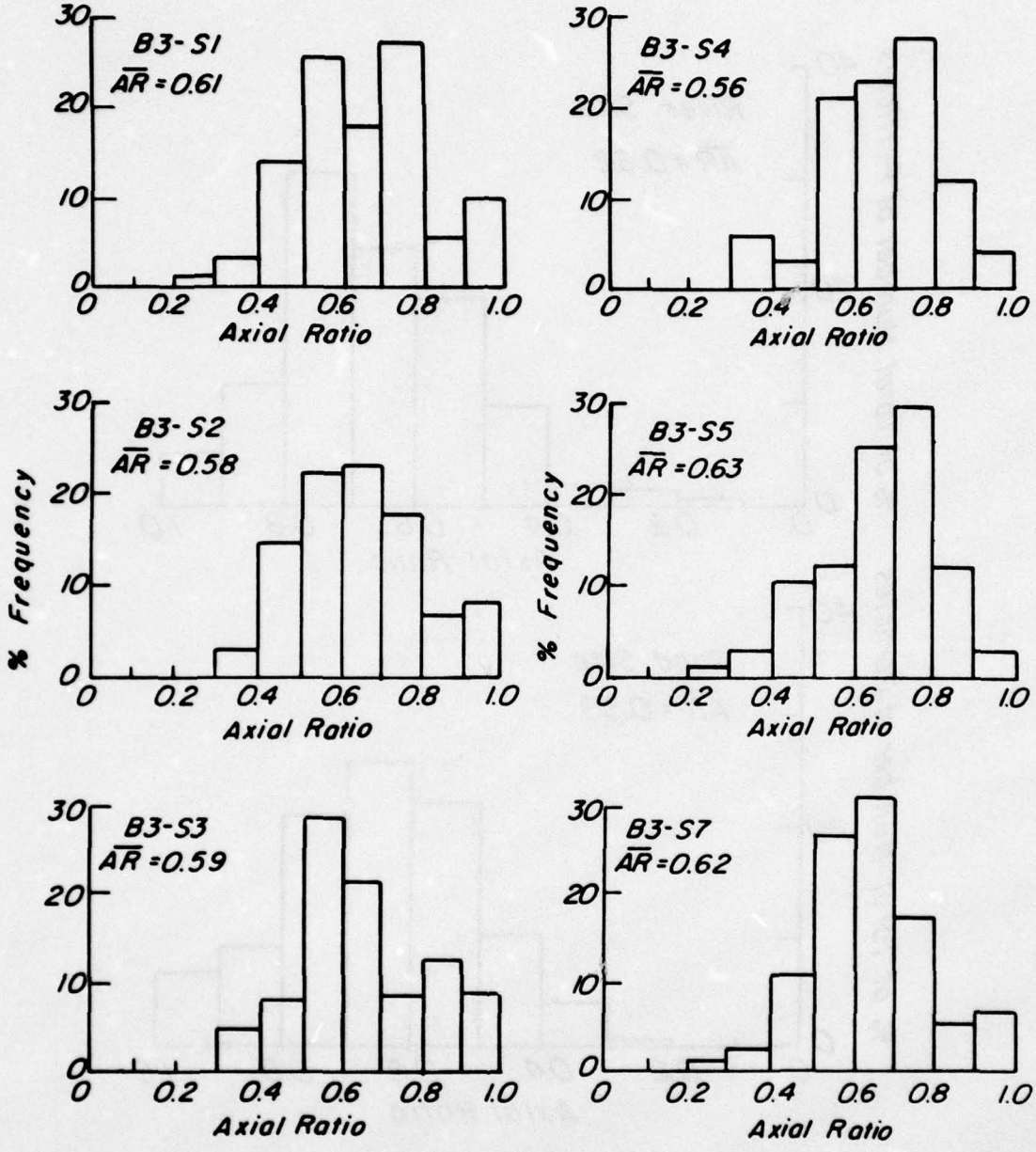

FIG. 10b PARTICLE AXIAL RATIO DISTRIBUTIONS FOR ROAD SITE SAMPLES

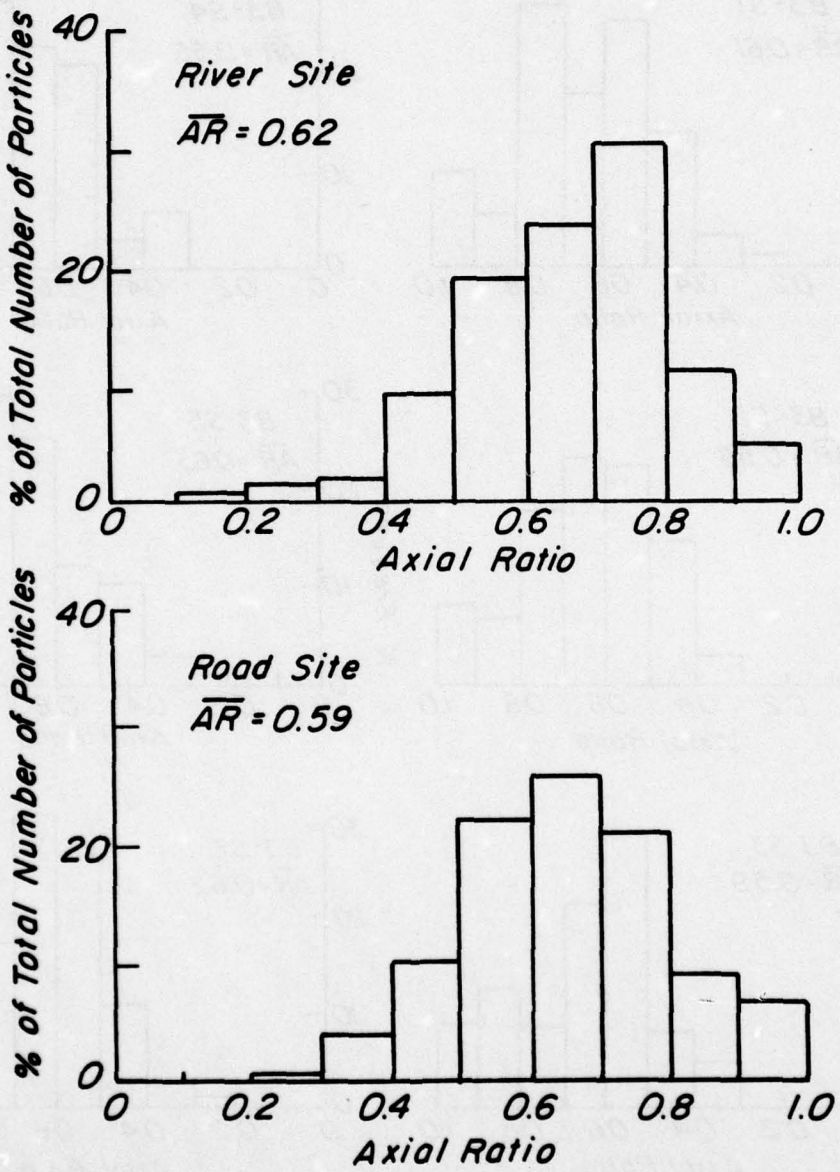

FIG. 11 AVERAGE AXIAL RATIO DISTRIBUTIONS FOR RIVER AND ROAD SITE SAMPLES

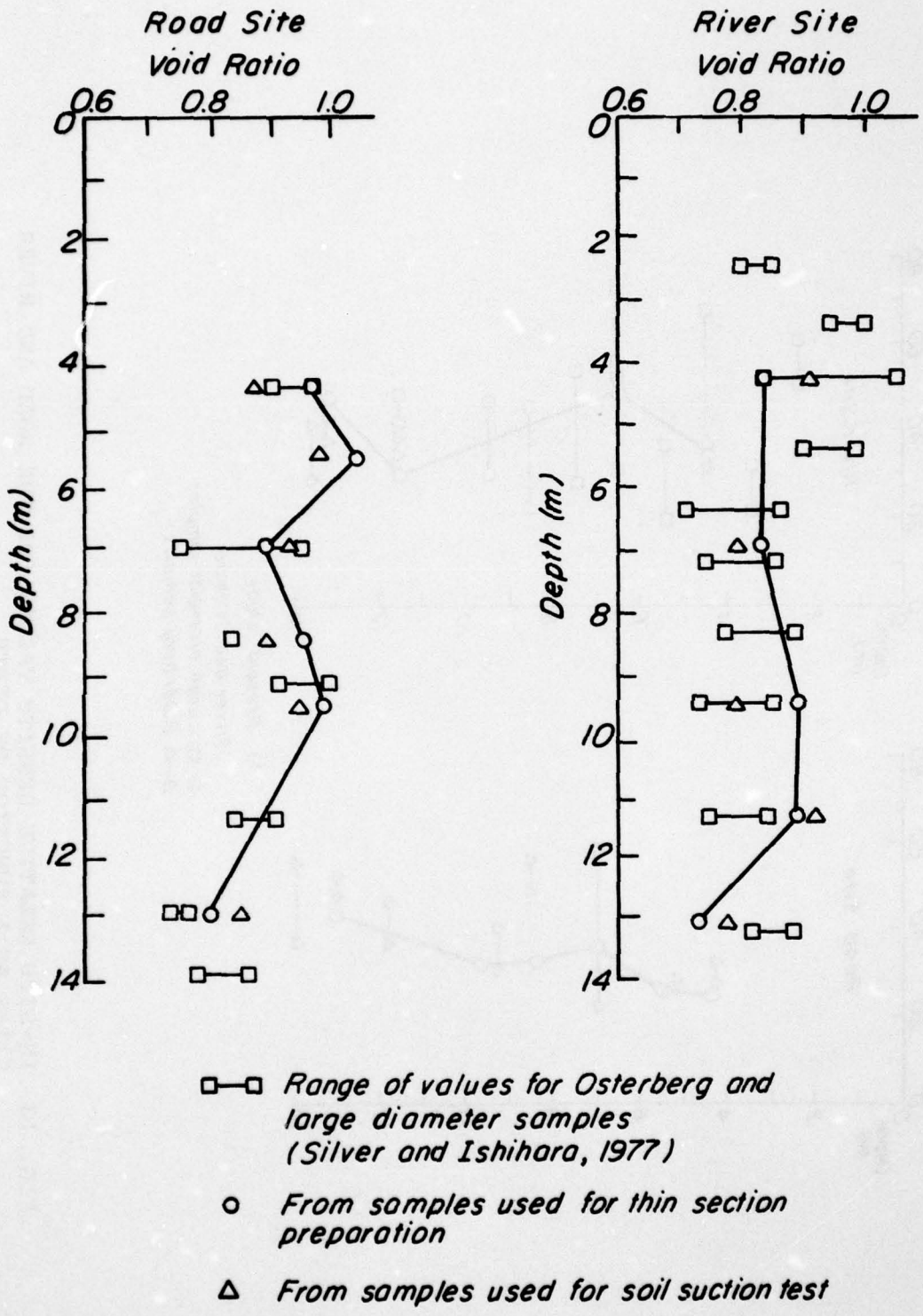

FIG. 12 RIVER AND ROAD SITE SAMPLE VOID RATIOS AS FUNCTIONS OF DEPTH

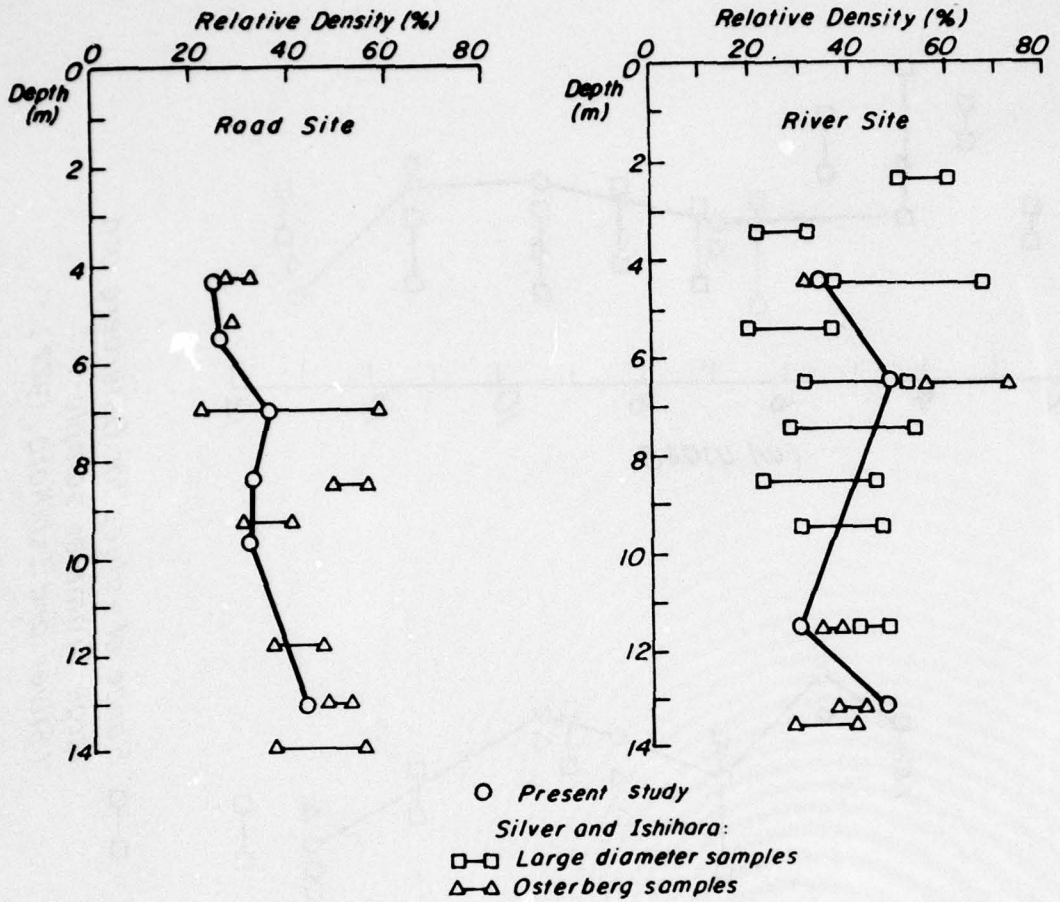

FIG. 13 IN-SITU RELATIVE DENSITY VALUES FOR THE ROAD AND RIVER SITES AS A FUNCTION OF DEPTH

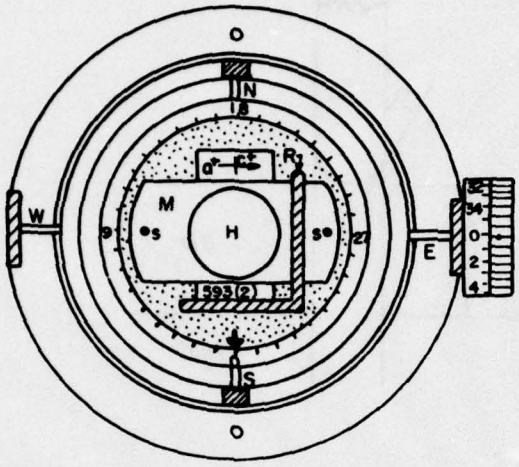

FIG. 14 UNIVERSAL STAGE LOOKING DOWN THE VERTICAL ROTATION AXIS

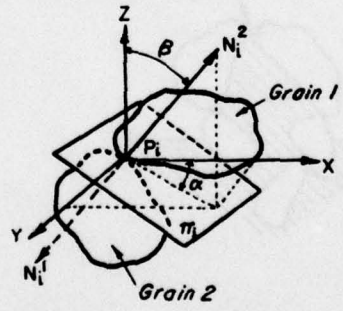

FIG. 15 MEASUREMENT OF NORMALS (N_i^1, N_i^2) TO TANGENT PLANE (π_i)

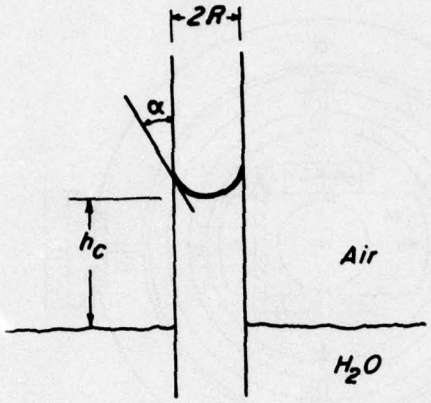

FIG. 16 ILLUSTRATION OF CAPILLARY RISE

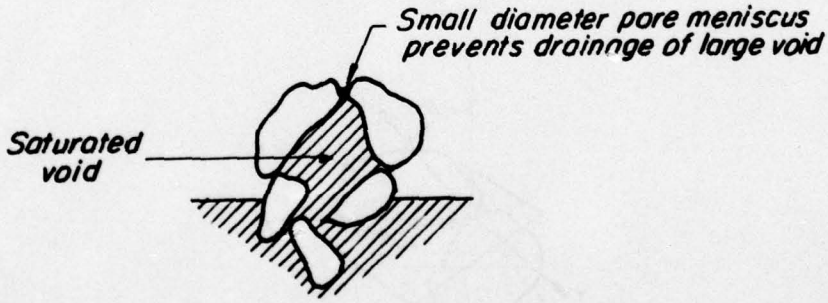

FIG. 17 A LARGE VOID ISOLATED BY SMALL DIAMETER PORES

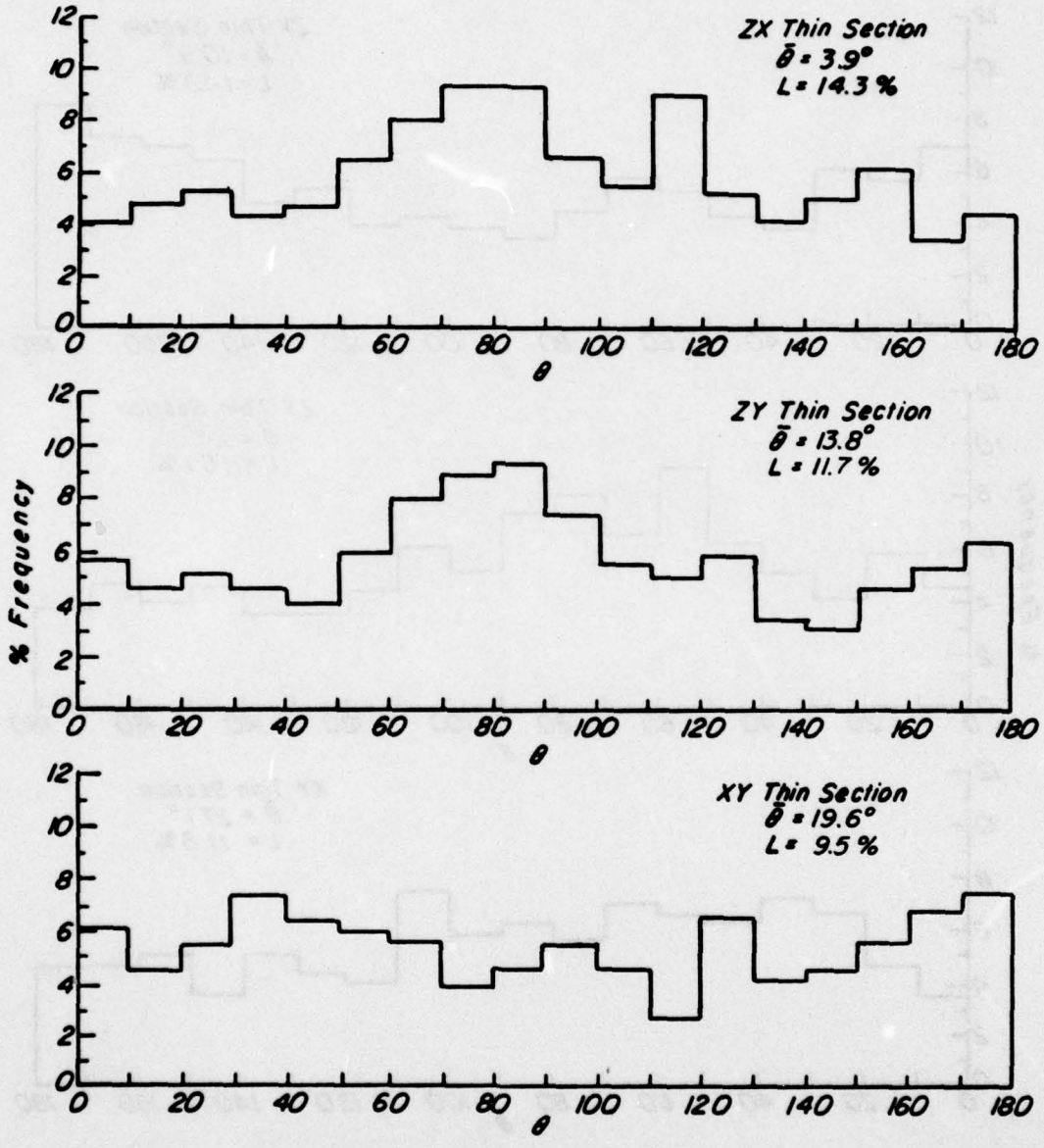

FIG. 18 HISTOGRAMS OF APPARENT PARTICLE LONG AXIS ORIENTATIONS FOR RIVER SITE SAMPLE B1-S3

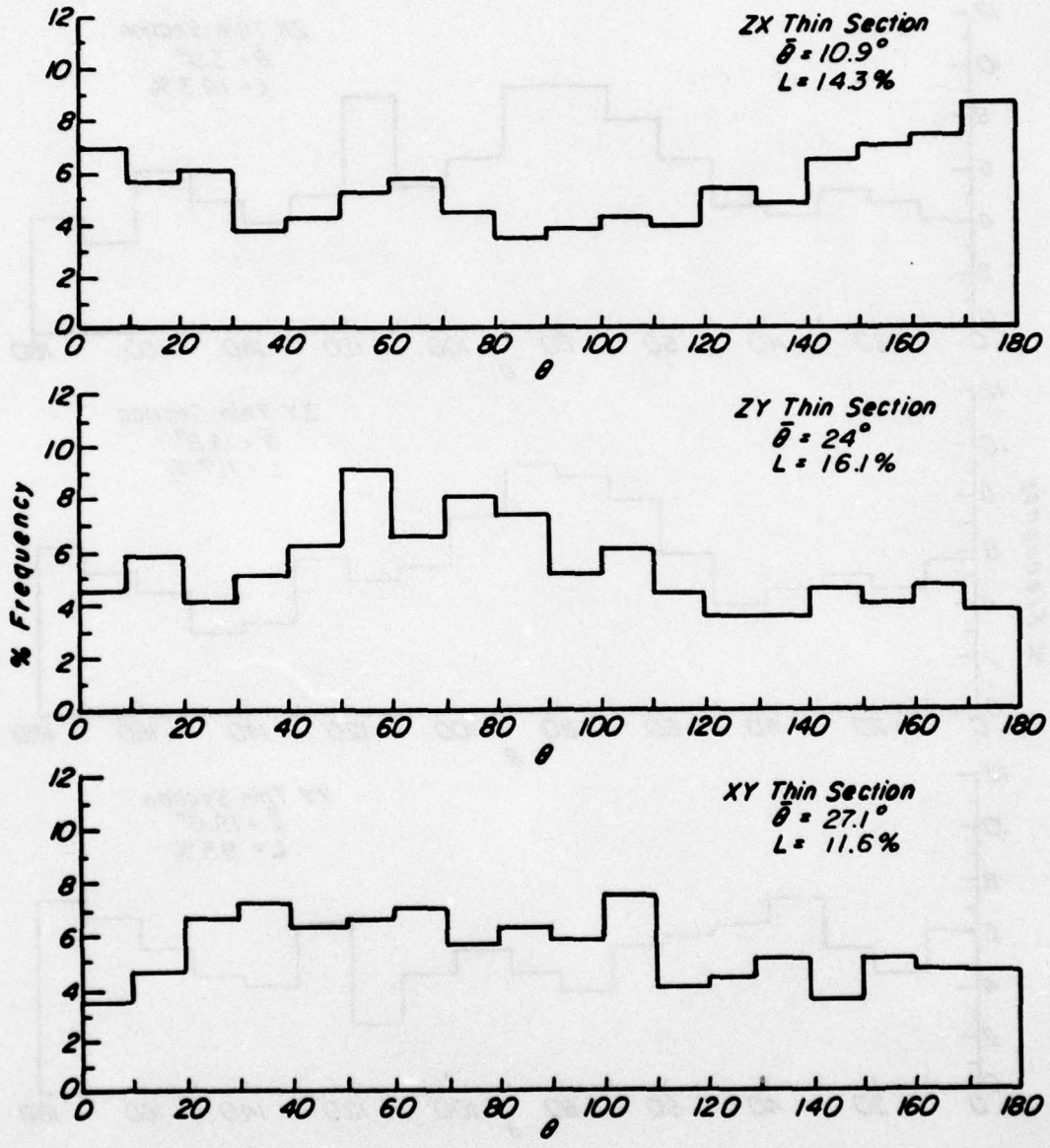

FIG. 19 HISTOGRAMS OF APPARENT PARTICLE LONG AXIS ORIENTATIONS FOR RIVER SITE SAMPLE B1-S4

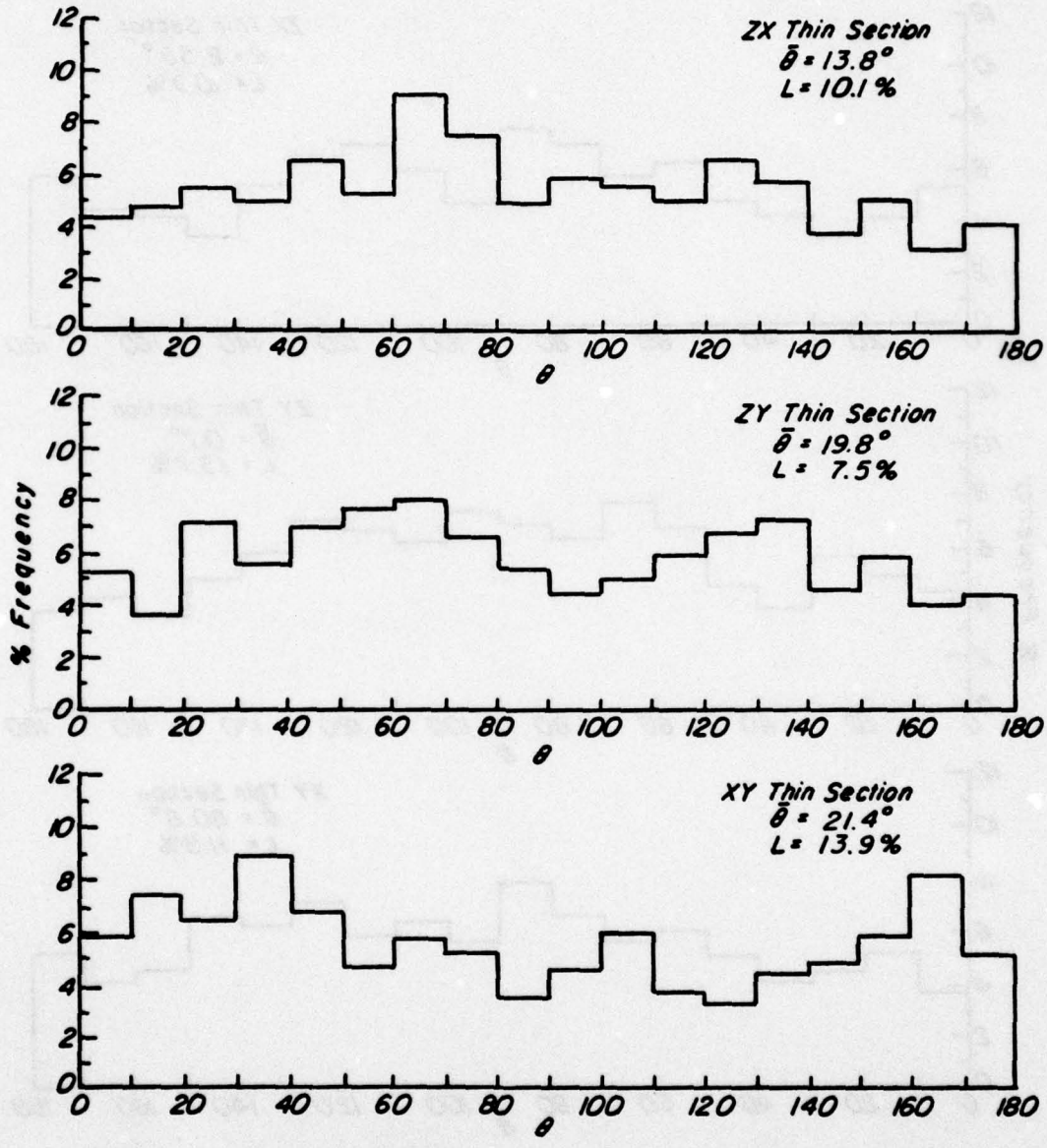

FIG. 20 HISTOGRAMS OF APPARENT PARTICLE LONG AXIS ORIENTATIONS FOR RIVER SITE SAMPLE B1-S5

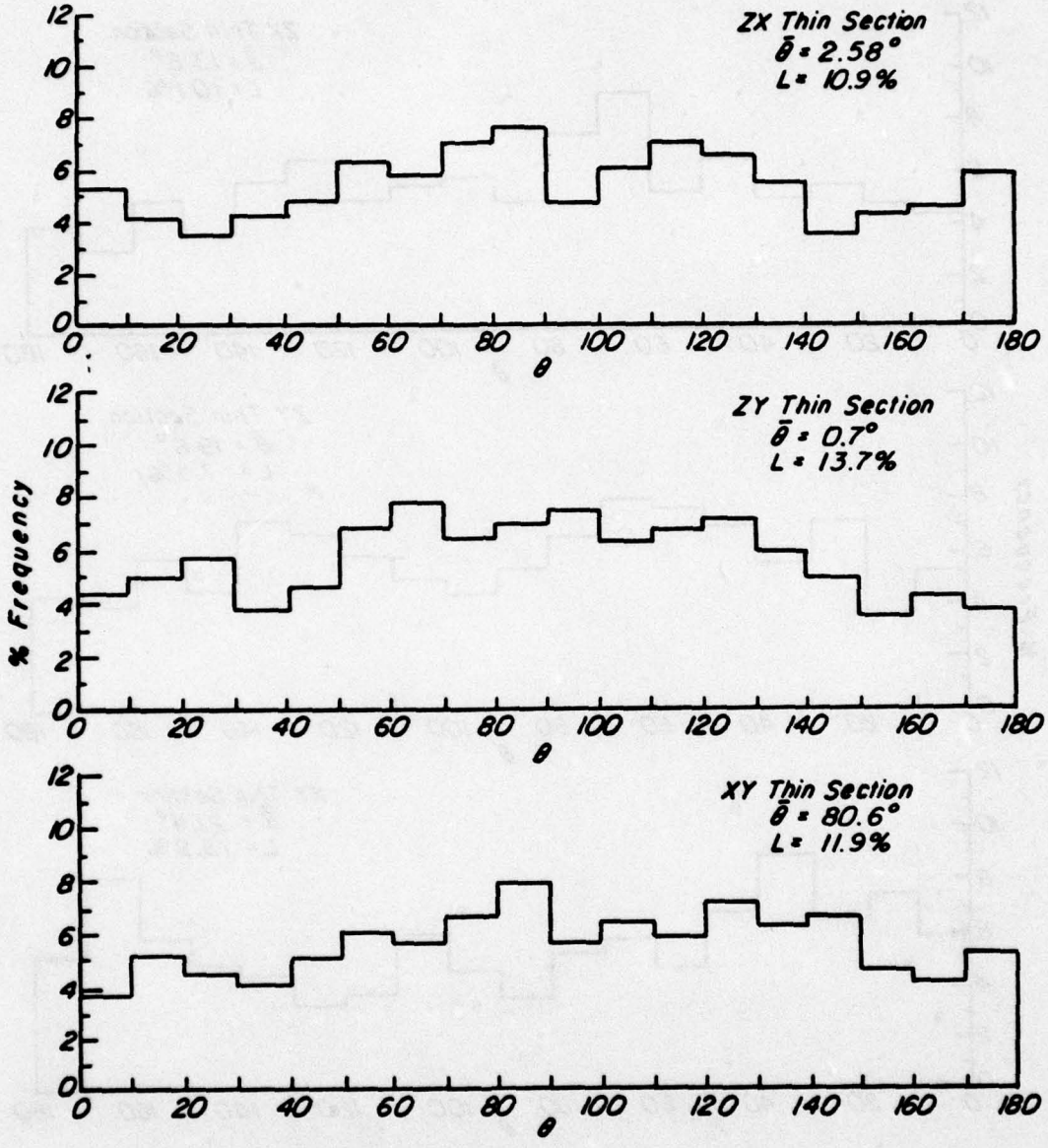

FIG. 21 HISTOGRAMS OF APPARENT PARTICLE LONG AXIS ORIENTATIONS FOR RIVER SITE SAMPLE B1-S6

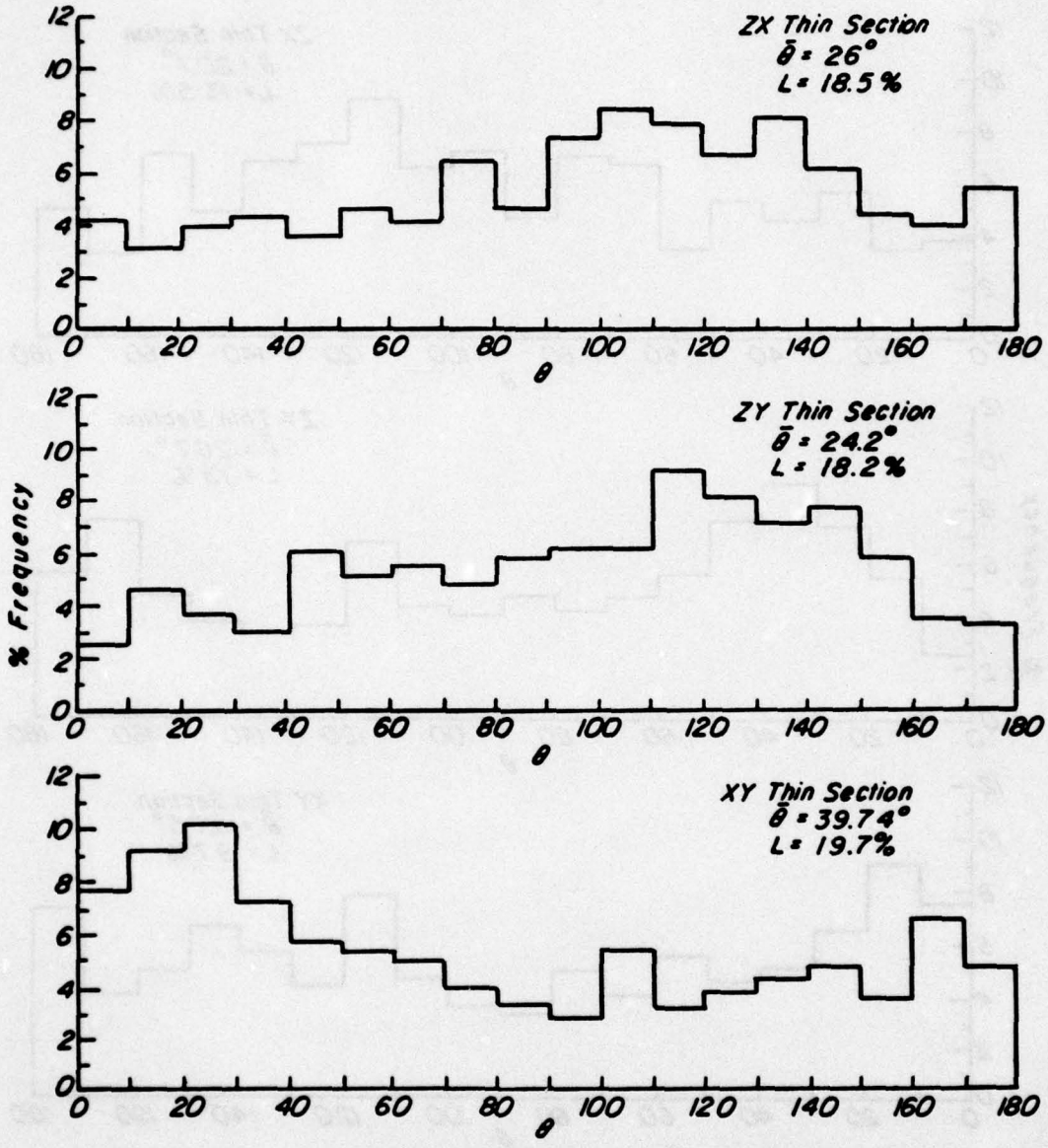

FIG. 22 HISTOGRAMS OF APPARENT PARTICLE LONG AXIS ORIENTATIONS FOR RIVER SITE SAMPLE B1-S7

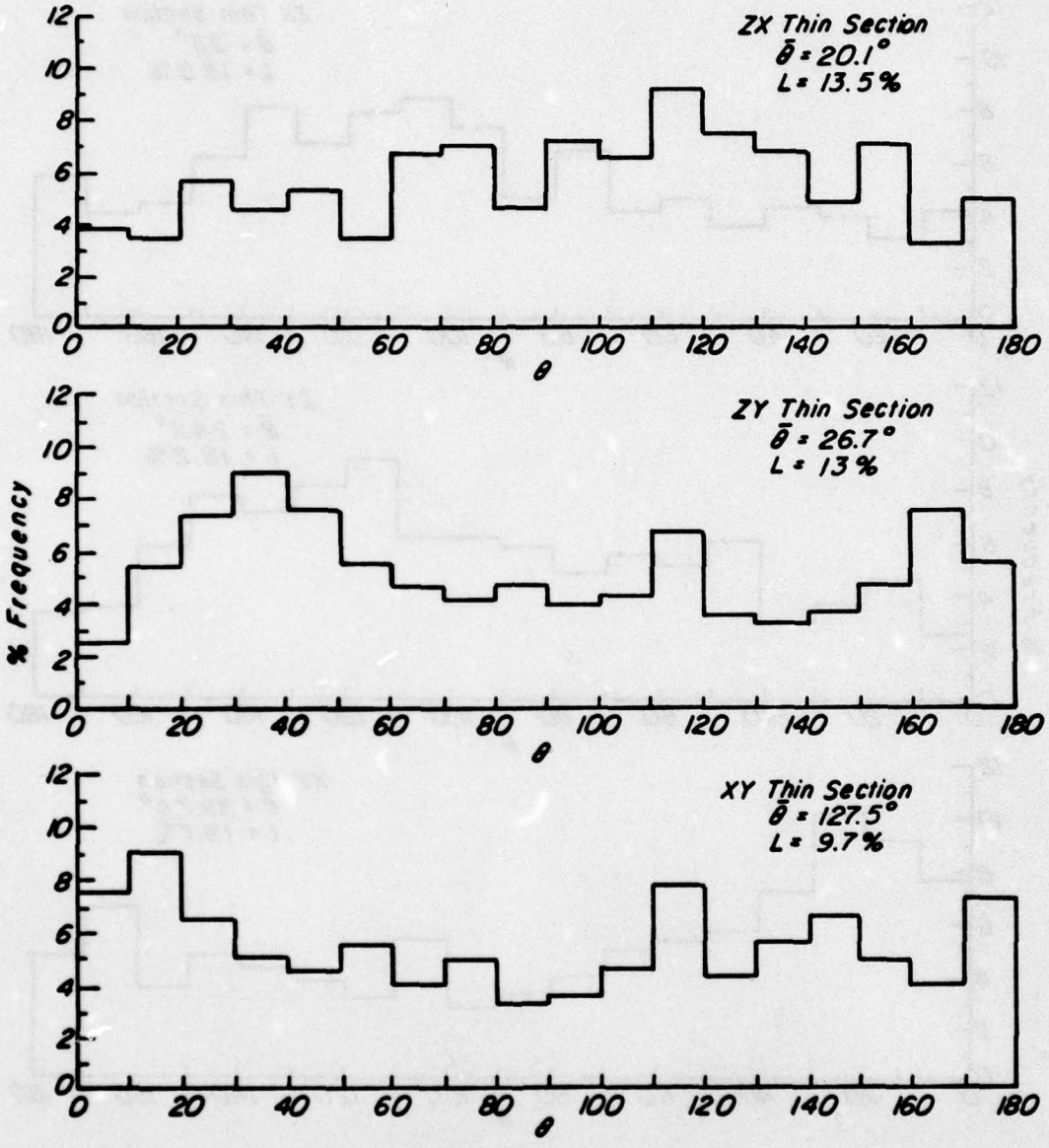

FIG. 23 HISTOGRAMS OF APPARENT PARTICLE LONG AXIS ORIENTATIONS FOR ROAD SITE SAMPLE B3-S1

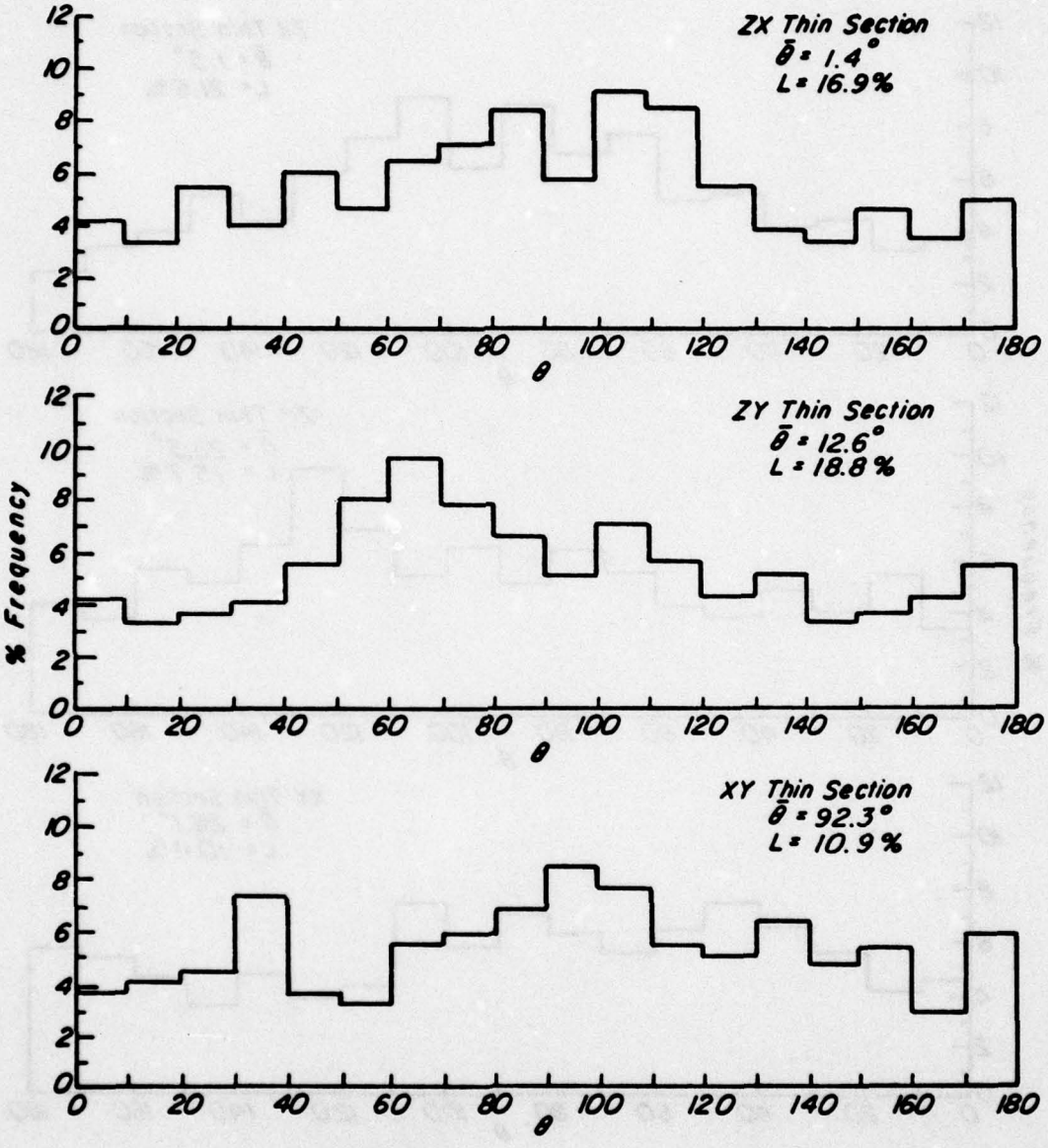

FIG. 24 HISTOGRAMS OF APPARENT PARTICLE LONG AXIS ORIENTATIONS FOR ROAD SITE SAMPLE B3-S2

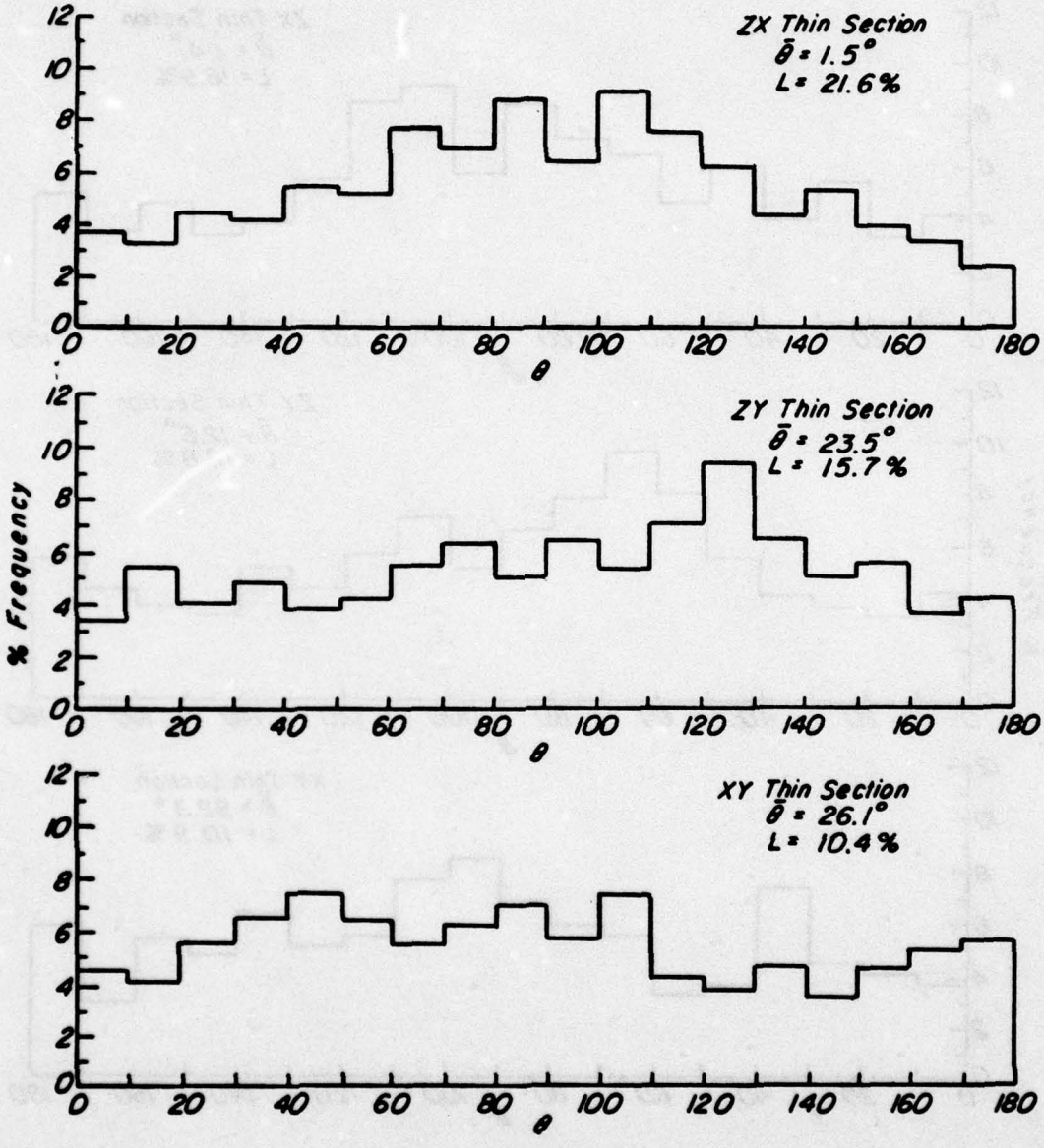

FIG. 25 HISTOGRAMS OF APPARENT PARTICLE LONG AXIS ORIENTATIONS FOR ROAD SITE SAMPLE B3-S3

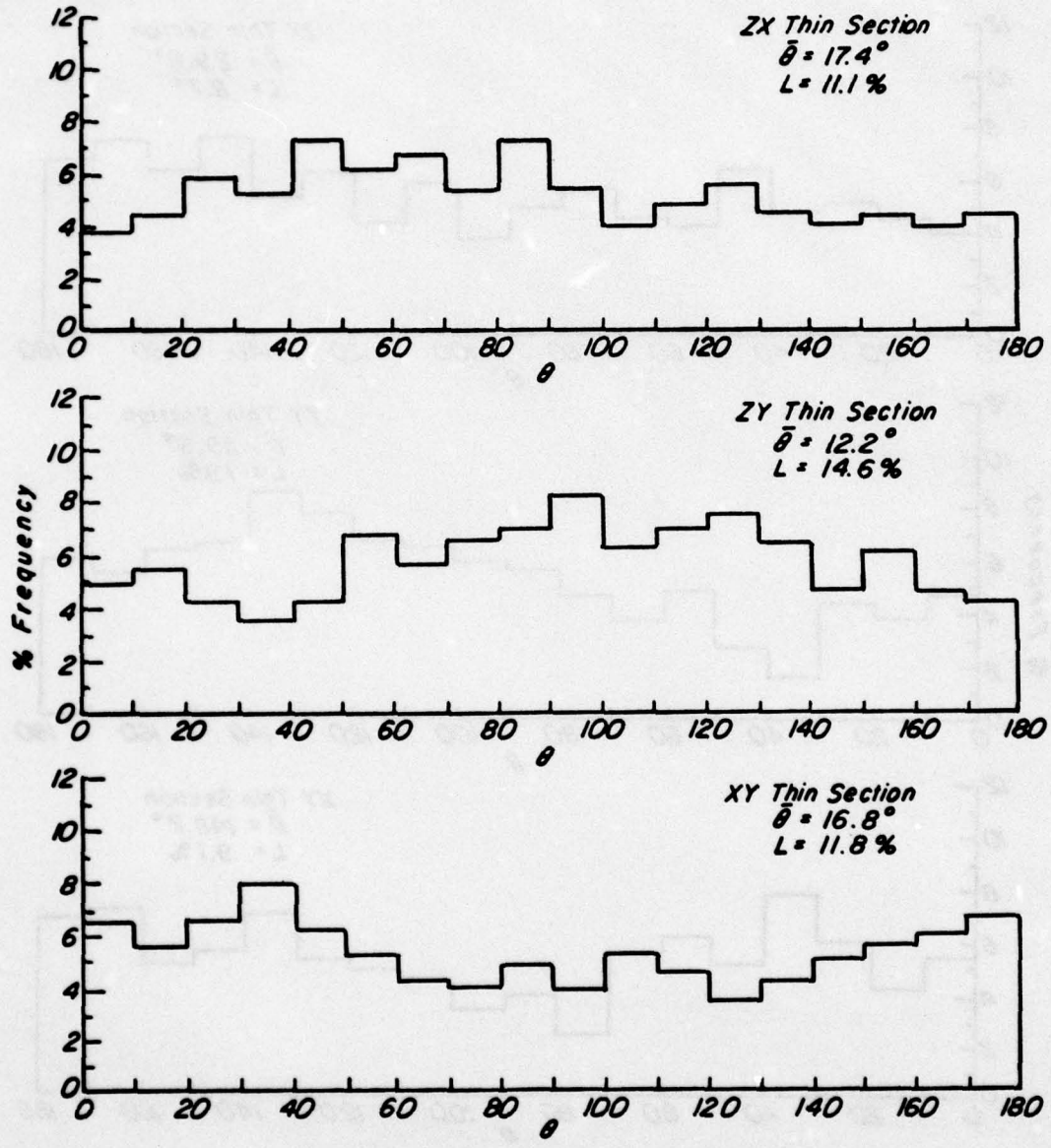

FIG. 26 HISTOGRAMS OF APPARENT PARTICLE LONG AXIS ORIENTATIONS FOR ROAD SITE SAMPLE B3-S4

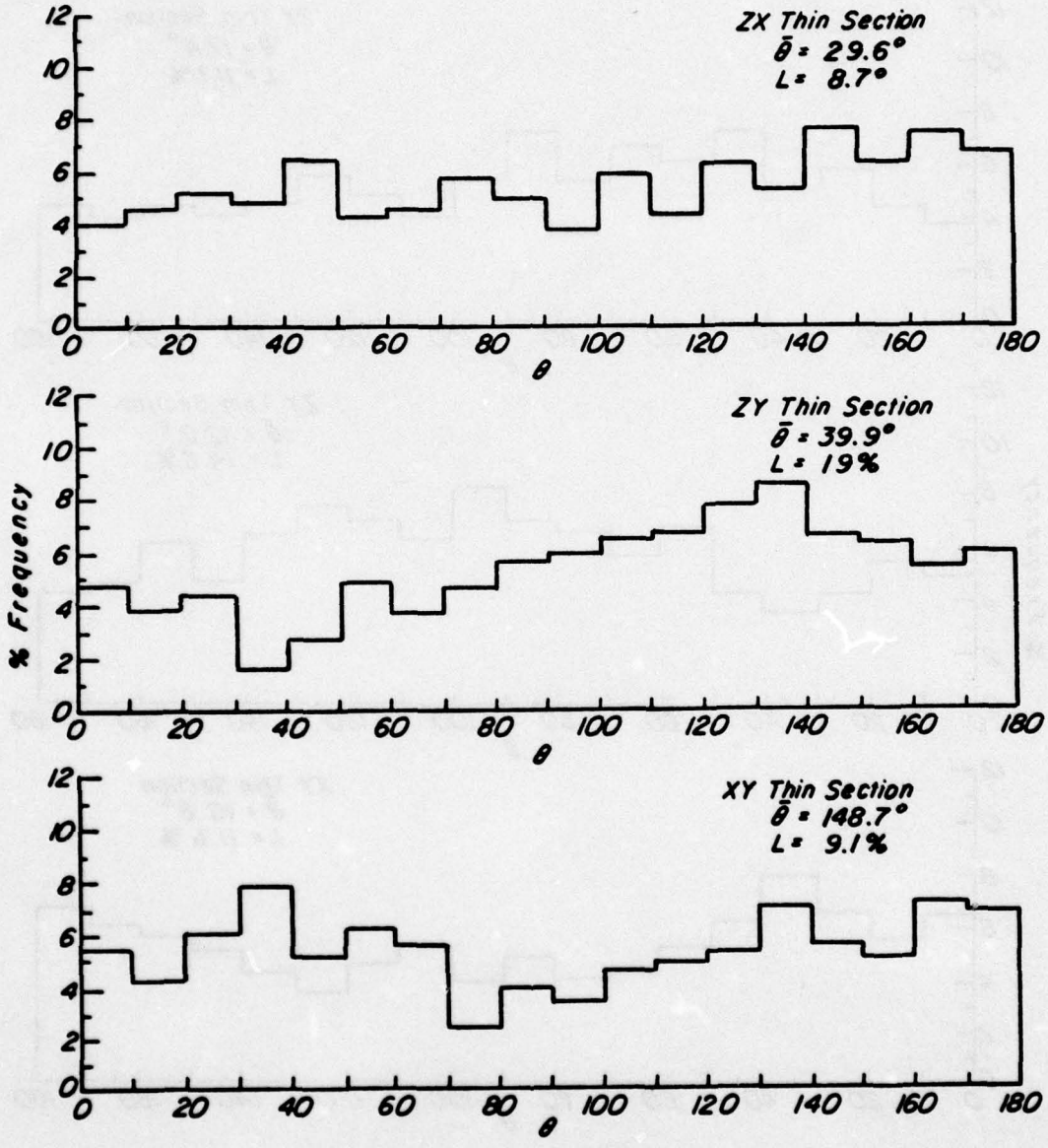

FIG. 27 HISTOGRAMS OF APPARENT PARTICLE LONG AXIS ORIENTATIONS FOR ROAD SITE SAMPLE B3-S5

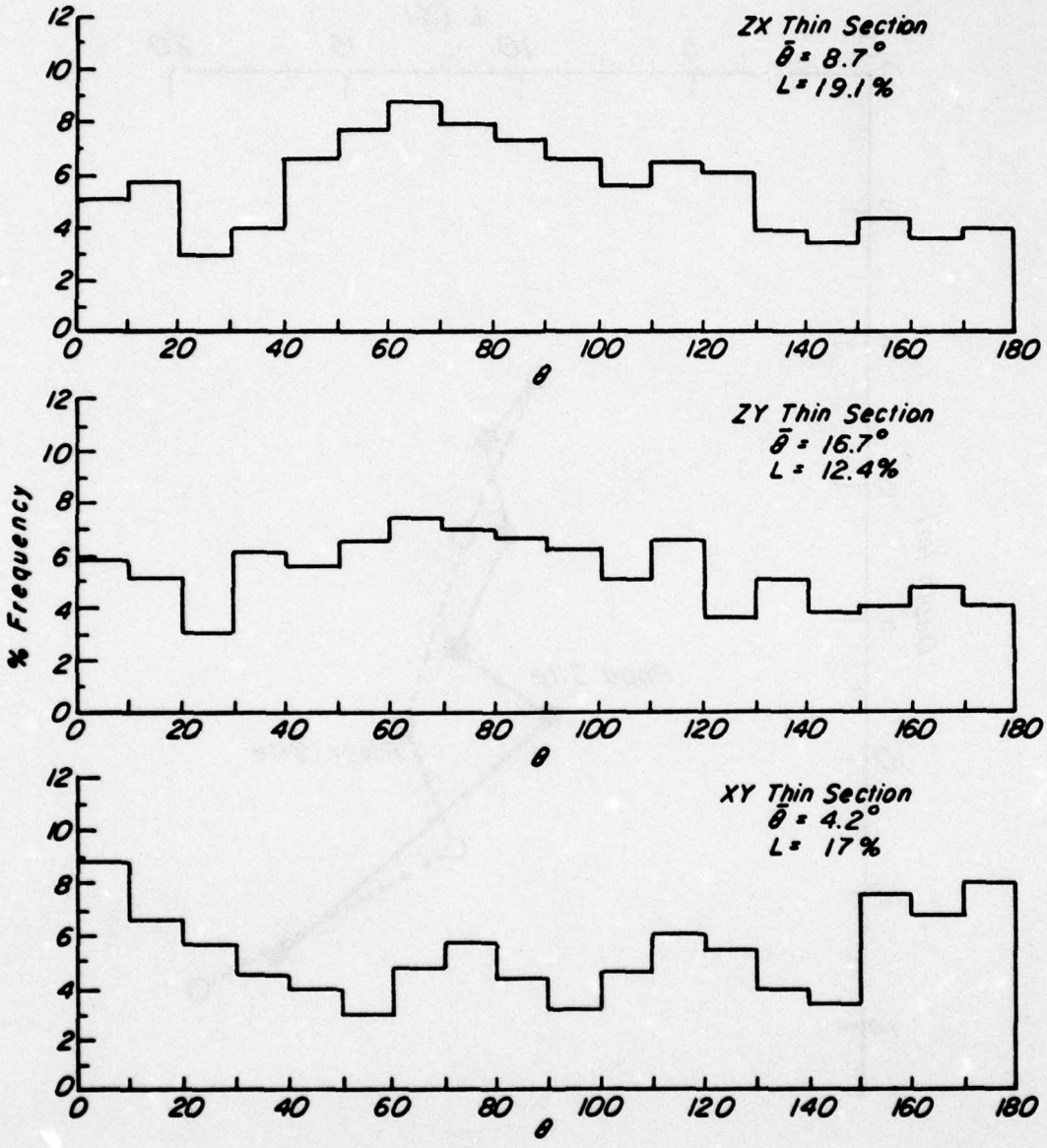

FIG. 28 HISTOGRAMS OF APPARENT PARTICLE LONG AXIS ORIENTATIONS FOR ROAD SITE SAMPLE B3-S7

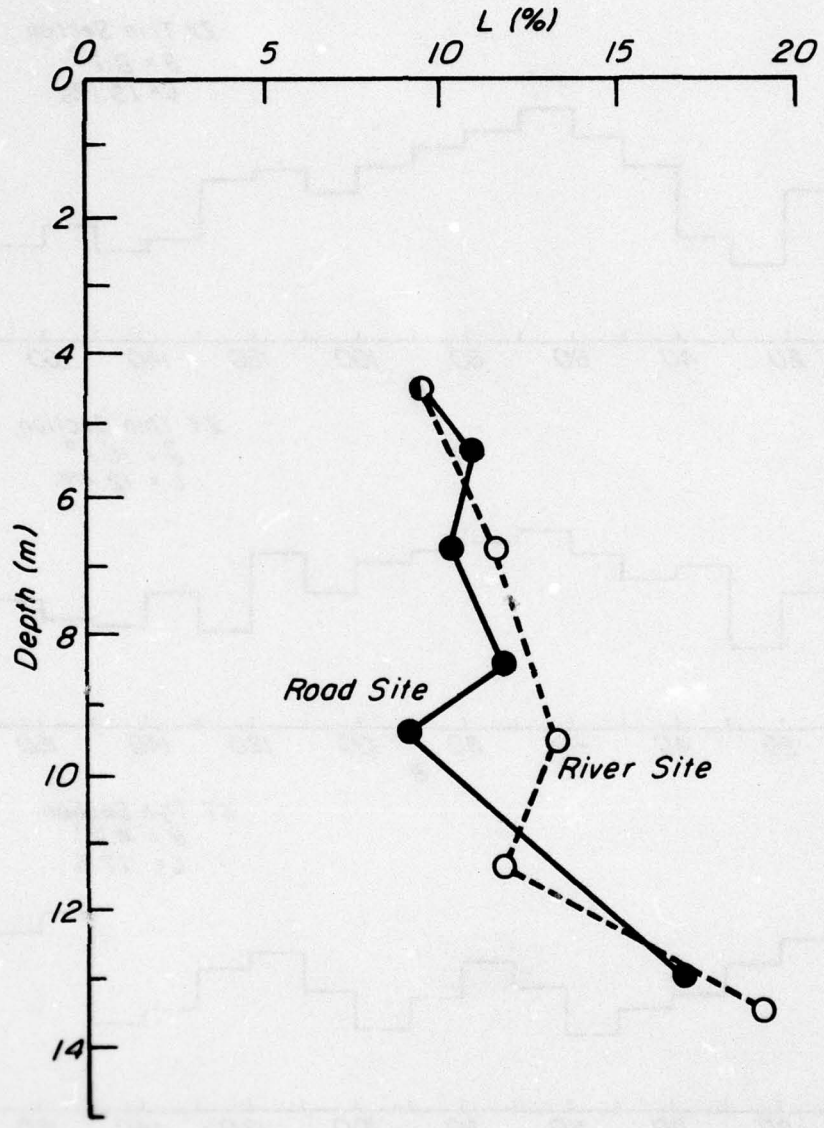

FIG. 29 RESULTANT VECTOR MAGNITUDES OBTAINED FROM HORIZONTAL THIN SECTIONS AS A FUNCTION OF DEPTH

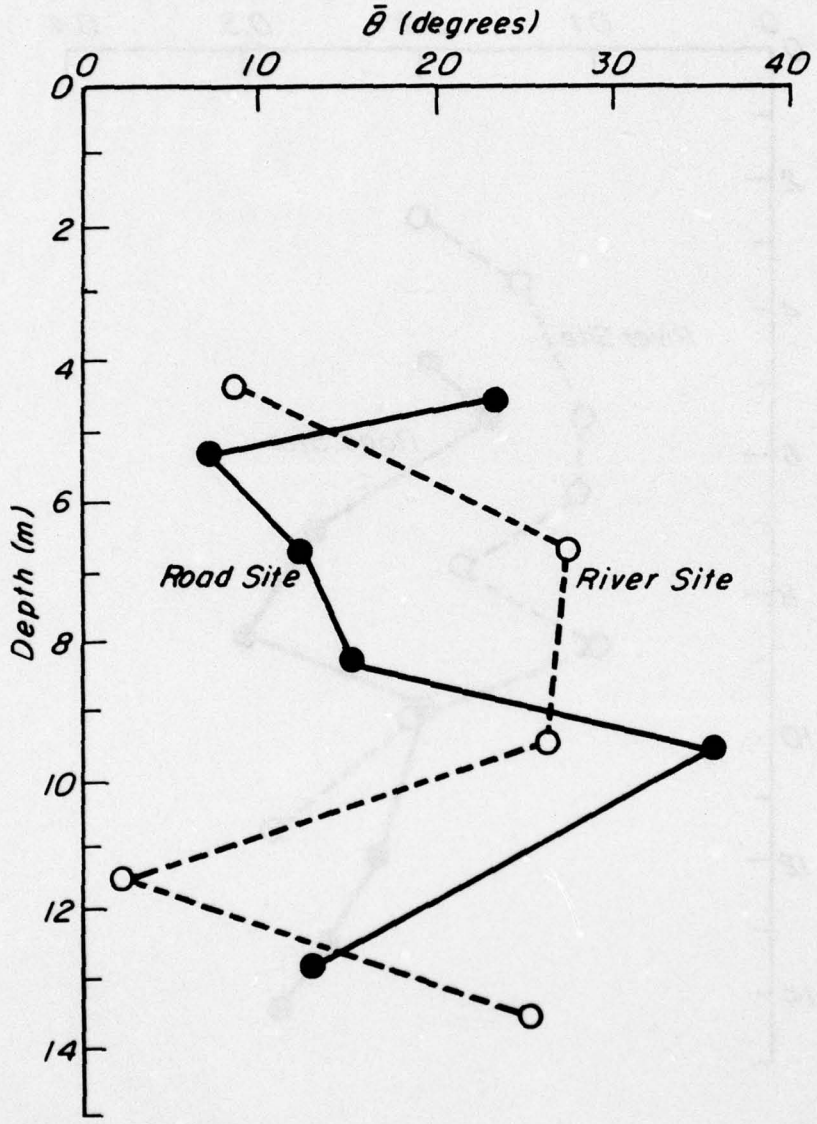

FIG. 30 AVERAGE INCLINATIONS OF APPARENT PARTICLE LONG AXES TO THE VERTICAL DIRECTION

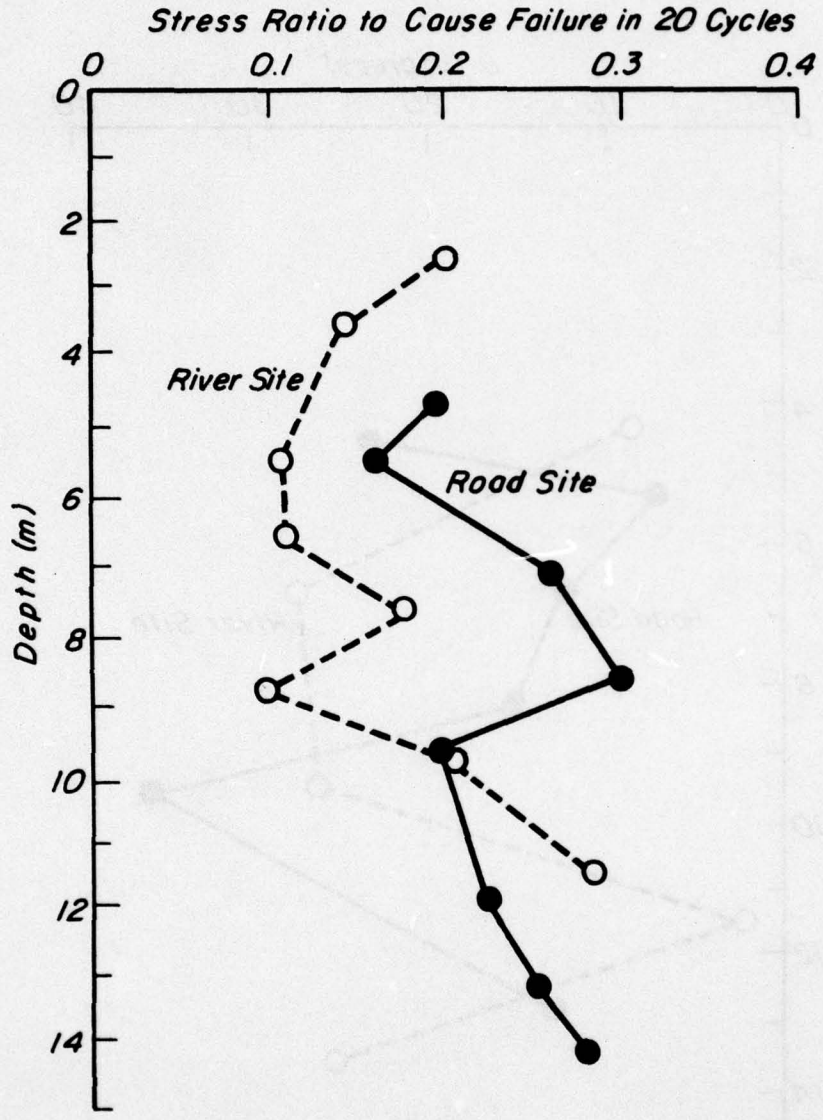

FIG. 31 COMPARISON OF IN-SITU CYCLIC TRIAXIAL STRENGTH (FAILURE IN 20 CYCLES) AS A FUNCTION OF DEPTH AT THE ROAD AND RIVER SITES
(From Silver and Ishihara, 1977)

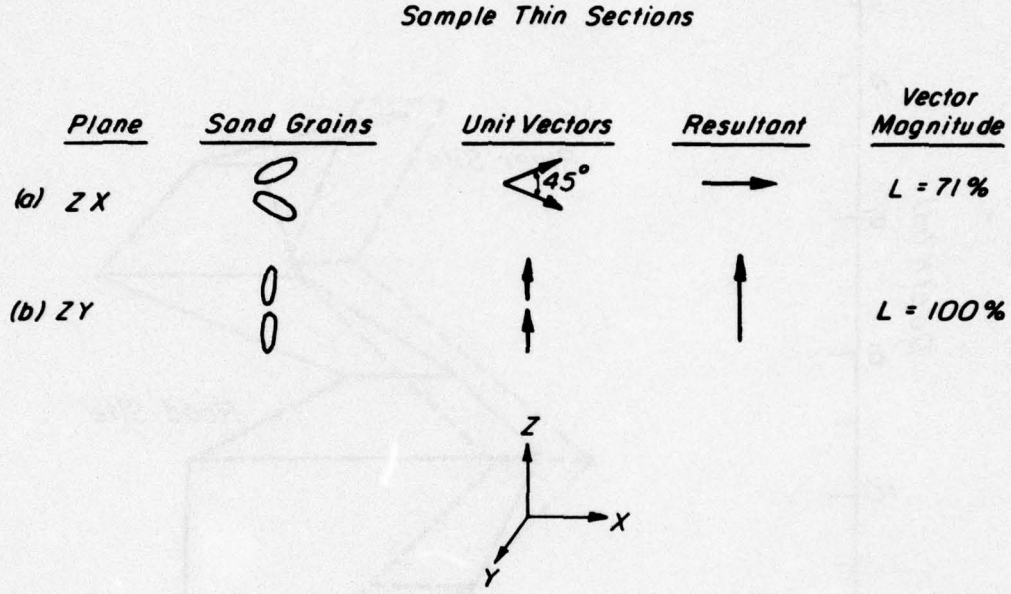

FIG. 32 ILLUSTRATION OF THE DEPENDENCE OF OBSERVED VECTOR MAGNITUDES, L, ON THIN SECTION ORIENTATION

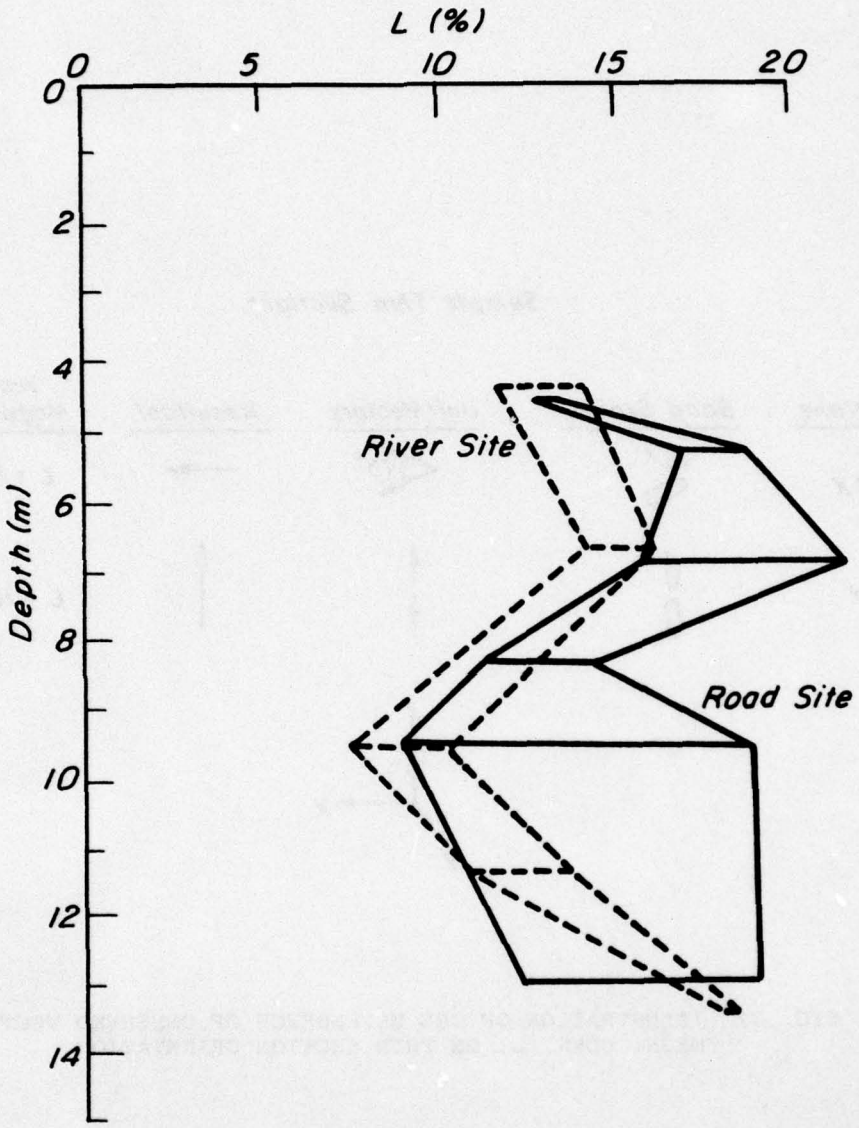

FIG. 33 RESULTANT VECTOR MAGNITUDES OBTAINED FROM VERTICAL THIN SECTIONS AS A FUNCTION OF DEPTH

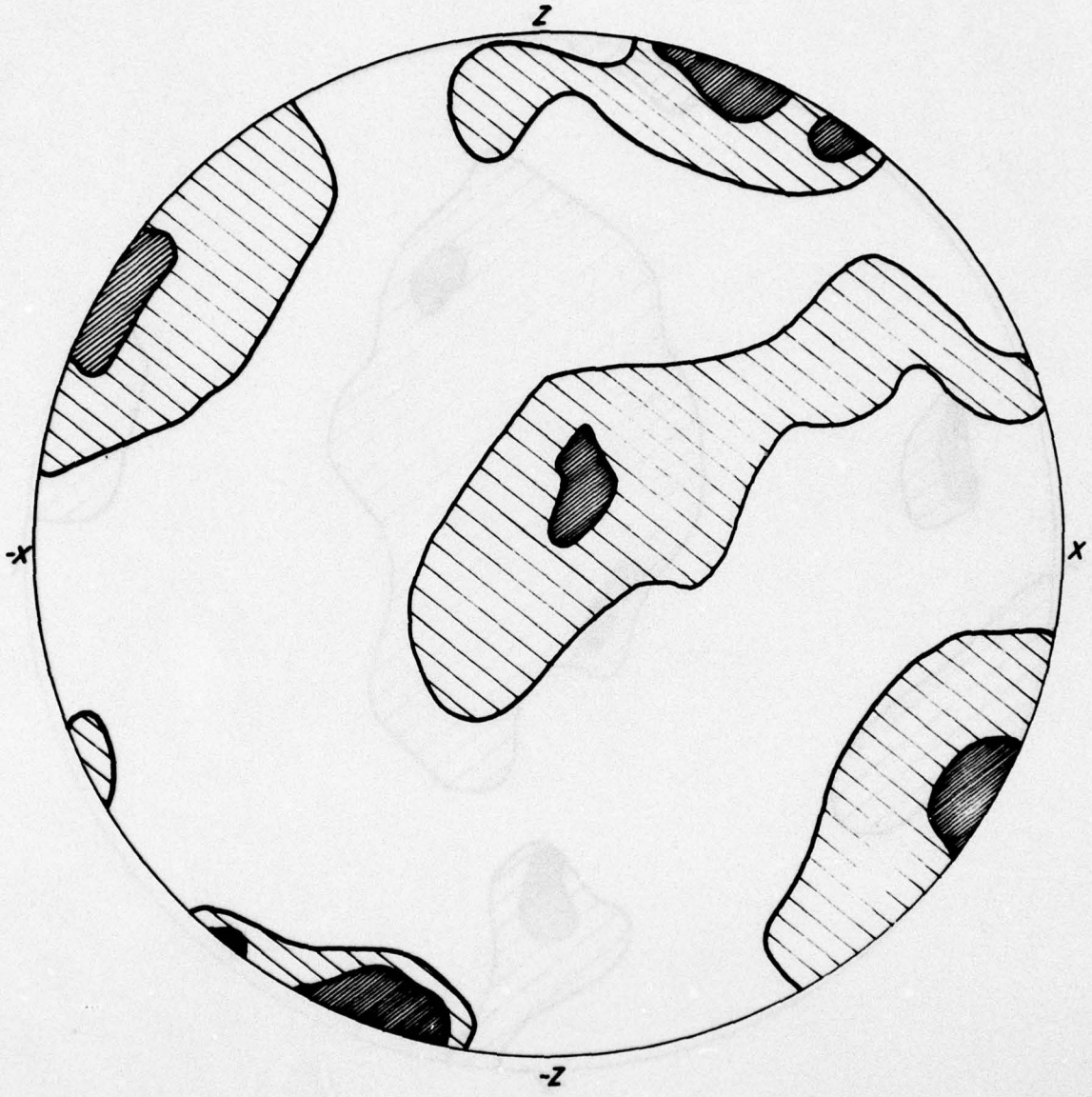

FIG. 34 EQUAL AREA STEREONET SHOWING THE DISTRIBUTION OF INTER-PARTICLE CONTACT NORMALS IN RIVER SITE SAMPLE B1-S3

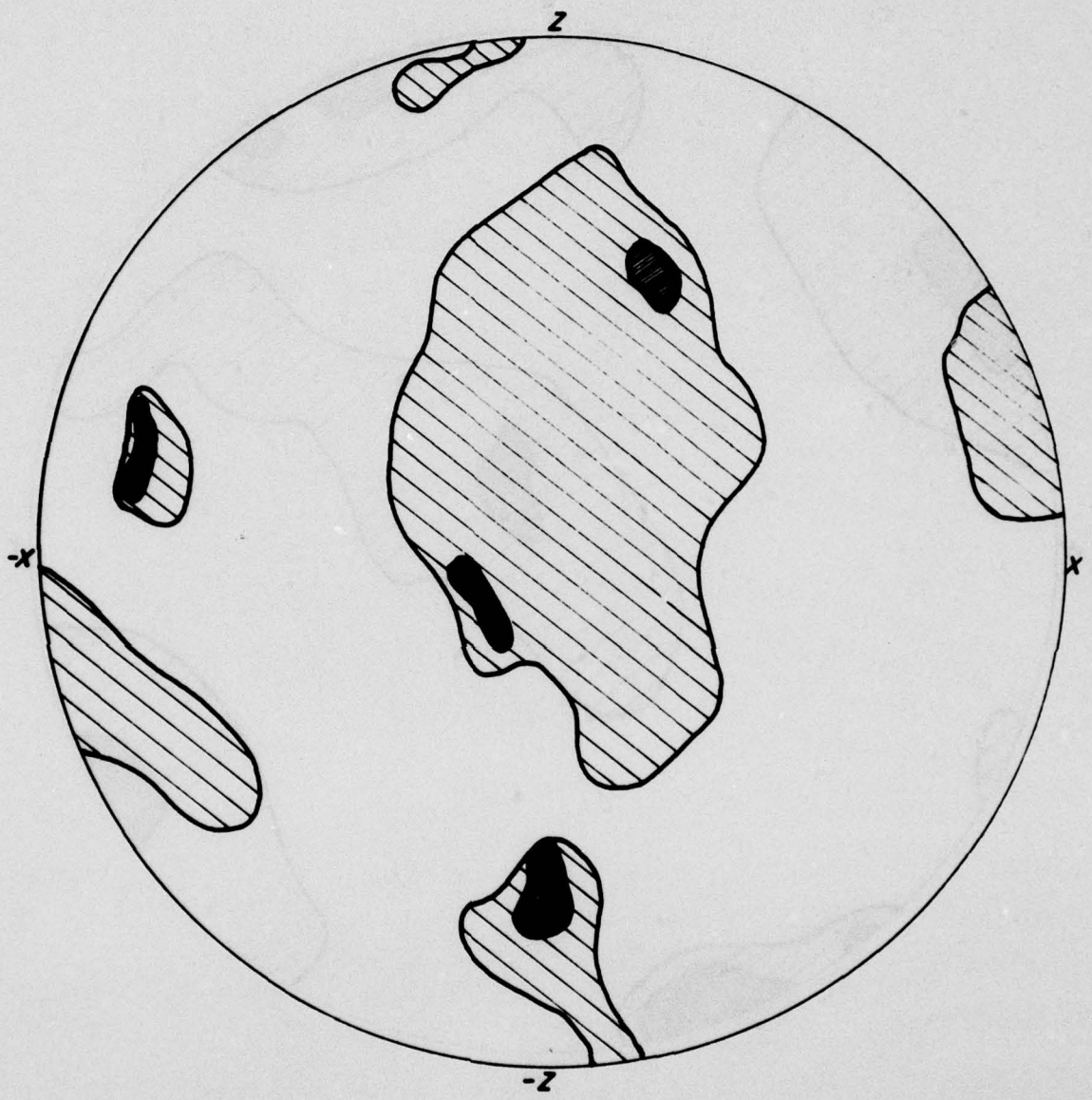

FIG. 35 EQUAL AREA STEREONET SHOWING DISTRIBUTION OF INTERPARTICLE CONTACT NORMALS IN RIVER SITE SAMPLE B1-S4

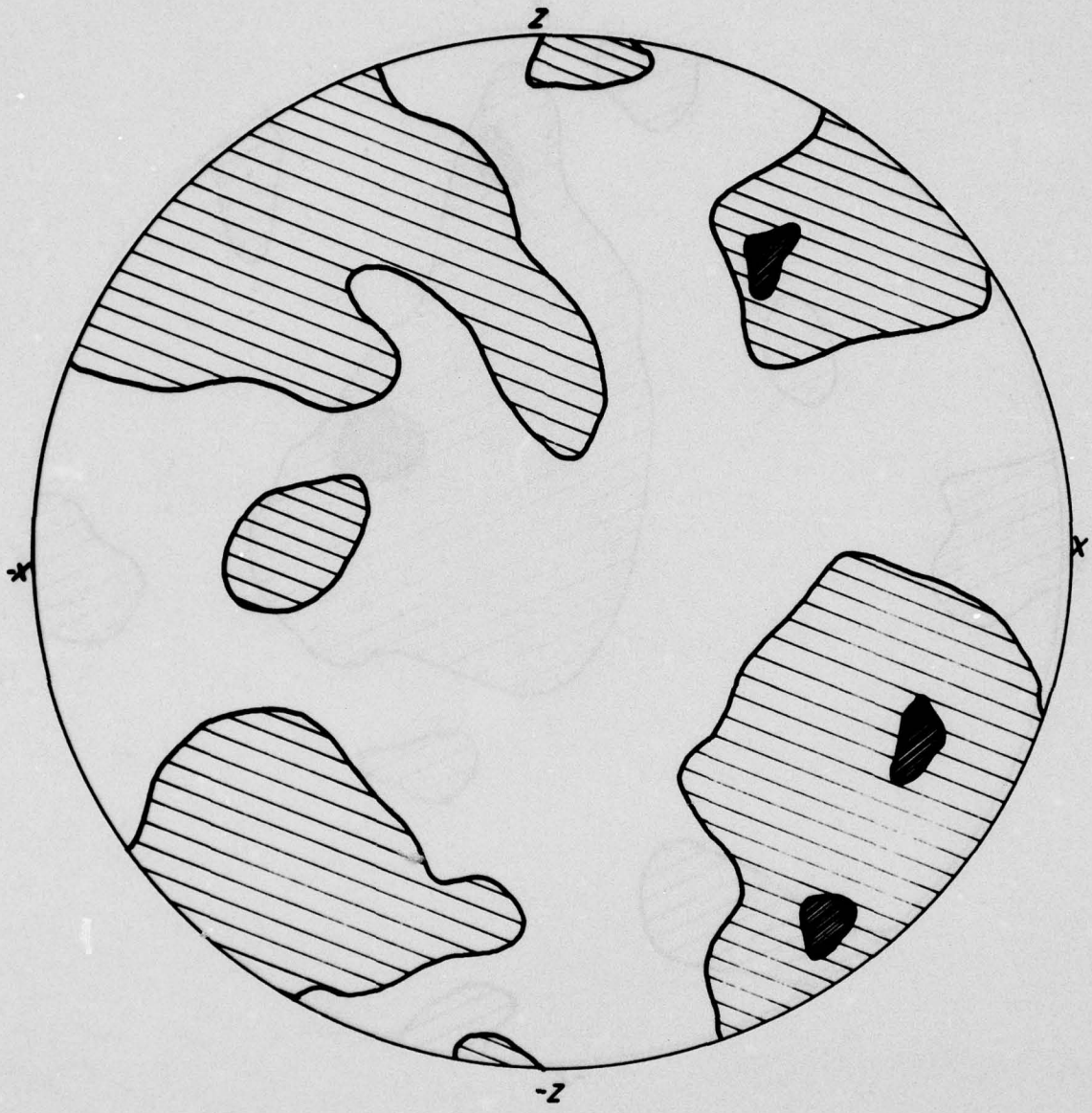

FIG. 36 EQUAL AREA STEREONET SHOWING THE DISTRIBUTION OF INTER-PARTICLE CONTACT NORMALS IN RIVER SITE SAMPLE B1-S5

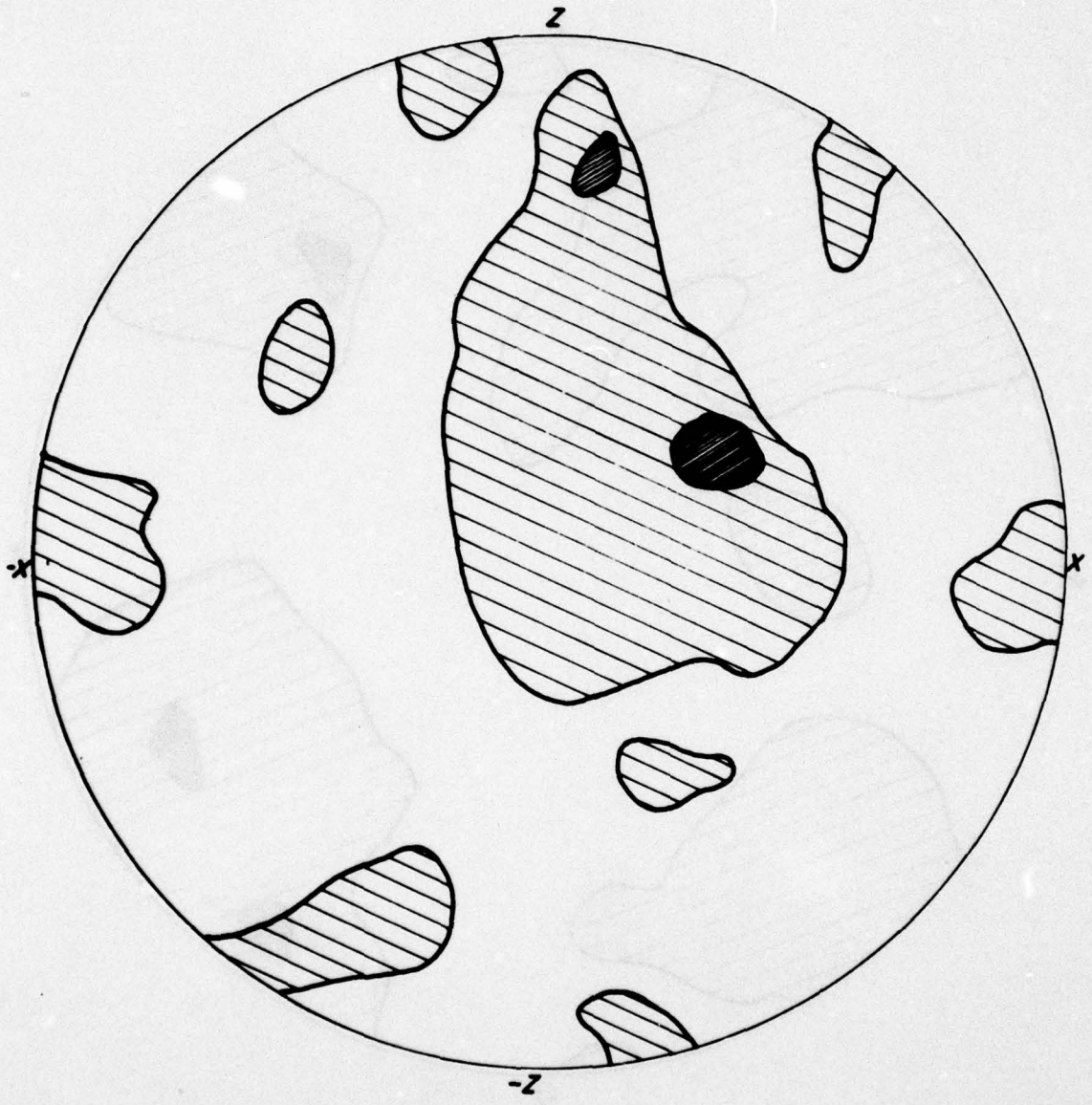

FIG. 37 EQUAL AREA STEREONET SHOWING THE DISTRIBUTION OF INTER-PARTICLE CONTACT NORMALS IN RIVER SITE SAMPLES B1-S6

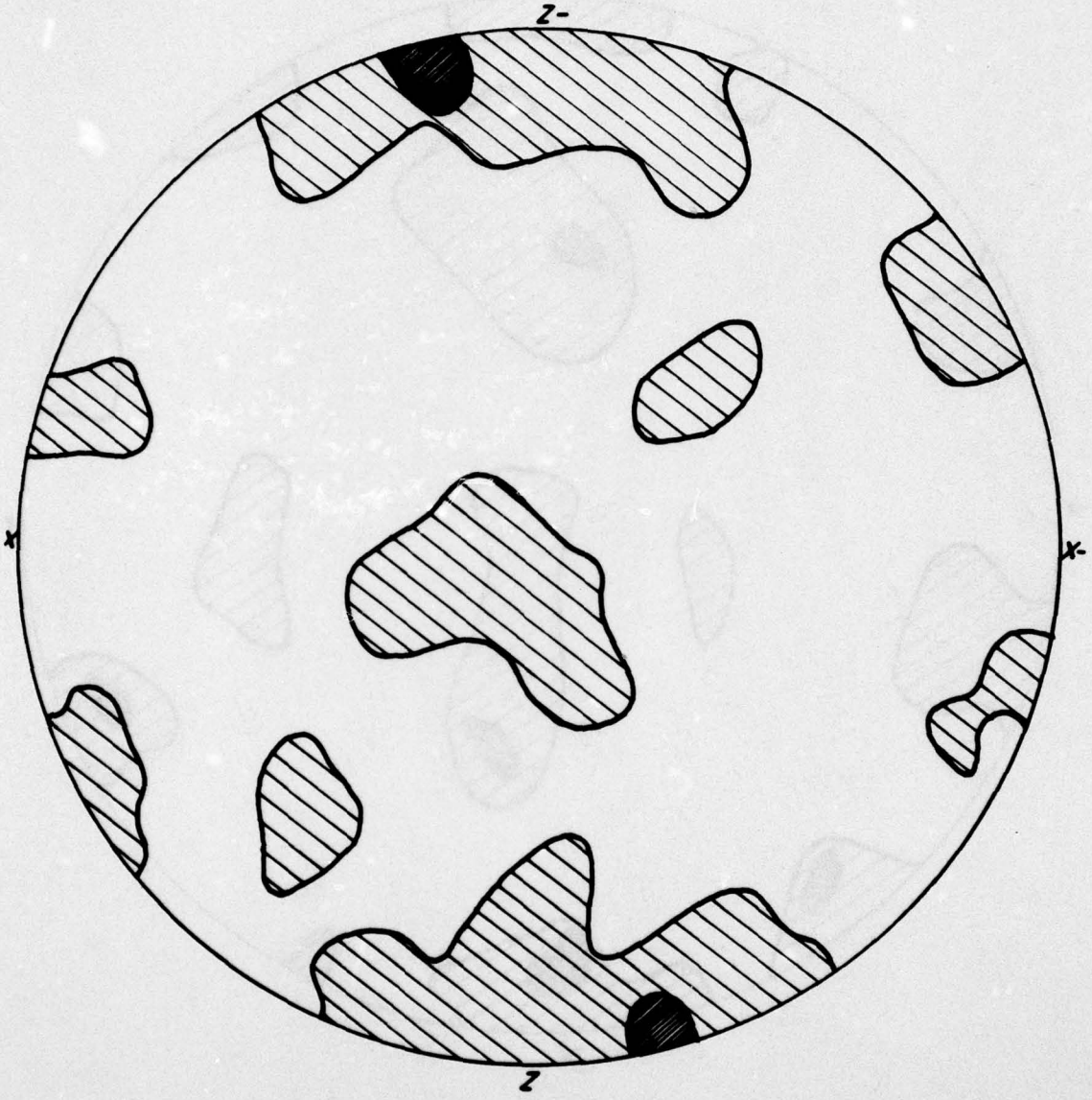

FIG. 38 EQUAL AREA STEREONET SHOWING THE DISTRIBUTION OF INTER-PARTICLE CONTACT NORMALS IN RIVER SITE SAMPLE B1-S7

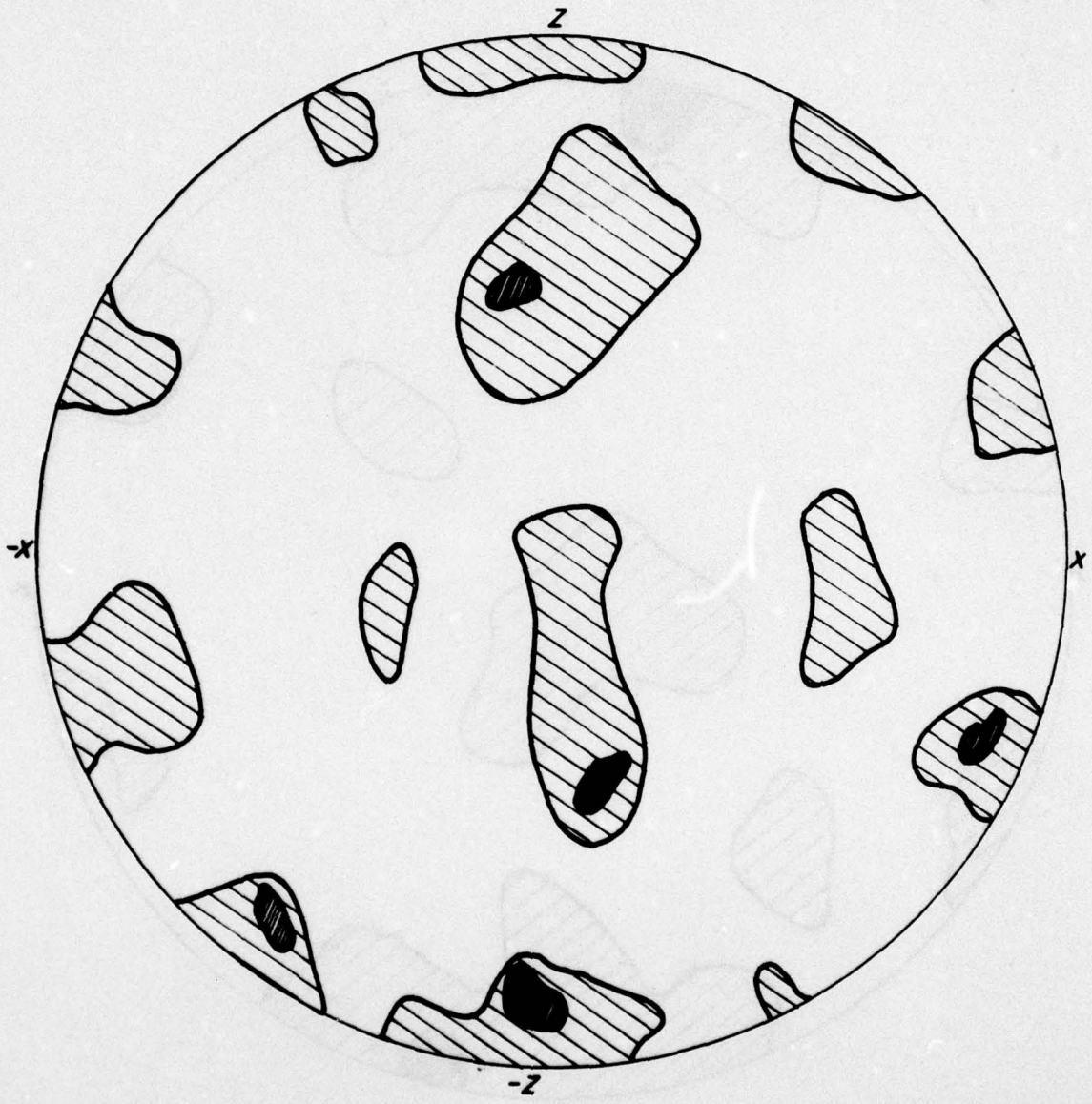

FIG. 39 EQUAL AREA STEREONET SHOWING THE DISTRIBUTION OF INTER-PARTICLE CONTACT NORMALS FOR ROAD SITE SAMPLE B3-S1

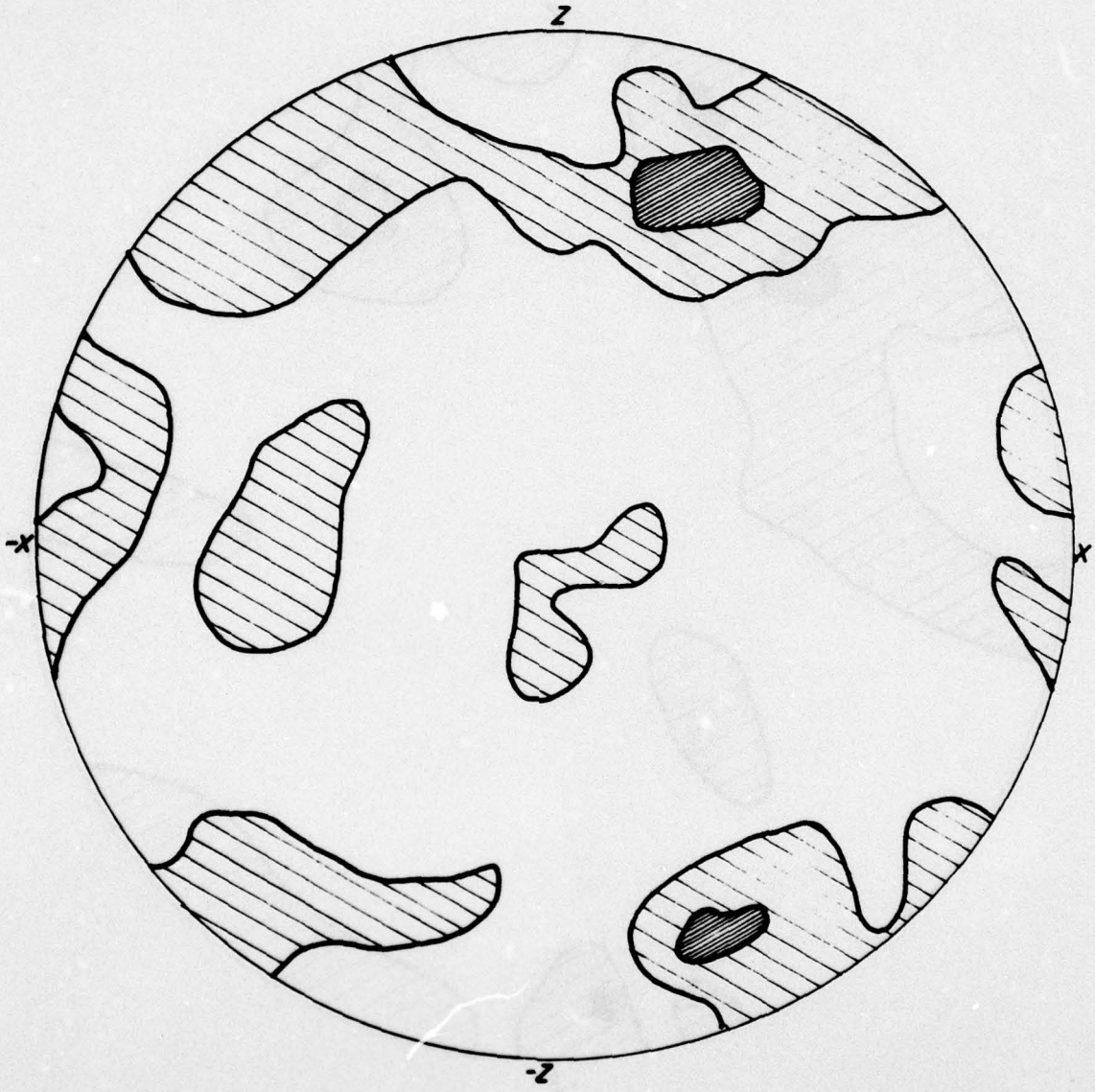

FIG. 40 EQUAL AREA STEREONET SHOWING THE DISTRIBUTION OF INTER-PARTICLE CONTACT NORMALS IN ROAD SITE SAMPLE B3-S2

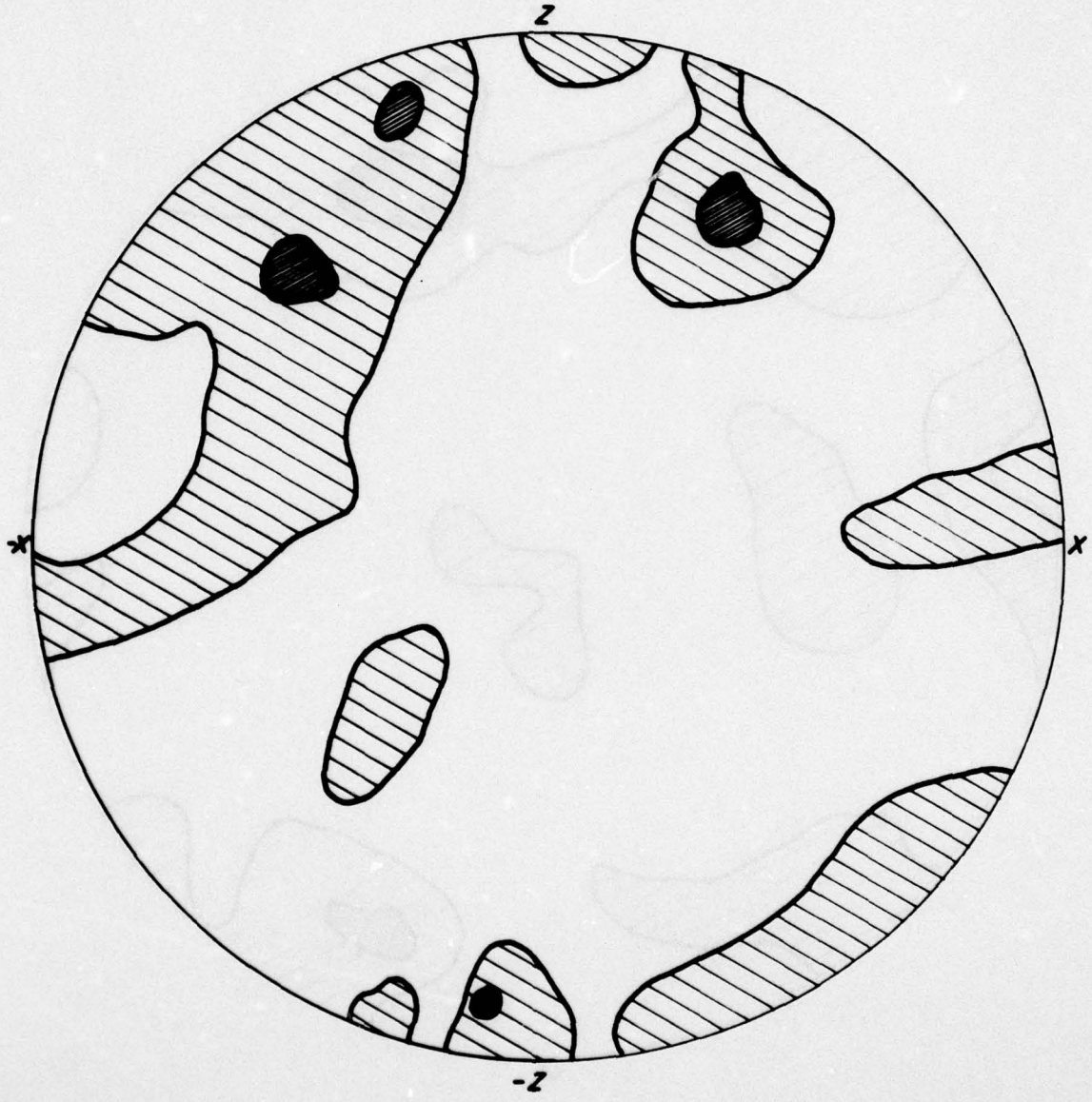

FIG. 41 EQUAL AREA STEREONET SHOWING THE DISTRIBUTION OF INTER-PARTICLE CONTACT NORMALS IN ROAD SITE SAMPLE B3-S3

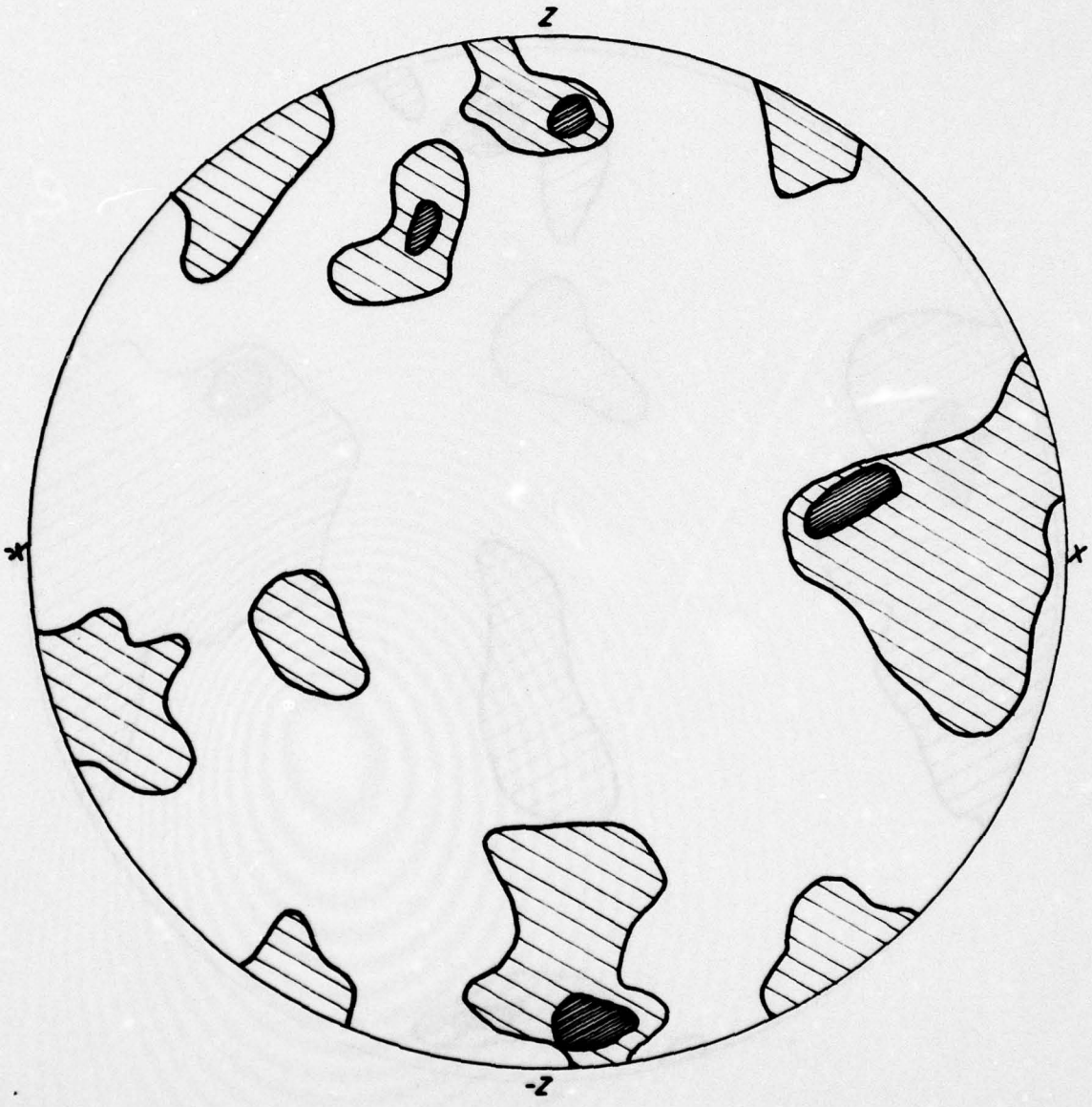

FIG. 42 EQUAL AREA STEREONET SHOWING DISTRIBUTION OF INTER-PARTICLE CONTACT NORMALS IN ROAD SITE SAMPLE B3-S4

AD-A061 145 CALIFORNIA UNIV BERKELEY OFFICE OF RESEARCH SERVICES F/G 8/7
FABRIC ANALYSIS OF UNDISTURBED SANDS FROM NIIGATA, JAPAN.(U)
SEP 78 J K MITCHELL, F J GUZIKOWSKI DACA39-76-M-0344
UNCLASSIFIED WES-TR-S-78-11 NL

2 OF 2
ADA
061145

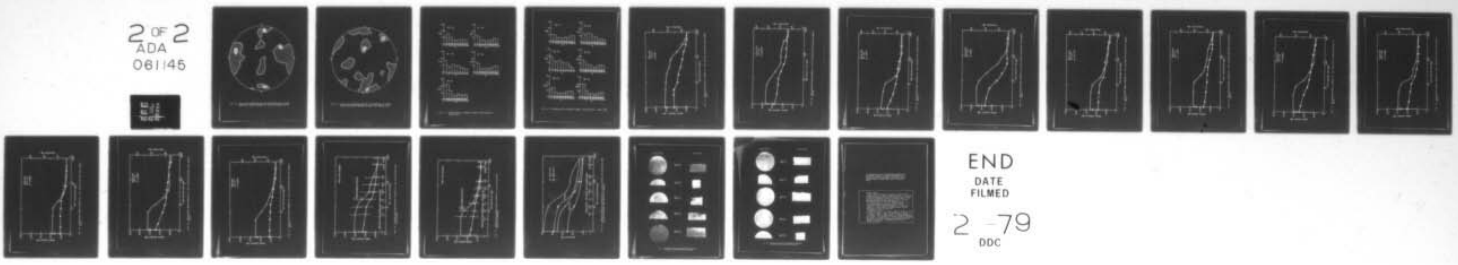

END
DATE
FILMED
2-79
DDC

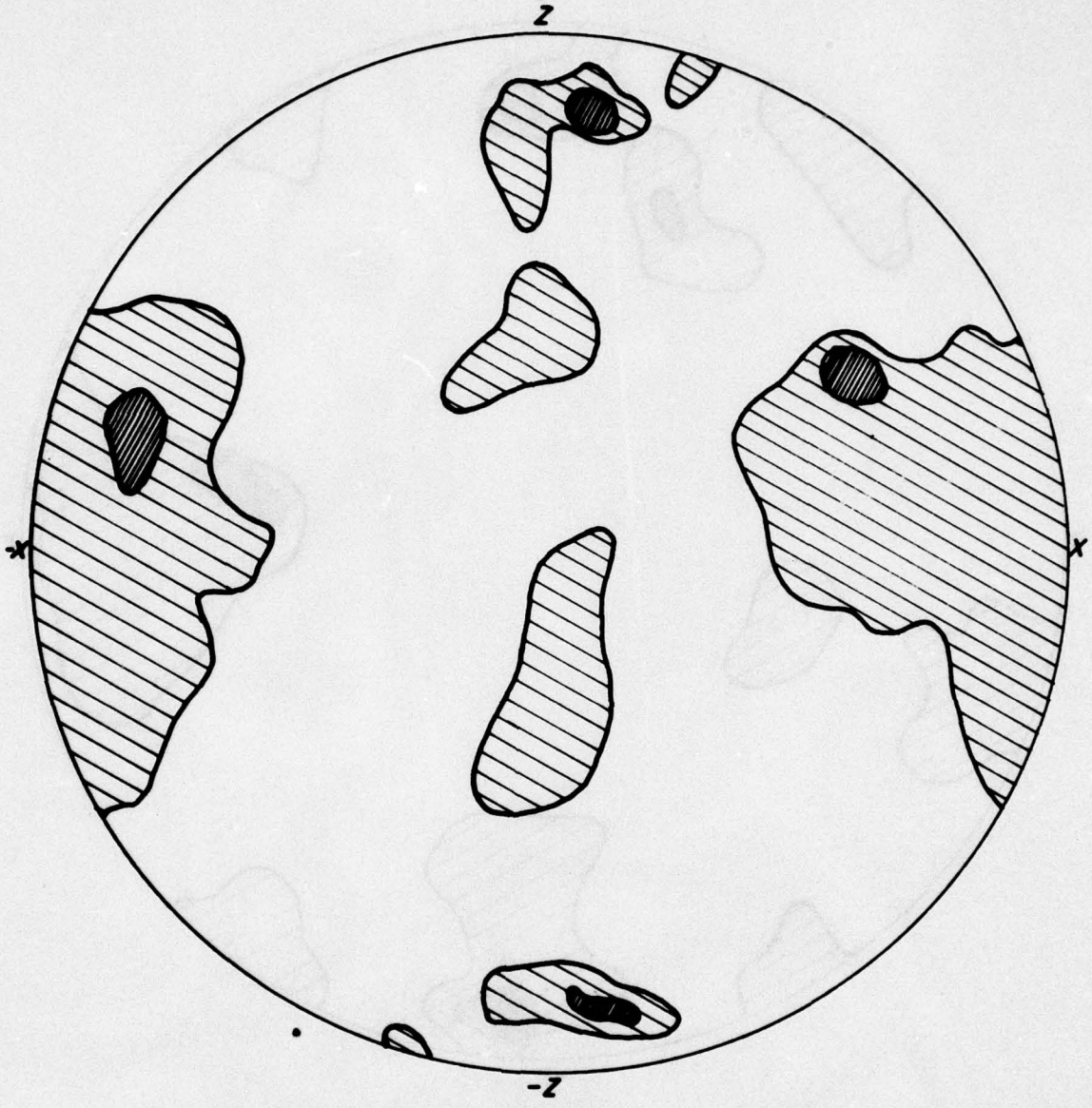

FIG. 43 EQUAL AREA STEREONET SHOWING DISTRIBUTION OF INTER-PARTICLE CONTACT NORMALS IN ROAD SITE SAMPLE B3-S5

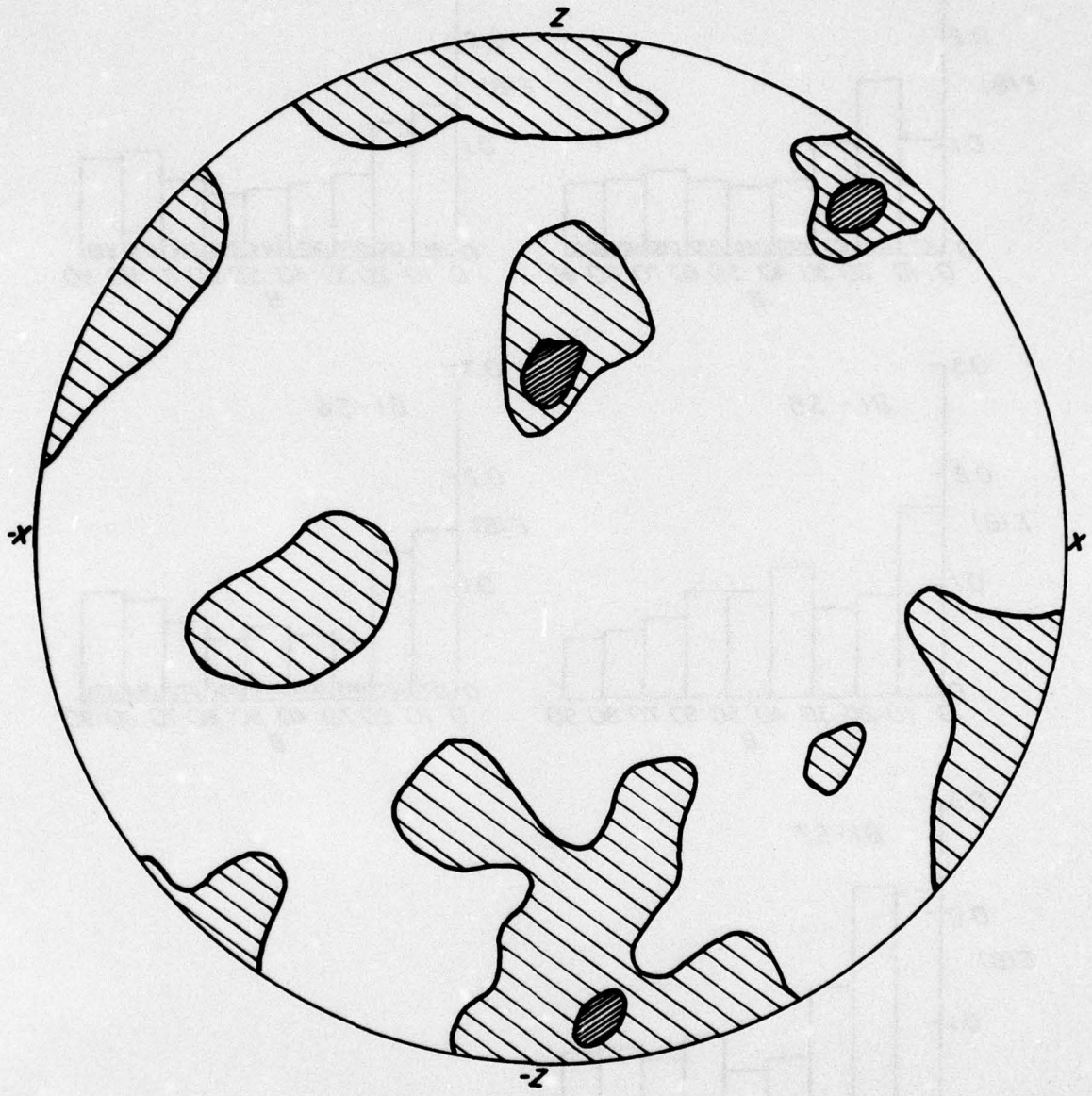

FIG. 44 EQUAL AREA STEREONET SHOWING DISTRIBUTION OF INTER-PARTICLE CONTACT NORMALS IN ROAD SITE SAMPLE B3-S7

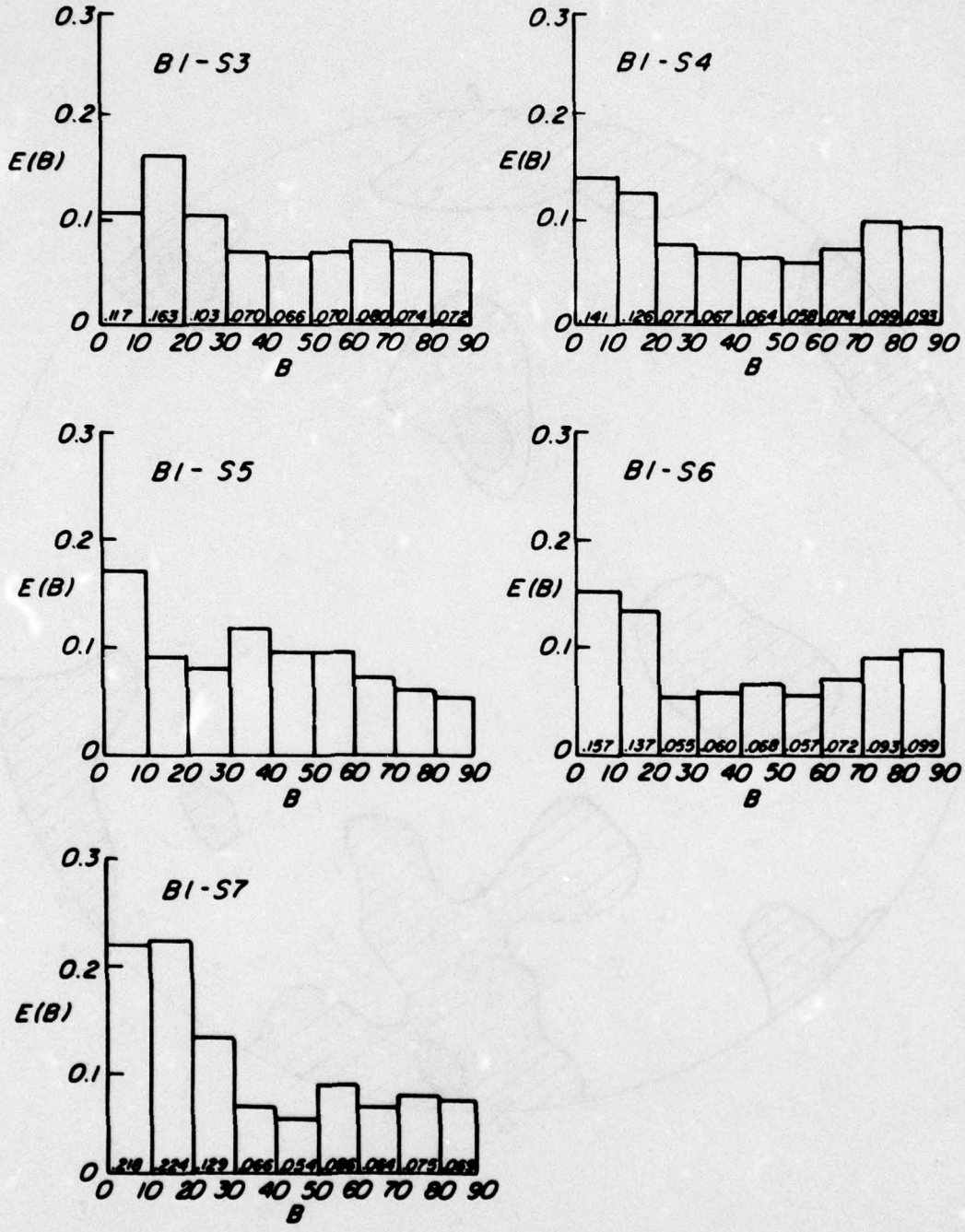

FIG. 45 INTERPARTICLE CONTACT NORMAL DISTRIBUTION - RIVER SITE

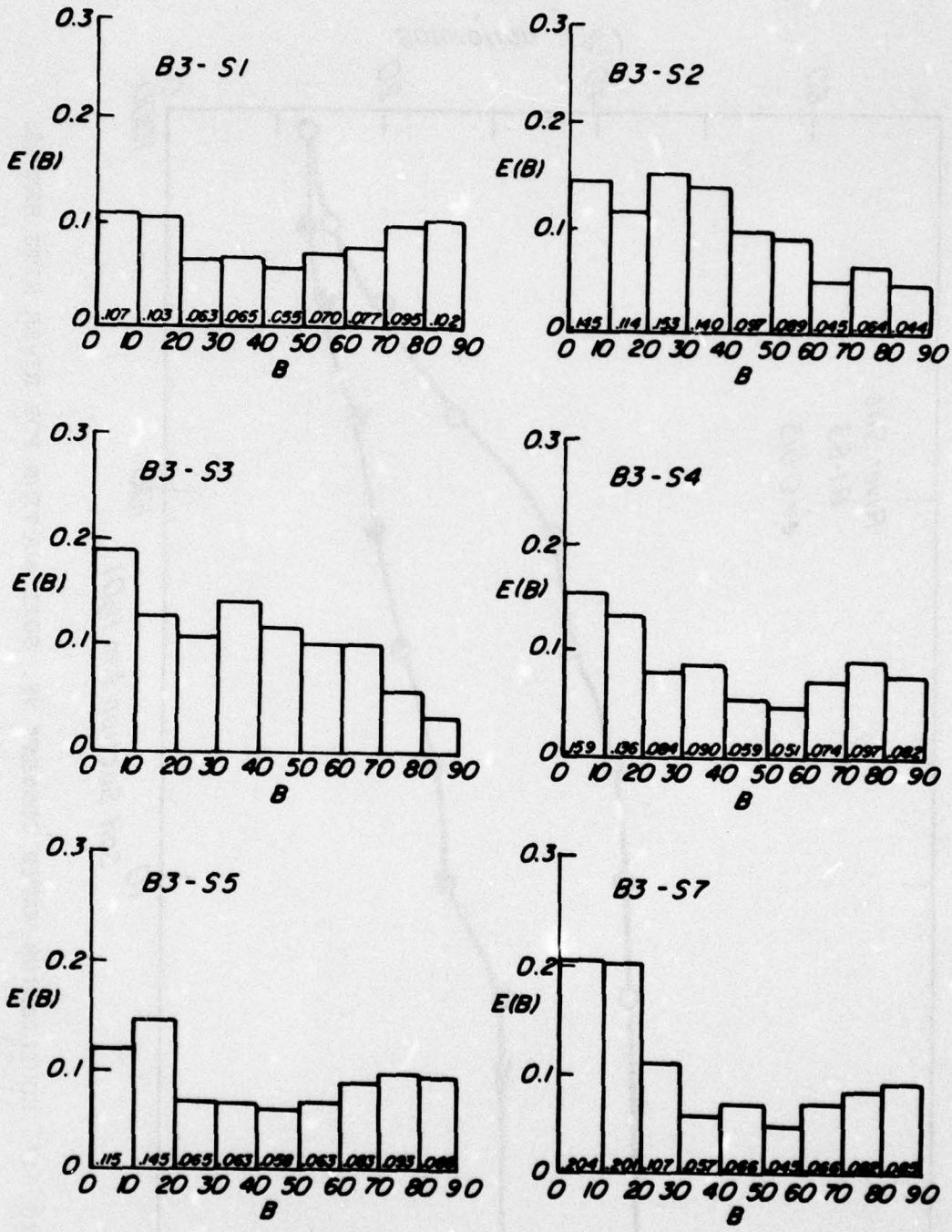

FIG. 46 INTERPARTICLE CONTACT NORMAL DISTRIBUTION - ROAD SITE

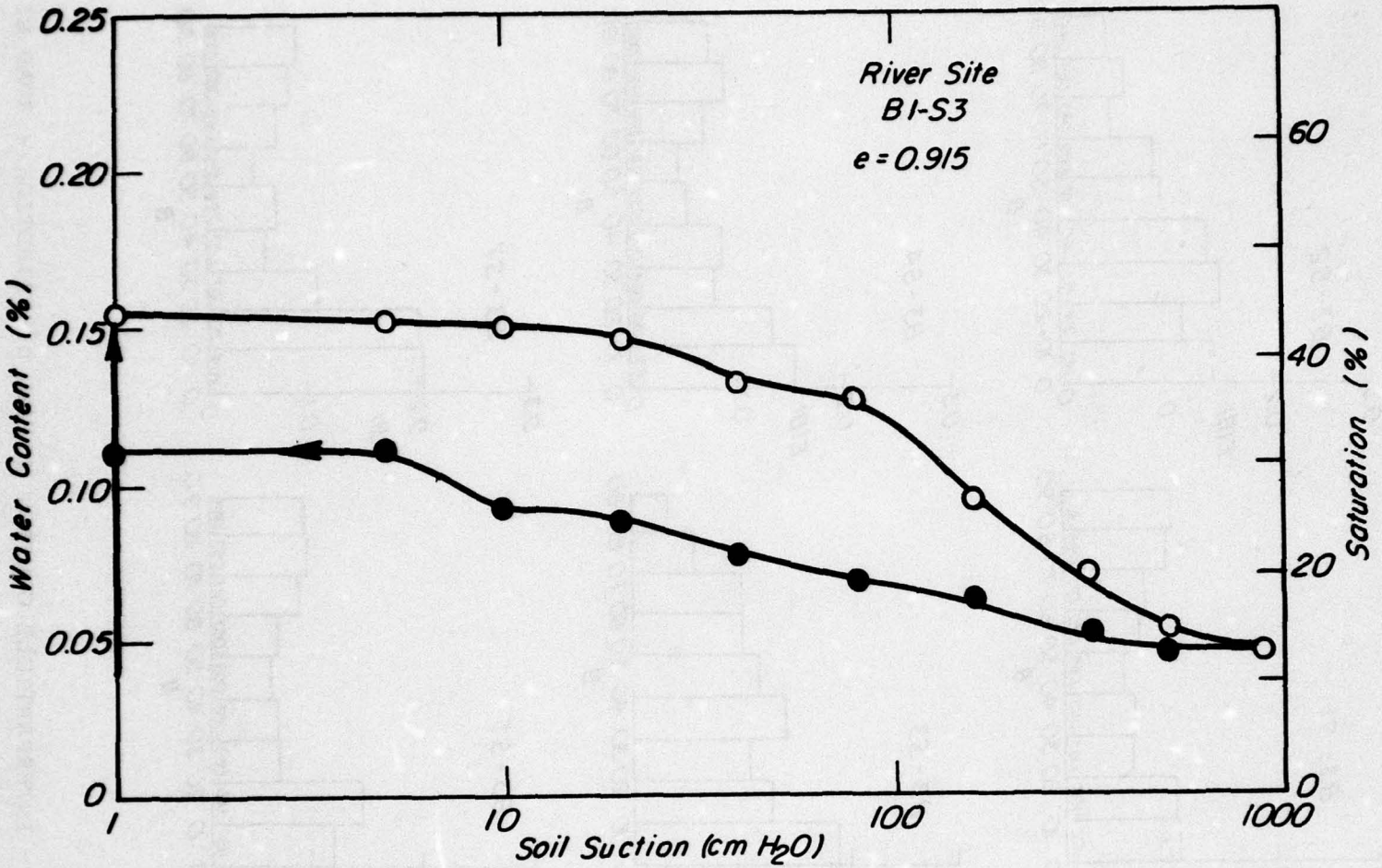

FIG. 47 EQUILIBRIUM WATER CONTENT VS. SOIL SUCTION FOR RIVER SITE SAMPLE B1-S3

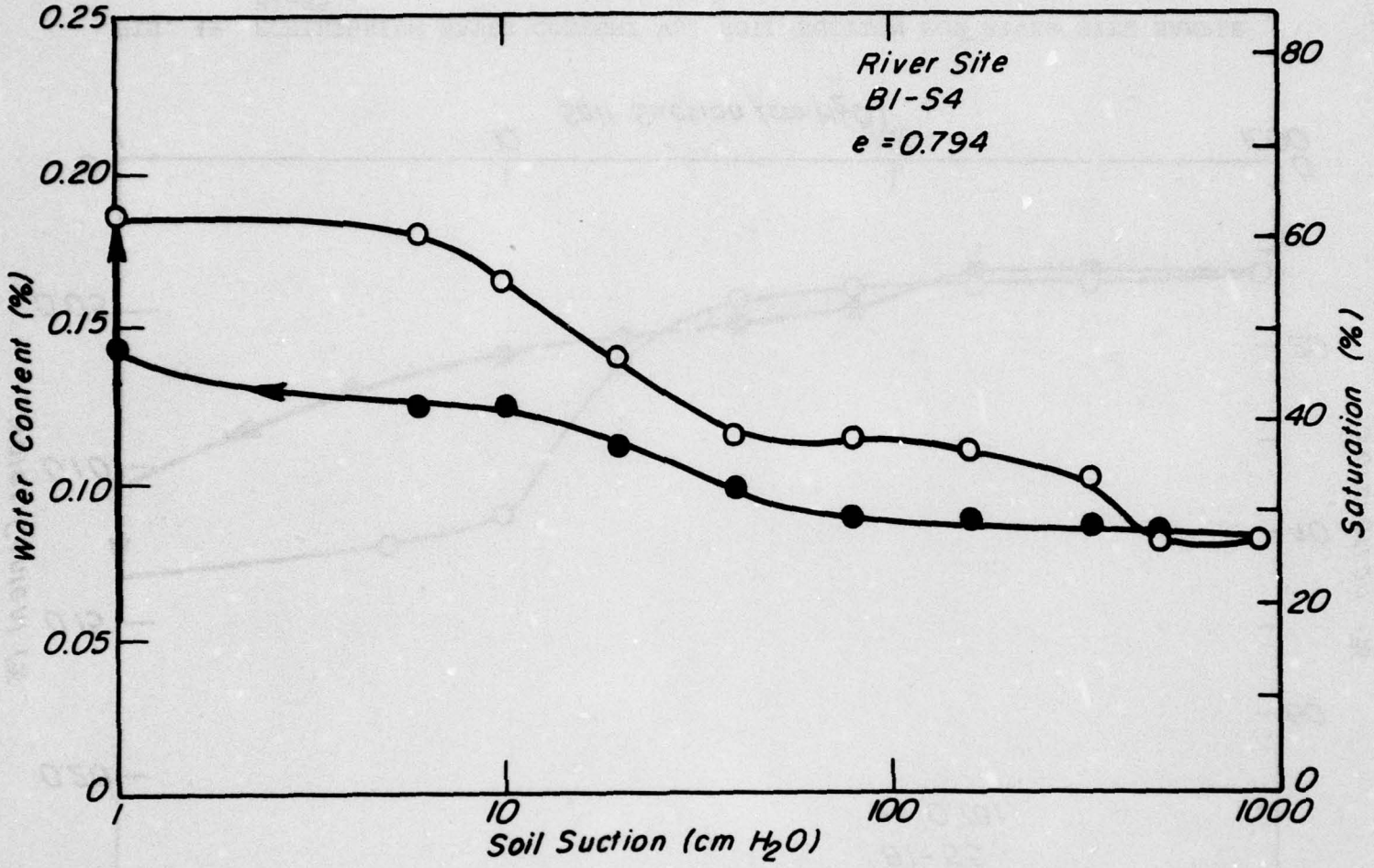

FIG. 48 EQUILIBRIUM WATER CONTENT VS. SOIL SUCTION FOR RIVER SITE SAMPLE B1-S4

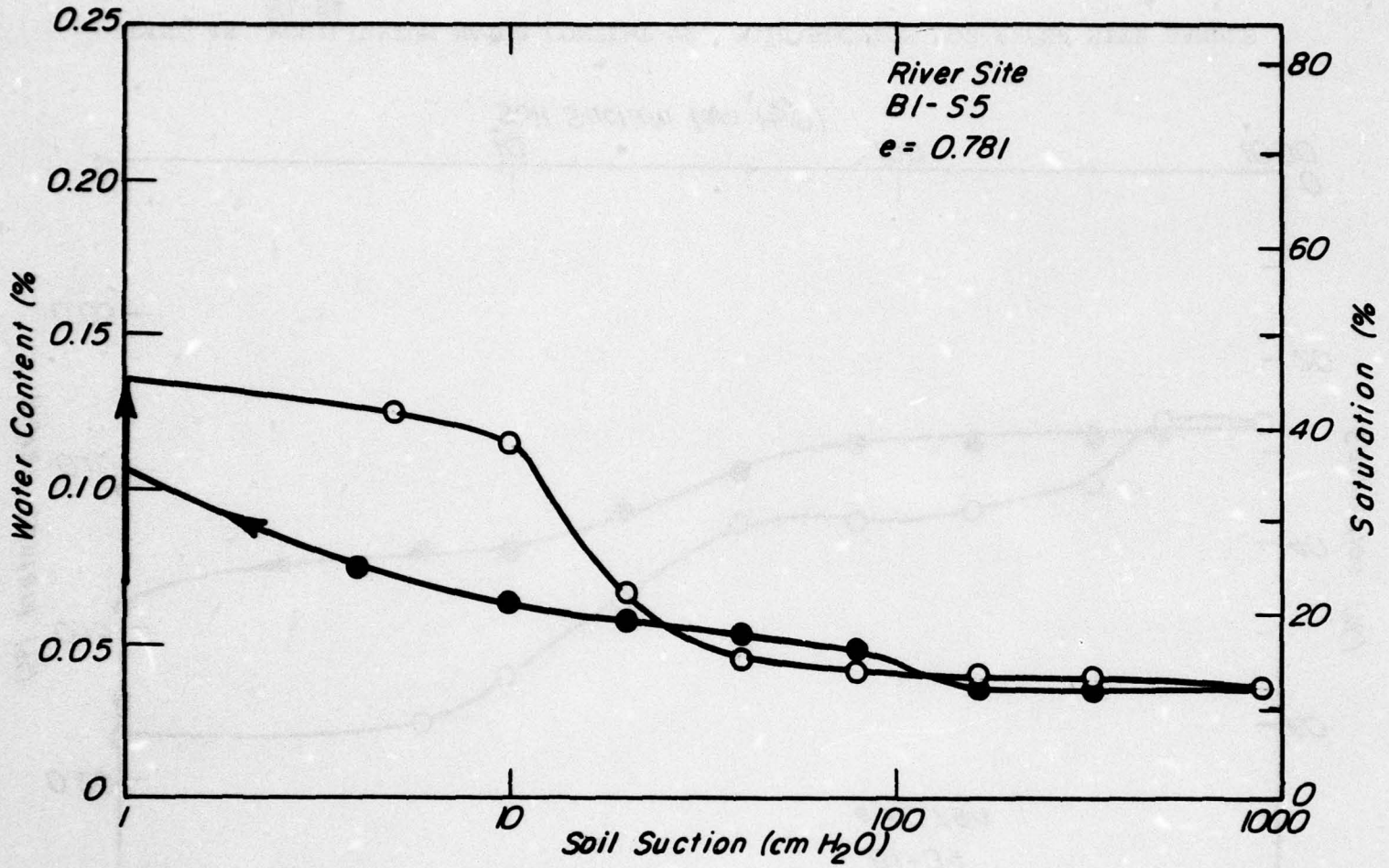

FIG. 49 EQUILIBRIUM WATER CONTENT VS. SOIL SUCTION FOR RIVER SITE SAMPLE B1-S5

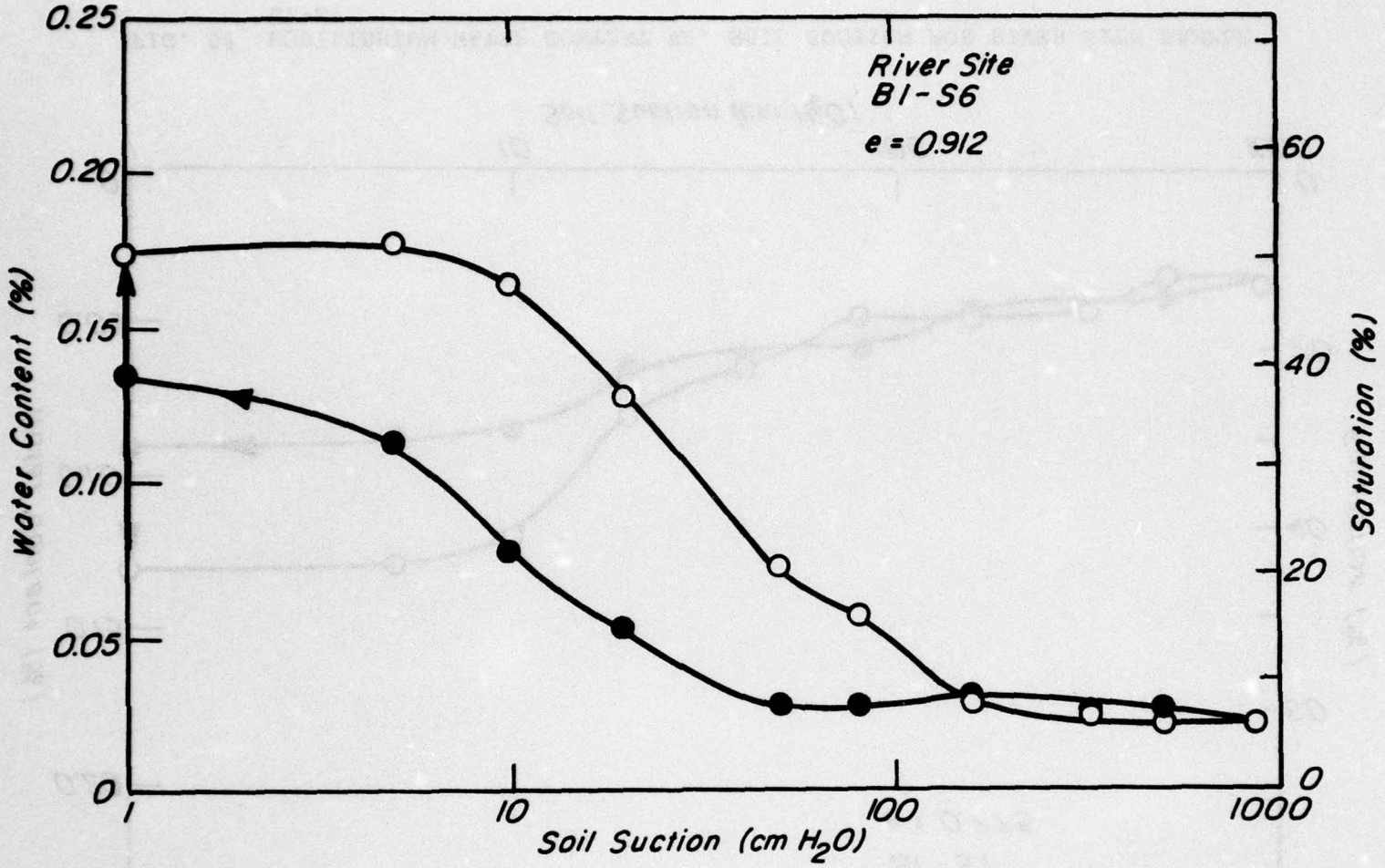

FIG. 50 EQUILIBRIUM WATER CONTENT VS. SOIL SUCTION FOR RIVER SITE SAMPLE B1-S6

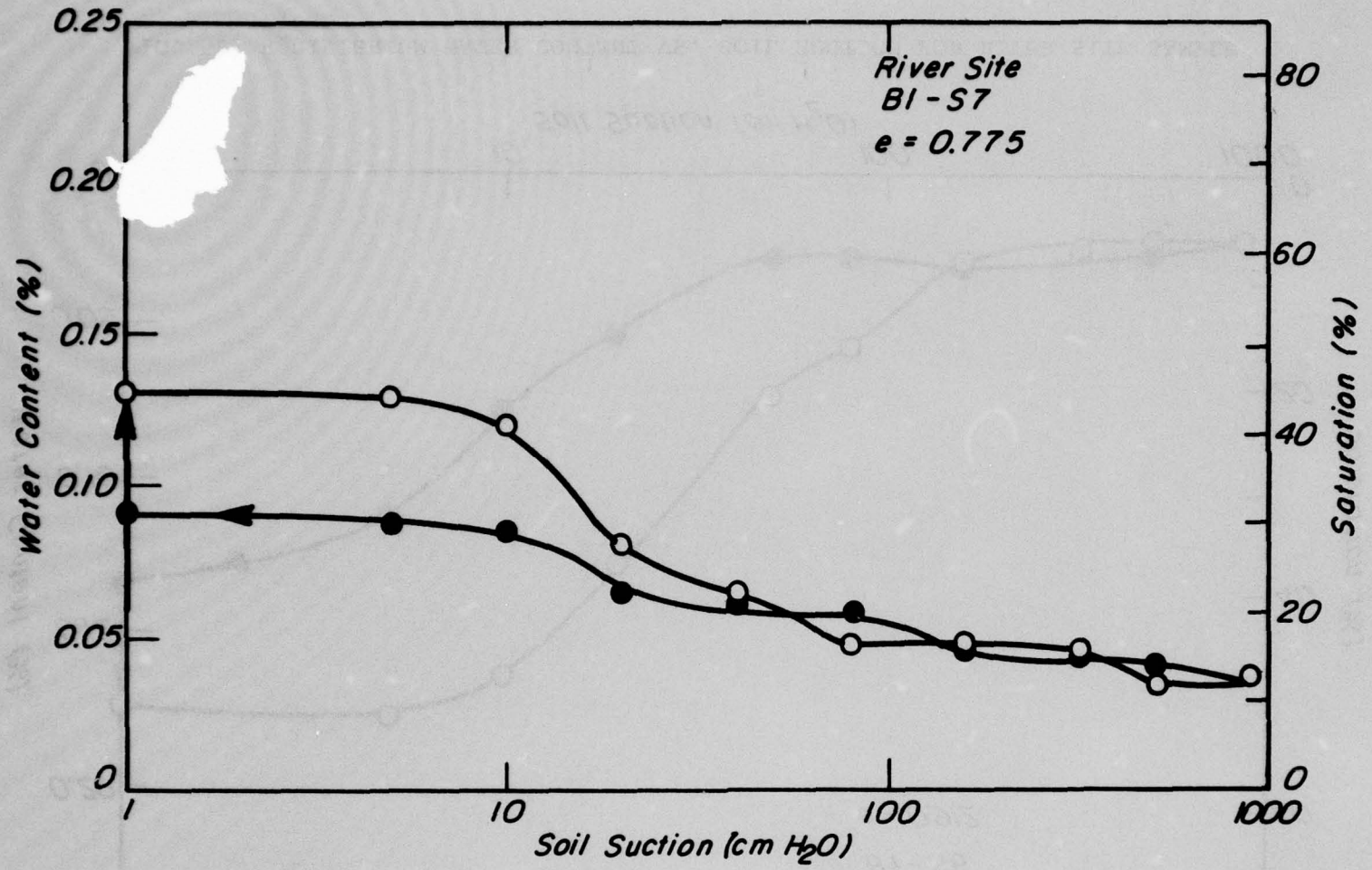

FIG. 51 EQUILIBRIUM WATER CONTENT VS. SOIL SUCTION FOR RIVER SITE SAMPLE B1-S7

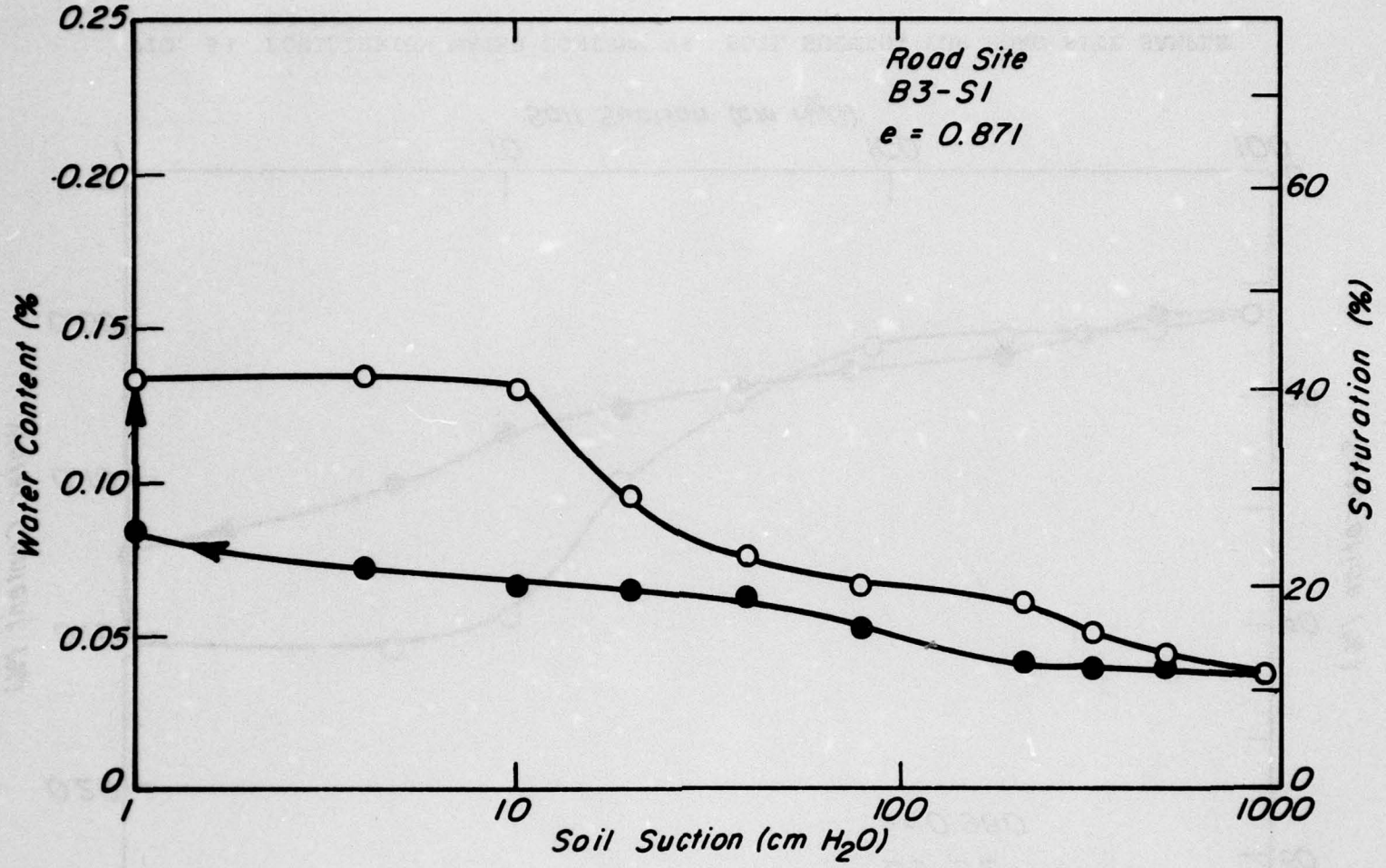

FIG. 52 EQUILIBRIUM WATER CONTENT VS. SOIL SUCTION FOR ROAD SITE SAMPLE B3-S1

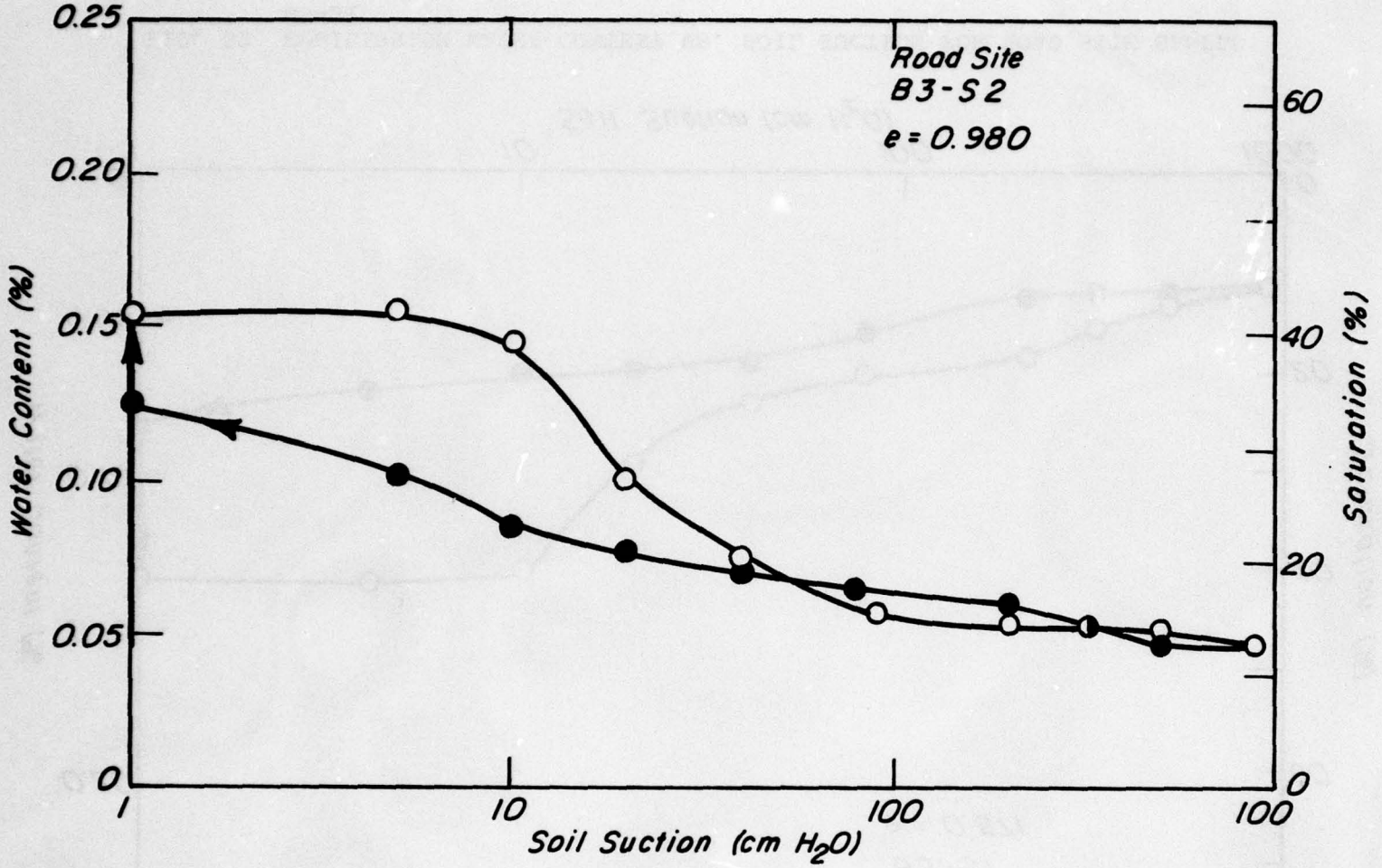

FIG. 53 EQUILIBRIUM WATER CONTENT VS. SOIL SUCTION FOR ROAD SITE SAMPLE B3-S2

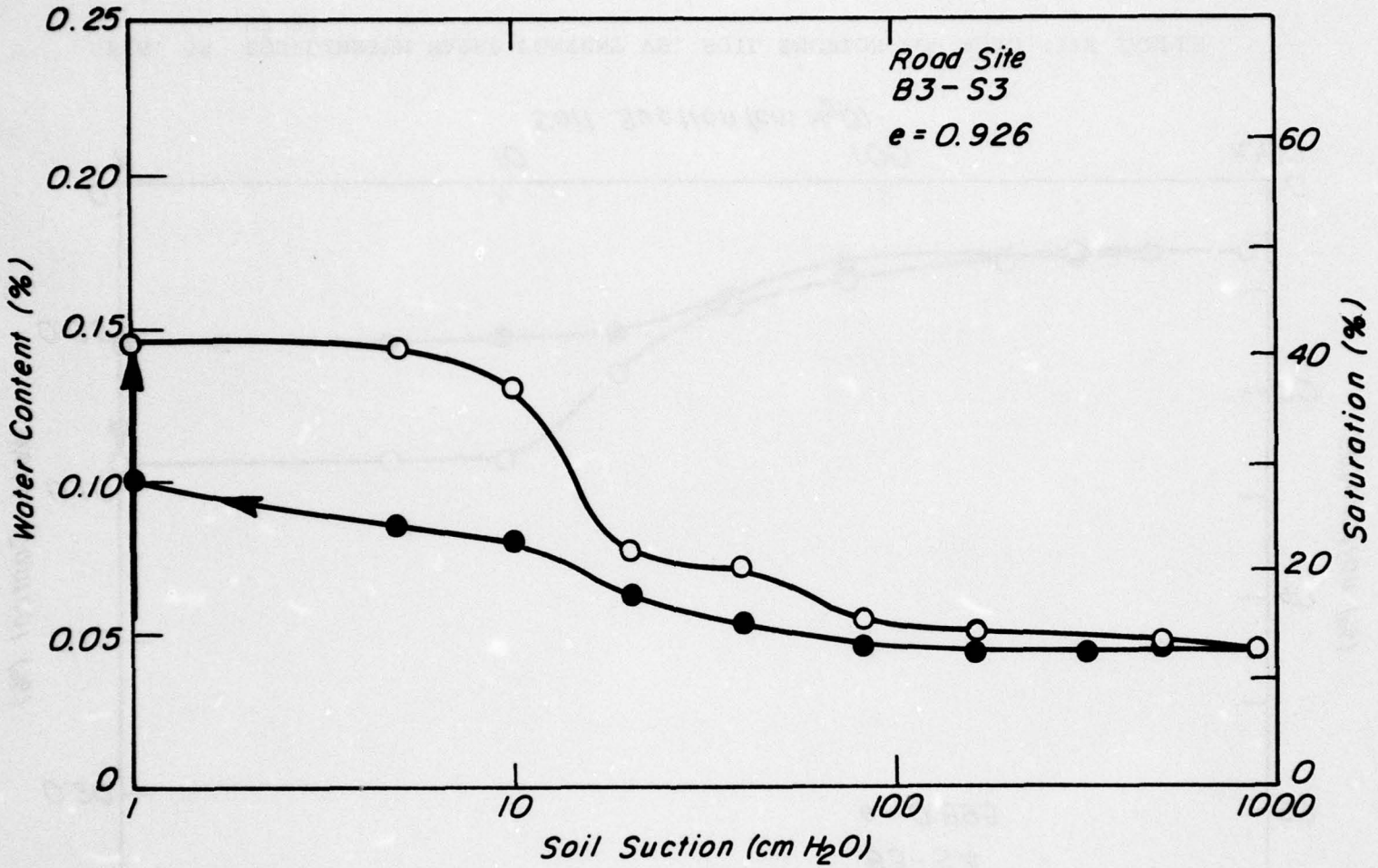

FIG. 54 EQUILIBRIUM WATER CONTENT VS. SOIL SUCTION FOR ROAD SITE SAMPLE B3-S3

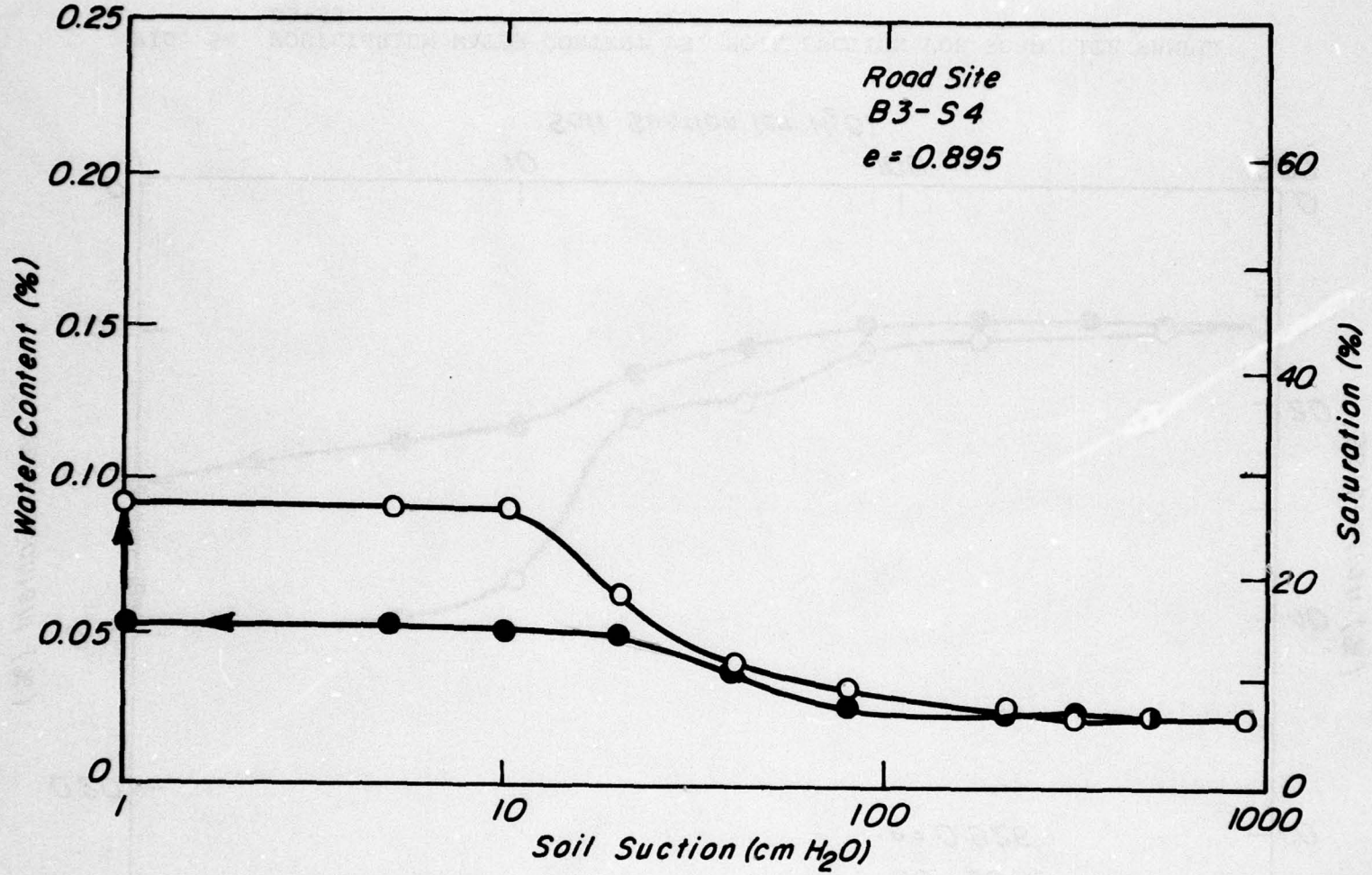

FIG. 55 EQUILIBRIUM WATER CONTENT VS. SOIL SUCTION FOR ROAD SITE SAMPLE B3-S4

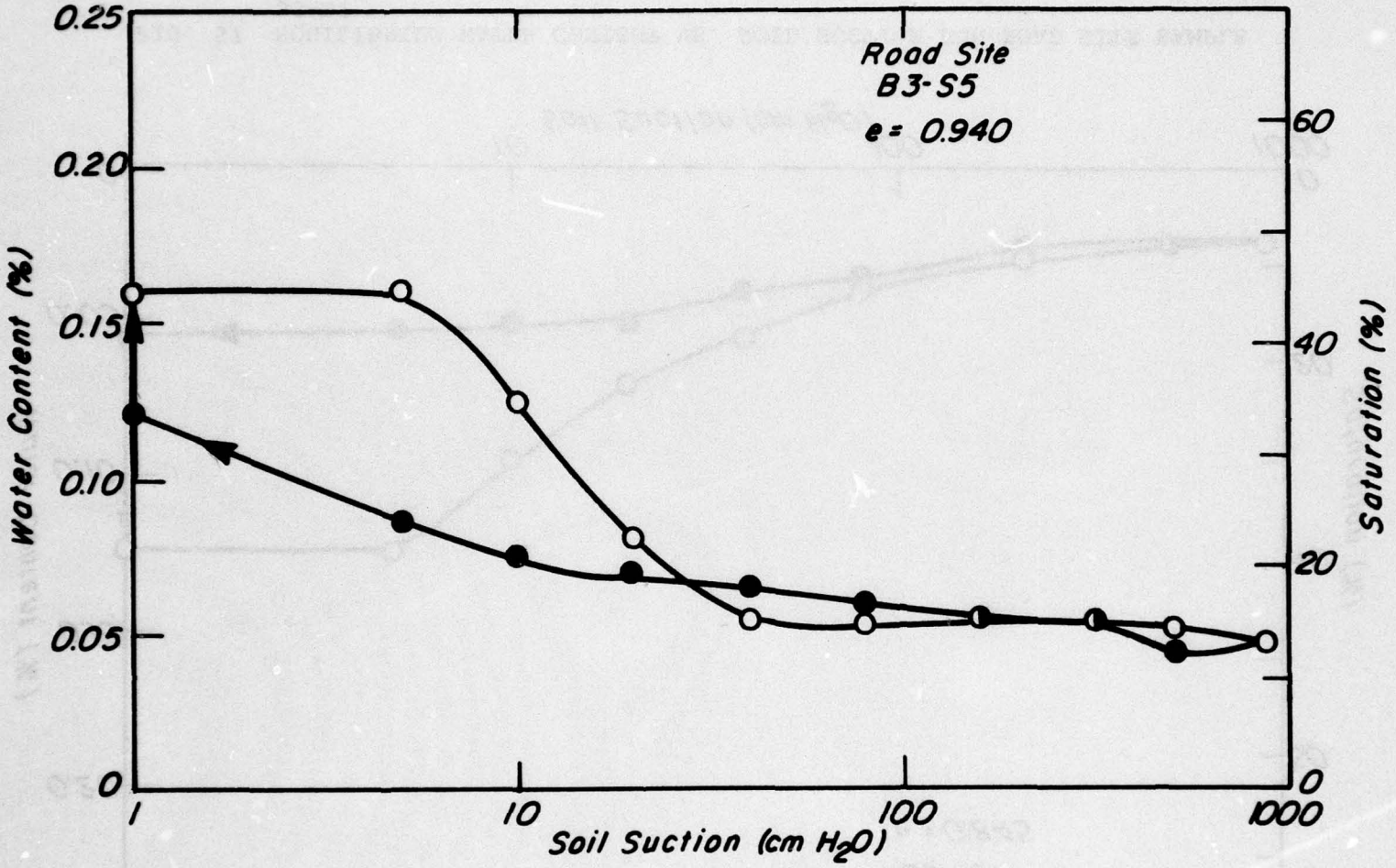

FIG. 56 EQUILIBRIUM WATER CONTENT VS. SOIL SUCTION FOR ROAD SITE SAMPLE B3-S5

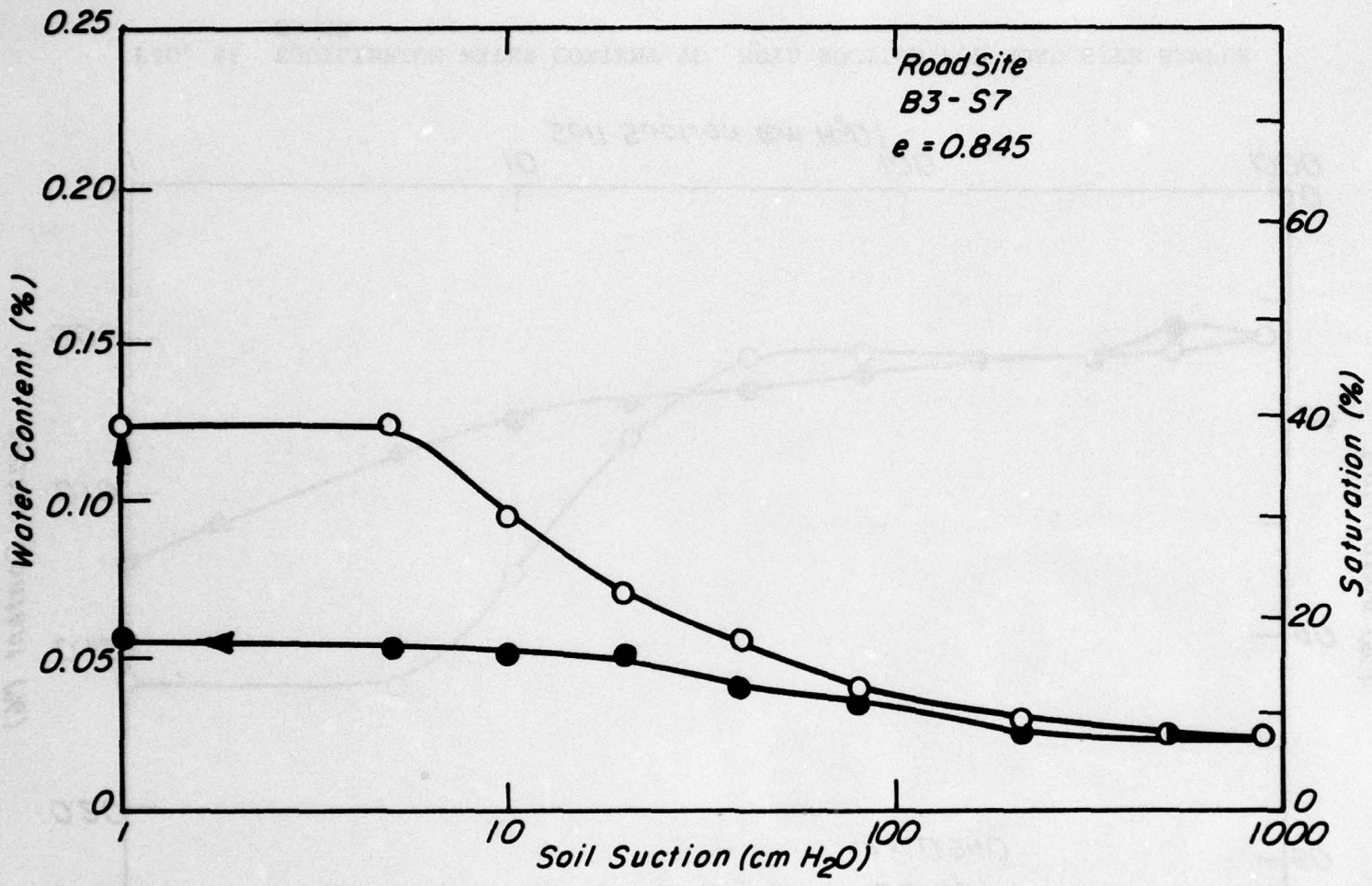

FIG. 57 EQUILIBRIUM WATER CONTENT VS. SOIL SUCTION FOR ROAD SITE SAMPLE B3-S7

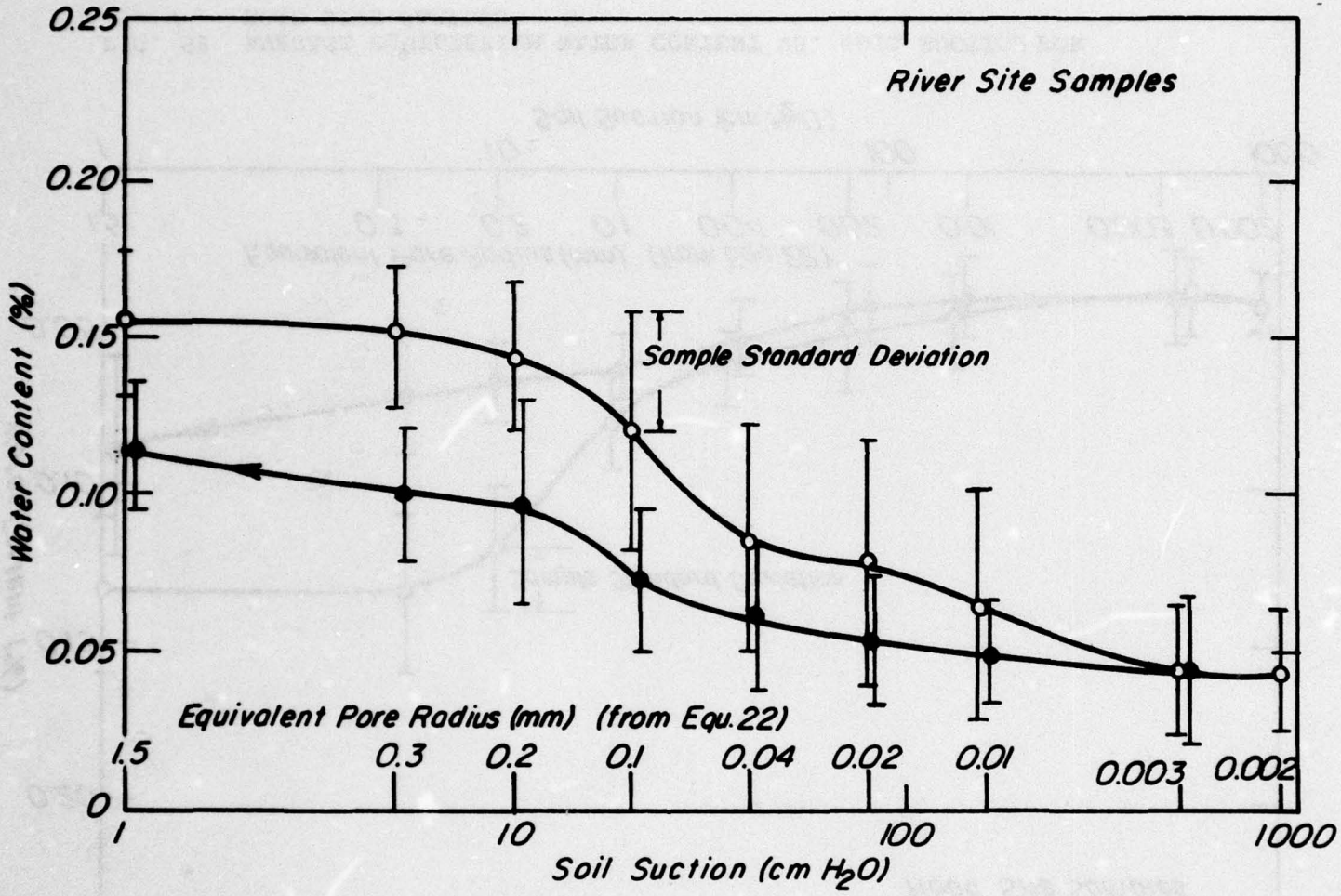

FIG. 58 AVERAGE EQUILIBRIUM WATER CONTENT VS. SOIL SUCTION FOR RIVER SITE SAMPLES

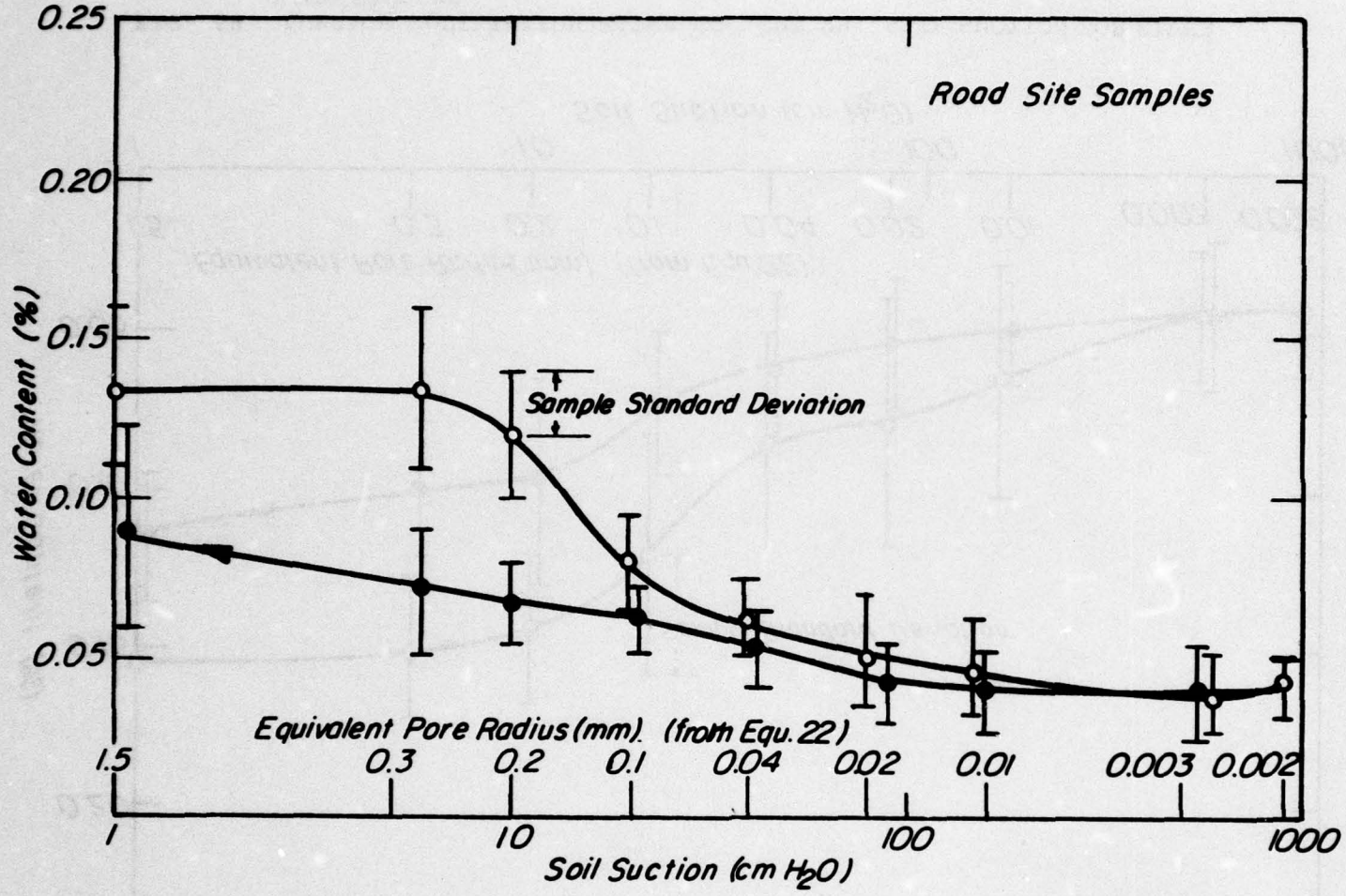

FIG. 59 AVERAGE EQUILIBRIUM WATER CONTENT VS. SOIL SUCTION FOR ROAD SITE SAMPLES

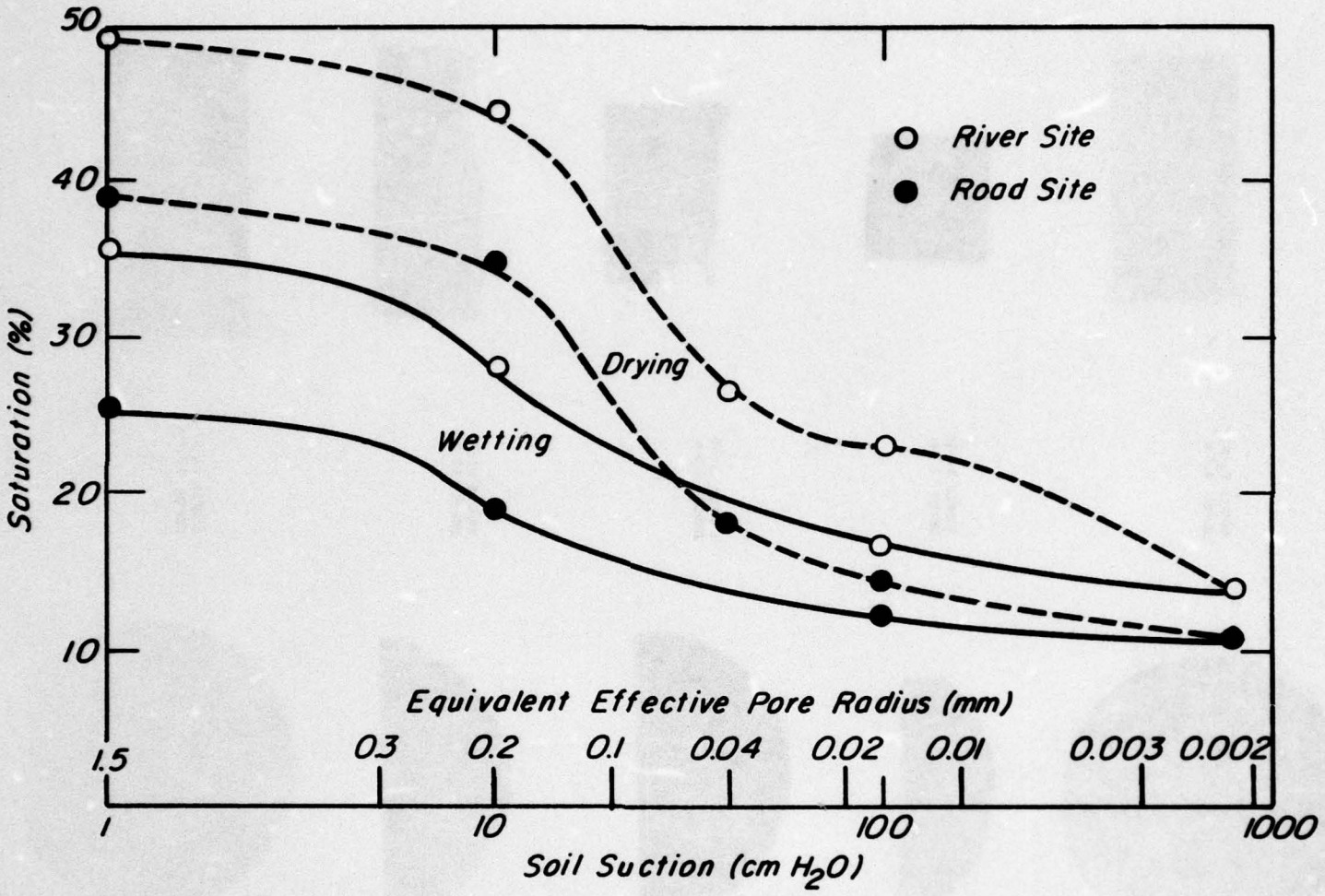

FIG. 60 AVERAGE DEGREE OF SATURATION VS. SOIL SUCTION AND EFFECTIVE PORE RADIUS FOR RIVER AND ROAD SITE SAMPLES

HORIZONTAL SECTIONS

VERTICAL SECTIONS

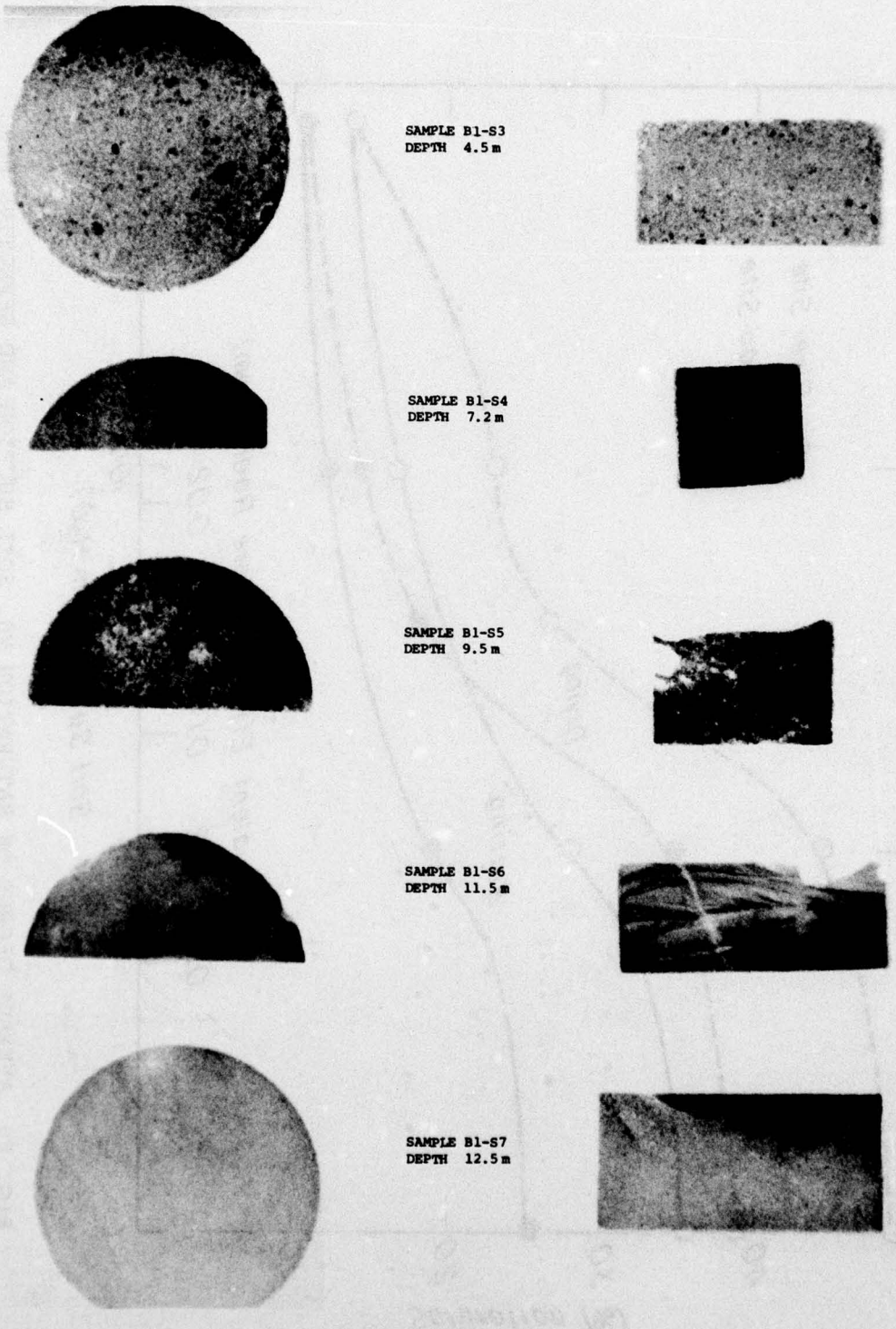

SAMPLE B1-S3
DEPTH 4.5 m

SAMPLE B1-S4
DEPTH 7.2 m

SAMPLE B1-S5
DEPTH 9.5 m

SAMPLE B1-S6
DEPTH 11.5 m

SAMPLE B1-S7
DEPTH 12.5 m

FIG. 61 ACTUAL-SIZE, POSITIVE X-RADIOGRAPHS OF HORIZONTAL AND VERTICAL SLICES FROM RIVER SITE SAMPLES

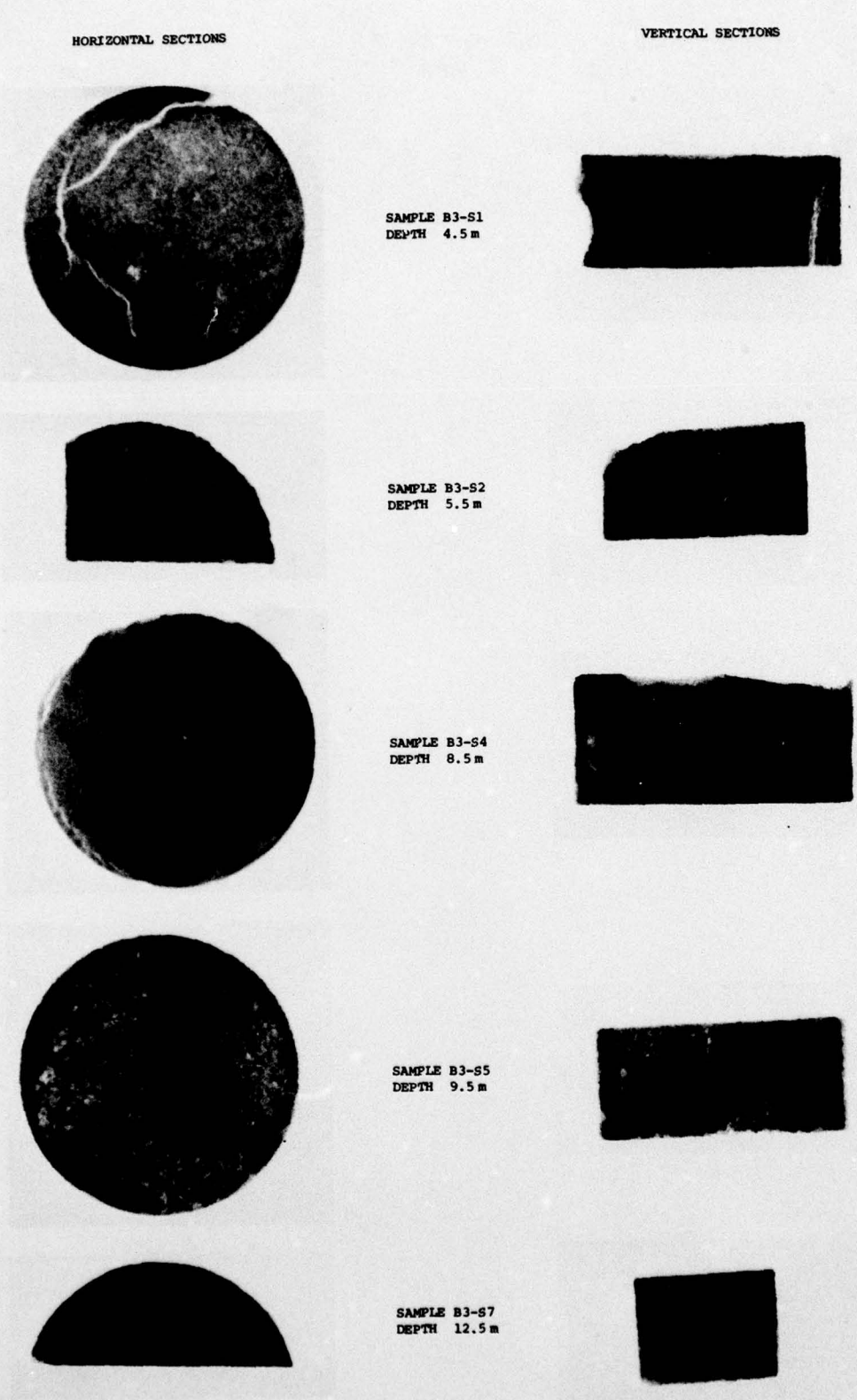

FIG. 62. ACTUAL-SIZE, POSITIVE X-RADIOGRAPHS OF HORIZONTAL AND VERTICAL SLICES FROM ROAD SITE SAMPLES

In accordance with letter from DAEN-RDC, DAEN-ASI dated 22 July 1977, Subject: Facsimile Catalog Cards for Laboratory Technical Publications, a facsimile catalog card in Library of Congress MARC format is reproduced below.

Mitchell, James K
Fabric analysis of undisturbed sands from Niigata, Japan / by James K. Mitchell, Frank J. Guzikowski, Willem C. B. Villet, College of Engineering, Office of Research Services, University of California, Berkeley, California. Vicksburg, Miss. : U. S. Waterways Experiment Station ; Springfield, Va. : available from National Technical Information Service, 1978.
xii, 41, [63] p. : ill. ; 27 cm. (Technical report - U. S. Army Engineer Waterways Experiment Station ; S-78-11)
Prepared for Office, Chief of Engineers, U. S. Army, Washington, D. C., under Contract No. DACA39-76-M0344 (Project 4A161102AT22, Task A2, Work Unit 005)
References: p. 40-41.
1. Liquefaction (Soils). 2. Niigata, Japan. 3. Sands. 4. Soil structure. 5. Soils -- Japan. 6. Undisturbed soil samples. I. Guzikowski, Frank J., joint author. II. Villet, Willem C. B., joint author. III. California. University. College of Engineering. Office of Research Services. IV. United States. Army. Corps of Engineers. V. Series: United States. Waterways Experiment Station, Vicksburg, Miss. Technical report ; S-78-11.
TA7.W34 no.S-78-11